NASA CR-66772

THE MODIFICATION AND USE OF A GROUND-BASED PHOTOMETER FOR EVALUATION OF SATELLITE MATERIALS

By D. C. Romick, R. H. Emmons, R. J. Preski, and E. D. Kalasky

GER-13830
7 June 1968

Prepared under Contract No. NAS1-6436 by
Goodyear Aerospace Corporation
Akron, Ohio

for

NATIONAL AERONAUTICS AND SPACE ADMINISTRATION

Langley Research Center
Langley Station, Hampton, Va.

THE MODIFICATION AND USE OF A GROUND-BASED PHOTOMETER FOR EVALUATION OF SATELLITE MATERIALS

By D. C. Romick, R. H. Emmons, R. J. Preski, and E. D. Kalasky
Goodyear Aerospace Corporation
Akron, Ohio

ABSTRACT

Goodyear Aerospace Corporation (GAC) has developed a cryogenically cooled multipurpose (photometric and polarimetric), five-color (U-B-V-R-I) photometric system and performed photometric observations on the Echo I, PAGEOS I, Echo II, and Explorer XIX satellites during four observation periods.

The new photometric-polarimetric system has been shown to be an accurate as well as a versatile instrument during the various observation periods.

Multicolor photometric and polarimetric observations indicate that the aluminized Mylar satellites, Echo I and PAGEOS I, degrade very slowly, if at all, in the space environment. Echo I, which has been in orbit for almost eight years, has shown little change in its optical properties until the last observation period. The slight diminishing in the reflectance and specularity obtained photometrically then may be correlated with the satellite's interaction with the earth's upper atmosphere. The PAGEOS I satellite has shown negligible change in its optical properties; the slight variations that have been indicated have not followed any consistent trend and are within the limits which might reasonably be expected from variations in atmospheric conditions and other factors involved. Multicolor photometric and polarimetric observations of the Echo II satellite performed thus far have shown considerable variation from laboratory measured values for Alodine in air; however the meaning of this is not yet clear. Additional data taken during the next observation period should go far toward resolving the questions raised by Echo II concerning its true rate of degradation in the space environment. V-band observations performed on the Explorer XIX satellite indicate that the present optical and physical properties are close to prelaunch design values. The information contained in the Explorer XIX observational data on spin rate and other characteristics strongly attest to the potential capability of this method of measurement of orbiting satellite characteristics.

CONTENTS

	Page
SUMMARY	1
INTRODUCTION	2
SYMBOLS	3
THEORY	5
Photometry	5
Polarimetry	10
DEVELOPMENT OF EXTENDED RANGE (U-B-V-R-I) INSTRUMENTATION SYSTEM	11
General	11
Objectives	12
Concept Development	12
Preliminary Design	17
Design Phase	17
Fabrication	43
Checkout and Acceptance Testing	44
Operation and Maintenance Manual	64
SATELLITE PHOTOMETRIC/POLARIMETRIC MEASUREMENTS	69
Field Preparation	69
Satellite Predictions and Orbital Geometry	71
Observation Procedure	71
Field Operations	73
Data Reduction and Analysis	74
Discussion of Results	77
Accuracy of Results	101
CONCLUSIONS AND RECOMMENDATIONS	106
Conclusions	106
Recommendations	107
REFERENCES	108

ILLUSTRATIONS

Figure		Page
1	Schematic diagram of photometric and polarimetric configurations	14
2	Response curves for achromatic half-wave plate	16
3	Normalized response functions for the UBVRI spectral regions	18
4	Photomultiplier and cryogenic housing	20

ILLUSTRATIONS (Continued)

Figure		Page
5	Cryogenic system installation	21
6	Insulated feed line routing of the cryogenic system	23
7	Under temperature alarm and cryogenic schematic diagram	25
8	Curbside wall of forward compartment	27
9	Five-color photometer head - Right Side	28
10	Streetside wall of forward compartment	29
11	Five-color photometer head - Left Side	30
12	Schematic diagram of mirrors and beam splitters	34
13	Cryogenic system and emergency shut down valves	37
14	Photometer control assembly	39
15	Logic boards in rear of photometer control assembly	40
16	Legend for monitor panel meter readings	41
17	Electronic unit - Exterior View	45
18	Electronic unit - Interior view, nearing completion	46
19	Photometer control assembly, nearing completion	47
20	Power unit assembly	48
21	New five-color instrumentation - Telescope Installation	49
22	Pair of logic boards	53
23	Photometric intensity values in UBVRI	61
24	Comparison of integrated and non-integrated polarimetric signal for Arcturus	62
25	Polarimetric signature of Arcturus with polaroid parallel to the declination axis	63
26	Photometric signature of the PAGEOS rocket body	65
27	Photometric signature of Explorer XIX	66
28	Photometric signature of an Agena rocket body	67

ILLUSTRATIONS (Continued)

Figure		Page
29	Photometric signature of the star Sidus Ludoviciana	68
30	Block diagram of computer data flow	76
31	Primary extinction coefficients	79
32	Specularity of Echo I from Autumn 1967 observations	84
33	Specularity of PAGEOS I from 6 March 1967 observations (V_{20}-band)	87
34	Effect of time in orbit on specularity	88
35	Effect of time in orbit on surface reflectance	89
36	Satellite polarization measurements - U band	95
37	Satellite polarization measurements - B band	96
38	Satellite polarization measurements - V band	97
39	Satellite polarization measurements - R band	98
40	Satellite polarization measurements - I band	99
41	Echo II polarization measurements - V band	100

TABLES

Table		Page
I	Five-color (U-B-V-R-I) Photomultiplier System Characteristics	32
II	Amplifier Gains	51
III	Observing Sites	70
IV	Second Order Extinction Coefficients	78
V	Scale Factors Obtained from Observations	78
VI	Construction and Orbit Parameters of Observed Satellites	81
VII	Optical and Physical Parameters of Echo I	83
VIII	Optical and Physical Parameters of PAGEOS I	85

TABLES (Continued)

Table		Page
IX	Optical and Physical Parameters of Echo II	91
X	Optical and Physical Parameters of Explorer XIX	92
XI	Polarimetric Observations	94
XII	Accuracy of Standard Star Observations at Palomar	101
XIII	Accuracy of Standard Star Observations at Yuma	102
XIV	Probable Error of Echo I Results	103
XV	Probable Error of PAGEOS I Results	103
XVI	Probable Error of Echo II Results	104
XVII	Probable Error of Explorer XIX Results	104
XVIII	Average Values of Probable Error of Percent Polarization	106

THE MODIFICATION AND USE OF A GROUND-BASED PHOTOMETER FOR EVALUATION OF SATELLITE MATERIALS

By D. C. Romick, R. H Emmons, R. J. Preski, and E. D. Kalasky
Goodyear Aerospace Corporation

SUMMARY

During the present contract period, Goodyear Aerospace Corporation (GAC) developed a cryogenically cooled multipurpose (photometric and polarimetric), five-color (U-B-V-R-I) photometric system and performed photometric observations on the Echo I, PAGEOS I, Echo II, and Explorer XIX satellites during four observation periods.

The new photometric-polarimetric system has been shown to be an accurate as well as a versatile instrument during the various observation periods.

The four series of observations performed under the present contract, using the NASA Mobile Satellite Photometric Observatory and the two photometric heads, (U-B-V and U-B-V-R-I) are as follows:

(1) Summer, 1966, at Palomar Mt., California; U-B-V photometric observations on Echo I

(2) Winter, 1967, at Phoenix and Yuma, Arizona; U-B-V-R-I photometric and polarimetric observations on Echo I, PAGEOS I, and Echo II

(3) Summer, 1967, at Akron, Ohio; U-B-V photometric observations on Echo I, PAGEOS I, Echo II, and Explorer XIX

(4) Autumn, 1967, at Akron, Ohio; U-B-V-R-I photometric observations on Echo I, PAGEOS I, and Echo II

Multicolor photometric and polarimetric observations indicate that the aluminized Mylar satellites, Echo I and PAGEOS I, degrade very slowly, if at all, in the space environment. Echo I, which has been in orbit for almost eight years, has shown little change in its optical properties until the last observation period. The slight diminishing in the reflectance and specularity obtained photometrically then may be correlated with the satellite's interaction with the earth's upper atmosphere. The PAGEOS I satellite has shown negligible change in its optical properties; the slight variations that have been indicated have not followed any consistent trend and are within the limits which might reasonably be expected from variations in atmospheric conditions and other factors involved. Multicolor photometric and polarimetric observations of the Echo II satellite performed thus far have shown considerable variation from laboratory measured values for Alodine in air; however the meaning of this is not yet clear. Additional data taken during the next observation period should go far toward resolving the questions raised by Echo II concerning its true rate of degradation in the space environment. V-band observations performed on the Explorer XIX satellite indicate that the present optical and physical properties are close to prelaunch design values. The information contained in the Explorer XIX observational data on spin rate and other characteristics strongly attest to the potential capability of this method of measurement of orbiting satellite characteristics.

INTRODUCTION

During the period from 1 July 1966 to 14 June 1968, GAC has been under contract to the NASA Langley Research Center (Contract NAS 1-6436) for modification and use of a ground-based photometric system for evaluation of satellite materials in orbit. This contract was preceded by other contracts beginning in 1964. The first effort, covered under NAS 1-3114, Amendment 5, made use of a visual comparison photometer and a separate photoelectric photometer on a 3-inch telescope to determine the specularity of the Echo I satellite (Reference 1).

The second contract (NAS 1-4669) was a 6-month program definition study for evaluating satellite materials by ground-based photometry. This study was followed by the development and fabrication of a 24-inch mobile photometric observatory for NASA (Contract NAS 1-5580, Reference 2). The initial photometric instrumentation was limited to the U, B, and V spectral bands. That system was later used for the photometric surveillance of the Passive Geodetic Satellite (PAGEOS) under Contract NAS 1-6189 (Reference 3).

The objectives of the present effort, as set forth in the work statement for Contract NAS 1-6436 are to:

(1) Extend the capability of the photoelectric photometer (constructed under Contract NAS 1-5580), from a single channel U-B-V device to a four channel U-B-V-R-I device

(2) Determine for the PAGEOS I, Echo I, Echo II, and Explorer XIX satellites by use of photoelectric photometry

   (a) Satellite stellar magnitude, solar reflectivity, and specular component of reflected light as a function of wavelength

   (b) Satellite diameter and local variations in radius of curvature

(3) Determine and compare the degree of polarization of the reflected solar radiation from the Echo II satellite with that from PAGEOS and Echo I

This final report summarizes the work performed, the results from the satellite observations, and the general conclusions to be drawn from this effort. Other items delivered as a part of this contract are:

(1) Drawings and microfilm copies of drawings of the new mobile photometric observatory equipment

(2) A revised Operations and Maintenance Manual for the mobile photometric observatory

(3) Copies of nine computer programs used for satellite predictions and data reduction and analysis

(4) A computer program users manual for the nine computer programs listed in Item (3) above

The computer program manual is submitted as a separate report.

SYMBOLS

Å	angstrom unit, 10^{-10} meters
A_{sp}	weighting coefficient for specular reflection
A_3	constant
antilog	antilogarithm operator: the number corresponding to the base 10 logarithm term which follows
B	blue band-pass filter stellar magnitude, standard system*
B_d	weighting coefficient for diffuse reflection
B-V	B-V standard system color index, stellar magnitudes*
b	blue band-pass filter stellar magnitude, natural system
b-v	b-v natural system color index, stellar magnitudes
D	slant range, distance from satellite to observer, feet
d	galvanometer deflection, inches (target + sky + dark) - (sky + dark)
E_d	diffuse component of illuminance
E_s	solar illuminance on the satellite
E_{sp}	specular component of illuminance
E_0	illuminance value at zero stellar magnitude
F	standard error of estimate
$f(\psi)$	Russell phase function
G_x	the function $(1 - k''_{u-b} X)$
H_x	the function $(1 - k''_{r-i} X)$
I_{max}	maximum light intensity component
I_{min}	minimum light intensity component
I_1	measured light intensity component
I_2	measured light intensity of perpendicular component
I_{2A}	adjusted I_2
J_x	the function $(1 - k''_{b-v} X)$
K_x	the function $(1 - k''_{v-r} X)$
k	constant
k'	primary atmospheric extinction coefficients
k''	second-order atmospheric extinction coefficients
M	mean value
m	stellar magnitude
P	degree of polarization
P_{mag}	polarization magnitude
$P_{\%}$	percent polarization
R	satellite radius, feet
R_c	radius of curvature, feet
R-I	R-I standard system color index, stellar magnitudes*
r-i	r-i natural system color index, stellar magnitudes

*Always extra-atmospheric; values for standard stars are obtainable from References 4, 5, and 6.

S	photometer gain, stellar magnitude units S = 2.5 $\log_{10}$ (photometer gain factor); also, specularity
U	ultraviolet band-pass filter stellar magnitude, standard system*
U-B	U-B standard system color index, stellar magnitudes*
u	ultraviolet band-pass filter stellar magnitude, natural system
u-b	u-b natural system color index, stellar magnitudes
V	visual band-pass filter stellar magnitude, standard system*
V-R	V-R standard system color index, stellar magnitudes*
v	visual band-pass filter stellar magnitude, natural system
v-r	v-r natural system color index, stellar magnitudes
X	atmospheric thickness, ($\cong$ secant z)
Z_1, Z_2, Z_3	coefficients in quadratic equation
z	angular distance from zenith
α	geocentric angle between earth-sun and earth-satellite vectors, radians
β	relative angle of the instrument head or half-wave plate
γ	reflectance, the ratio of the rate of reflection of radiant energy to its rate of incidence
ϵ	system transformation scale factor, V_{20} determination
ζ	calibration zero-point term, stellar magnitude units
η	apparent position angle of plane polarized light measured relative to the telescope
μ	system transformation scale factor, B-V determination; also, true parameter; also, micron unit (10^{-6} meters)
π	the constant 3.14159
ρ	system transformation scale factor, V_1 determination
σ	system transformation scale factor, V-R determination
τ	system transformation scale factor R-I determination
ψ	system transformation scale factor, U-B determination; also, phase angle between satellite-sun vector and satellite-observer vector, radians

Subscripts

B	denotes blue band data, standard system
b	denotes blue band data, natural system
b-v	denotes b-v color index data
d	denotes diffuse values
f	denotes a function
I	denotes infrared band data, standard system
i	denotes infrared band data, natural system
m	denotes stellar magnitudes

*Always extra-atmospheric; values for standard stars are obtainable from References 4, 5, and 6.

o	denotes extra-atmosphere value (i.e., extrapolated to X = 0)	t	denotes true value
⊙	denotes solar magnitude	U	denotes ultraviolet band data, standard system
R	denotes red band data, standard system	u	denotes ultraviolet band data, natural system
R_c	denotes radius of curvature	u-b	denotes u-b color index data
r	denotes red band data, natural system	V	denotes visual band data, standard system
r-i	denotes r-i color index data	v	denotes visual band data, natural system
S	denotes specularity value	v-r	denotes v-r color index data
s	denotes solar value	1, 20	denotes S-1, S-20 photocathode respectively when used with V or v bands
sp	denotes specular value		

Note: a bar above a symbol denotes mean value

THEORY

Photometry

The use of multicolor photometry to obtain high accuracy observations of stars, planets, nebulae, etc., has expanded rapidly in the past decade. Basically the same techniques which have been developed for stellar photometry have been incorporated into satellite photometry. These include use of

(1) The "standard system"; i.e., response functions (similar photomultipliers, filters, etc.), method of data reduction; i.e., transformation to the standard system, use of standard stars, etc., as described in References 5 and 6;

(2) good-to-excellent observation sites correlated to the season of the year;

(3) high speed computers to reduce the data;

(4) aids such as plots, tables, etc., in order to obtain the most accurate set of calibration coefficients from a series of stellar observations;

(5) independent observations of standard stars to determine the accuracy of the telescope-photometer system.

The method of stellar calibration has been described in detail for the U-B-V spectral regions in References 3 and 7 and will only be discussed briefly here. The theory was expanded to include the V-R-I bands during the present contract and measurements were made in these bands during the observation periods reported herein. The theory utilized for obtaining satellite optical and physical properties is presented in subsequent sections.

Stellar calibration. - The method of stellar calibration includes three separate types of observations of standard stars in the various spectral regions and uses six separate computer programs to reduce the data. The equations and description of techniques used to obtain the transformation and calibration parameters are basically the same as given by Hardie (Reference 7). The three calibration programs provide the following parameters:

(1) Second order Extinction Coefficients

$k''_{b-v_{20}}$, k''_{u-b}, k''_{v_1-r}, k''_{r-i}

(2) Transformation Scale Factors

ϵ, μ, ψ, ρ, σ, τ

(3) Primary Extinction Coefficients and Zero-Point Terms

$k'_{v_{20}}$, $k'_{b-v_{20}}$, k'_{u-b}, k'_{v_1}, k'_{v_1-r}, k'_{r-i}; $\zeta_{v_{20}}$, $\zeta_{b-v_{20}}$, ζ_{u-b}, ζ_{v_1}, ζ_{v_1-r}, ζ_{r-i}.

Satellite photometry. -

General: From careful observations of the intensity of sunlight reflected from a spherical artificial satellite, various inferences can be drawn concerning the present condition of its surface. For instance, the extent to which an initially specular reflecting surface has been degraded can be determined, as well as values of the mean and local effective radii of curvature of the satellite. In general, the following parameters may be obtained through the use of a ground-based photometric system: (1) stellar magnitude (normalized); (2) specularity and diffusivity of the surface of a satellite; (3) mean and local radii of curvature; and (4) reflectance, if radius of curvature is assumed. In this report the specular component of reflected light is called specularity. It is expressed as a percentage of the total reflected light.

Stellar magnitudes: Having previously determined the 22 extinction-calibration-transformation constants from the various stars used in the calibration programs, the extra-atmospheric stellar magnitudes of the various satellites may be determined. Equations (1) through (6) reduce the satellite photometric observations from their raw data galvanometer deflections and the separately determined zenith distances to the standard system U-B-V-R-I magnitudes and color indices.

$$V_{20} = \left[S_{v_{20}} - 2.5 \log \left(d_{v_{20}}\right)\right] - k'_{v_{20}} X + \epsilon(B-V_{20}) + \zeta_{v_{20}} \tag{1}$$

$$B-V_{20} = \mu J_x \left[\left(S_b - S_{v_{20}}\right) - 2.5 \log \frac{d_b}{d_{v_{20}}}\right] - \mu k'_{b-v_{20}} X + \zeta_{b-v_{20}} \tag{2}$$

$$U-B = \psi G_x \left[(S_u - S_b) - 2.5 \log \left(\frac{d_u}{d_b}\right)\right] - \psi k'_{u-b} X + \zeta_{u-b} \tag{3}$$

$$V_1 = \left[S_{v_1} - 2.5 \log \left(d_{v_1}\right)\right] - k'_{v_1} X + \rho(V_1 - R) + \zeta_{v_1} \tag{4}$$

$$V_1 - R = \sigma K_x \left[\left(S_{v_1} - S_r \right) - 2.5 \log \left(\frac{d_{v_1}}{d_r} \right) \right] - \sigma k'_{v_1} X + \zeta_{v_1} - r \tag{5}$$

$$R\text{-}I = \tau H_x \left[(S_r - S_i) - 2.5 \log \left(\frac{d_r}{d_i} \right) \right] - \tau k'_{r\text{-}i} X + \zeta_{r\text{-}i} \tag{6}$$

The terms are defined in the list of symbols.

This particular operation computes not only the stellar magnitude and phase angle of the satellite but also prints out such coordinates as slant range, height, altitude, azimuth, right ascension, declination, etc. for each time. In addition, the computer incorporates such correction factors as normalization of each observed intensity to a uniform slant range; e.g., 2640 statute miles for PAGEOS I, 1000 statute miles for Echo I and II, and allowance for the contribution of earth albedo.

Normalized slant range: Normalization of the photometric data to a uniform range is accomplished by applying the inverse square law of illumination to the illuminances, first having determined the satellite's slant range at observation time. Satellite photometric data must be normalized for the instantaneous slant range from the observer before a meaningful analysis can be made. The instantaneous slant range is computed for the times at which photometric data was taken from an accurate ephemeris of the satellite. It should be noted that a one-percent error in slant range will propagate an error of 0.02 in the normalized stellar magnitude.

Contribution of earth albedo: The correction for the contribution of the earth's albedo (earthshine) for a specular spherical satellite is a function of the satellite's orbital height and geocentric angle α (elongation) from the sun. The adjusted increment must then be applied as a correction to the reduced stellar magnitude of a near-specular spherical satellite before proceeding to determinations of effective radii of curvature and reflectance, and to the degree of specularity of the surface.

Satellite stellar magnitude at various effective wave lengths: The satellite stellar magnitudes may be determined in the U or near-ultraviolet band (3600 Å), B or blue band (4400 Å), V or visual band (5500 Å), R or red band (7000 Å), and I or near-infrared band (9000 Å). The specular illuminance (E_{sp}) of the radiation received in the U, B, V, R, or I spectral regions (depending on which spectral region is switched in at a given time) is given by:

$$\frac{E_{sp}}{E_0} = \text{antilog}\,(-0.4\, m_{sp}) = \frac{1}{4} \frac{E_s}{E_0} \left(\frac{R}{D} \right)^2 \tag{7}$$

Using this equation, the extra-atmospheric stellar magnitude, m_{sp}, for the specular component of a satellite can be determined. The stellar magnitudes for the diffuse spherical satellite are given by:

$$\frac{E_d}{E_0} = \text{antilog}\,(-0.4\, m_d) = \frac{2}{3} \frac{E_s}{E_0} \left(\frac{R}{D} \right)^2 f(\psi) \tag{8}$$

where

$$f(\psi) = \frac{1}{\pi} \left[\sin \psi + (\pi - \psi) \cos \psi \right] .$$

Determination of specular component of light reflected from a sphere's surface: The specular spherical satellite has a convex mirror surface that provides a small image reflection of the sun, equal in brightness regardless of the viewing angle. Conversely, a diffuse sphere in sunlight exhibits phases like the moon or Venus. The integrated light from the diffuse sphere is a function of the phase angle ψ, which is the angle formed at the satellite between lines to the sun and the observer. The phase angle is zero when the phase is full. The illuminance of the diffuse sphere increases as the phase angle decreases to the limit at the eclipse.

To determine the specularity of a satellite, photometric measurements are made over a wide range of phase angles. For moderate orbit inclinations these phase angles can be measured during single passes, when the satellite orbit has reached approximately the coplanar condition. For a polar-orbiting satellite, the range in phase angle during a single pass is limited, requiring the combination of carefully calibrated data from various passes to achieve the desired span of phase range.

The essential background and theory for the specularity determination is shown in Equations (7) and (8) (from R. Tousey, References 8 and 9). These equations make possible the prediction of the extra-atmospheric stellar magnitudes, m, of specular and diffuse spherical satellites. The Russell phase function, $f(\psi)$, (Reference 10) gives the dependence of illuminance upon phase angle for a perfectly diffuse sphere that obeys Lambert's cosine law of reflection. (This law states that the reflection from a small area is proportional to the cosine of the angle between the normal and the direction to the observer.) These equations provide for photometric discrimination between specular and diffuse spherical reflecting surfaces. How closely the photometric data conforms to one or the other must be determined.

Equation (9) (from Reference 11) is the regression equation that permits this determination, where A_{sp} and B_d are the weighting factors for the specular and diffuse components, respectively, of the reflected light. They are determined by a least-squares best fit to the normalized photometric data. Finally, Equation (10) (also from Reference 11) provides the fractional specularity.

The regression equation for determining specularity is:

$$\text{antilog } (-0.4\ m) = \frac{1}{4} A_{sp} + \frac{2}{3} B_d f(\psi) \tag{9}$$

$$\text{specularity, } S = \frac{A_{sp}}{A_{sp} + B_d} \tag{10}$$

where $$f(\psi) = \frac{1}{\pi} \sin \psi + (\pi - \psi) \cos \psi \quad .$$

Before the analysis can proceed, the photometric data must be carefully calibrated and normalized. Observations of nonvariable stars of known illuminance are generally performed both before and after the satellite pass. The photometric data is then processed and the atmospheric extinction coefficients are determined. Simultaneously with the tracking of the satellite, the following information is time-correlated with the photometric data:

(1) Elevation (atmospheric thickness)

(2) Slant range

(3) Earthshine (effect of earth albedo)

(4) Phase angle

The calibrated photometric data is then processed for extra-atmospheric illuminance, normalized to zero earthshine and to a uniform slant range by the inverse square law. A least-squares solution of the linear regression Equation (9) yields best-fit values for the intercept A_{sp} and the slope B_d, which are then employed in Equation (10) to determine specularity.

Mean and local radii of curvature: While the satellite's specularity is a microtexture characteristic, the mean and local radii of curvature of a nearly spherical satellite describe its size and macrotexture.

Having previously determined the diffuse-reflecting weighting coefficient, B_d, it is possible to remove from the normalized magnitudes the contribution of diffuse reflection in each, $-2.5 \log 2/3\, B_d f(\psi)$, to obtain purely specular magnitudes, m_{sp}. If a reasonable or previously measured value for the reflectance, γ, is adopted, the radius of curvature can next be determined in any optical band from the relation:

$$R_c \text{ (ft)} = \text{antilog}\left(\frac{m_\odot - m_{sp}}{5} - 0.5 \log S\gamma + \log D + 0.30103\right) \tag{11}$$

where $m_\odot$ is the U, B, V, R, or I magnitude of the sun for the date; D is the slant range in feet; R_c is the radius of curvature in feet; m_{sp} is the extra-atmospheric stellar magnitude contributed solely by the specular components of sunlight reflected from the satellite; and γ is the total reflectance. Since the observed illuminances depend on both γ and R_c in Equation (11), one may be obtained only if the other is known.

From Equation (11) the mean radius of curvature may be obtained from a large number of observations of the local radii of curvature. The range and variability of the local radius of curvature may be examined in light of the original design and available material for gross implications for a possible new mean radius of curvature.

Determination of reflectance if a radius of curvature is assumed: By solving Equation (11) for γ, one may obtain the reflectance for an assumed radius of curvature. The equation for this value is

$$\gamma = S^{-1} \text{ antilog}\left(\frac{m_\odot - m_{sp}}{2.5} - 2 \log R_c + 2 \log D + 0.60206\right) \tag{12}$$

As before, this refers to all five colors (U-B-V-R-I) when the values of m_{sp} are known.

The sun's visible radiation is constant in output to within one percent, but owing to the eccentricity of the earth's orbit, the sun's illuminance upon an earth satellite varies. For example, the sun's visual band stellar magnitude varies from -26.70 in early July to -26.78 in January. The corresponding distances are approximately 94.5×10^6 miles in July and 91.5×10^6 in January. These minor variations in magnitudes with the distance of the sun will be reflected in corresponding variations in the magnitudes for sunlit satellites, and for subsequent determinations of the satellite's effective radius of curvature, or U, B, V, R, or I reflectance, the instantaneous U, B, V, R, or I solar magnitude is required.

For each specularity determination a "figure of merit" is computed as:

$$\frac{\left\{\sum_{1}^{n}\left[\overline{f(\psi)} - f(\psi)\right]^2\right\}^{1/2}}{\sigma_{R_c}/\bar{R}_c}$$

This expression increases with the number of data points and the range of phase angles observed and decreases with increased target scintillation.

Polarimetry

The degree of polarization is defined as:

$$P = \left(\frac{I_{max} - I_{min}}{I_{max} + I_{min}}\right) . \tag{13}$$

The percent polarization is 100 P. The degree of polarization can be determined from the data reduction equation.

$$\frac{I_1 - I_{2A}}{I_1 + I_{2A}} = P \cos(2\eta - k\beta) + A_3 \tag{14}$$

where k = 2 for rotating instrument head (Wollaston prism)

k = 4 for rotating half-wave plate

The polarimetric data were corrected for systematic errors and reduced according to this equation which is developed in the computer program manual. The adjusted values of I_2 are determined by fitting a quadratic equation to the ratios of I_1/I_2 for each pre and post calibration nonpolarized star and by multiplying the polarized star and satellite values of I_2 by the quadratic equation determined from the weighted average values of quadratic coefficients. That is,

$$I_{2A} = I_2\left(Z_1 + Z_2\beta + Z_3\beta^2\right) \tag{15}$$

where Z_1, Z_2, Z_3 are the quadratic coefficients and β the various positions of the Wollaston prism or half-wave plate. This adjusted value of I_{2A} compensates for the factor dependence of the intensity for each position of the Wollaston prism or half-wave plate and the term A_3 compensates for any constant offset between photomultipliers.

The computed degree of polarization is converted to the polarization magnitude by the equation (Reference 12):

$$P_{mag} = 2.17 \tan h^{-1} P = 2.17 \tan h^{-1}\left(\frac{I_{max} - I_{min}}{I_{max} - I_{min}}\right) \quad \text{for } P < 1 \tag{16}$$

where P_{mag} is defined as

$$P_{mag} = 2.5 \log \left(\frac{I_{max}}{I_{min}} \right) . \quad (17)$$

The resulting polarization magnitude values for the polarized stars were compared with the published values in the Alfred Behr Catalog (Reference 12) and the percent-probable error of P was considered to be a measure of the accuracy of each value.

DEVELOPMENT OF EXTENDED RANGE (U-B-V-R-I) INSTRUMENTATION SYSTEM

General

One of the main tasks specified and carried out under this contract was the development and installation of a new extended range instrumentation capability in accordance with Section 3.3 of the contract work statement. The new system checkout and acceptance was carried out in accordance with Sections 4.1 and 4.2 of the work statement and an operation and maintenance manual was provided.

In general, the guidelines provided in the work statement proved sufficient to define the system, although subsequent meetings with the NASA project director and project office personnel during the conceptual design phase served to refine and more specifically direct the system concept toward its ultimate objectives. These provided a high data gathering capability, operating speed and flexibility for an increased level of compatibility with the characteristic requirements for satellite measurement inherent in the relatively short observation periods available during a typical pass.

In order to insure optimum design concepts, a careful period of combined preliminary configuration studies and consultations preceeded the establishment of the final design characteristics. Advice was enlisted from the leading astronomers engaged in photometric work. Dr. W A. Hiltner of Yerkes Observatory was retained as a consultant. In the final phase of concept formulation, Dr. Hiltner was brought to Akron to work with the GAC engineers involved. NASA project personnel also joined in these sessions. As a result, the concept developed proved to be remarkably sound. Very few changes of any kind were required during the design process and subsequent phases, and the formulated objectives were entirely fulfilled.

One conspicuous exception to lack of change required occurred in the case of the cooling system for the photomultipliers. While many portions of the original cryogenic system were satisfactory, and other parts were nearly so; nevertheless, there were several shortcomings which were sufficiently serious as to render the system unsatisfactory. Accordingly, a redesign of portions of the cryogenic system was undertaken and the modifications carried out subsequent to the first observation interval with the new system. The modified system was utilized for the subsequent observation intervals.

The entire new five-color, four-channel instrumentation system with the final cryogenic system has demonstrated full compliance with all objectives, high performance capability and operational flexibility, and displays smooth operating characteristics which signify the attributes of a truly sound high quality system.

Objectives

The system objectives that finally evolved from the initial concept development processes, and corresponding features incorporated in the design were as follows:

(1) A capability for very rapid data acquisition compatible with the short viewing times typically characteristic of satellites (a matter of minutes).

(2) A capability for working in a variety of optical color bands ranging well beyond both ends of the visible spectrum (from .3 to 1 μ).

(3) A sensitivity in all modes capable of working down to very faint satellites (8 to 10th magnitudes).

(4) An ability to handle high frequency scintillations giving very noisy signals by use of a variable signal integrating mode.

(5) A capability for making accurate polarimetric measurements (as well as plain photometric) with all the above listed attributes.

(6) A capability for continuous measurements in any two upper and lower region colors simultaneously.

(7) An ability to subtract out the sky background continuously.

(8) A versatility to use practically any combination of operating modes and to employ a wide variety of wide and narrow band filter combinations.

The system achieves a remarkable degree of versatility in providing all these features and capabilities. It does this by utilizing four photometric signal channels (each with its own photomultiplier) simultaneously, and an optical system which delivers the light gathered by the telescope to each channel in the proper manner corresponding to the various operating modes. Its operation is fully controlled and monitored from the operator's instrumentation control console in the forward compartment, where the separate photometric signals are also further processed, monitored, and recorded. The optical system can be set in the various operating configurations in a matter of seconds by means of external controls on the unit and in the instrument room. The manner in which these provisions are made and how they operate is described in detail in later sections. In addition, the cryogenic system which is necessary to satisfy the system requirements, along with associated optical path window heaters and other accessories are also discussed in later portions of this section.

Concept Development

The basic features of the system, including the use of paired channels, were a part of the initial concept and were specified in the contract work statement. These features included:

(1) Use of paired channels in each spectral region to separate sky background and polarization components.

(2) Use of filter wheels (or equivalent) to measure 3 or more color bands in each of these spectral regions.

(3) Use of 2 sets of these paired channels to permit coverage of 2 spectral regions with the U, B, and V bands in one and V, R, and I bands in the other. (This meant a total of 4 channels.)

(4) Utilization of this full 4 channel, 5 color U-B-V-R-I capability for either straight photometric measurement with sky background removed, or for polarimetric measurement.

(5) An electromagnetically shielded and thermally controlled environment to enhance performance of each of the 4 photomultipliers.

(6) An efficient optical system with protection from contamination, antidewing provisions, high transmissivity and/or reflectance, etc.

(7) Efficient sensor system with high quality photomultipliers and filters for each spectral measurement region.

(8) Efficient electronic signal processing system with suitable pre-amplifiers at the photomultiplier outputs.

(9) Stable power supplies and other elements as required to insure proper precision performance of the sensors and signal processing elements of the system.

(10) Effective monitoring and control provisions to promote flexibility and efficiency in operating the system so as to fully utilize its other capabilities.

(11) Adaptability for later incorporation of additional capabilities, such as extension to the 1 to 3 or 8 to 14 micron wavelength regions.

Most of the above features were incorporated into the early design concepts without difficulty, but some proved more challenging and resulted in concentration of effort toward arrangements that would:

(1) Minimize the light loss in the optics, primarily by reducing the required number of optical surfaces to a minimum.

(2) Provide a full, highly efficient polarimetric capability.

(3) Obtain maximum flexibility for various measurement modes, and maximum operational facility for quickly and easily converting from one mode to another.

The design concept for the system was strongly influenced by consideration of the most advanced high performance photometric instrumentation systems developed and used at leading astronomical observatories carrying out precision photometric and polarimetric work. Especially attractive, in terms of our objectives, were the features incorporated into the latest system developed by Dr. Hiltner of Yerkes Observatory, which incorporated clever effective means for noise cancellation in sensitive polarization measurement of stars.

These influences were instrumental in directing the concept toward the basic arrangement shown schematically in Figure 1. One of the main problems was that of deciding how best to provide efficient polarization component separation over the entire wavelength range of the system (0.31 to 1.0 μ, or beyond), while retaining the maximum operating facility for fast data-gathering. Latest advances in this area had led to employment of quarter-wave and half-wave plates for rotation of the polarization plane, but these characteristically operated

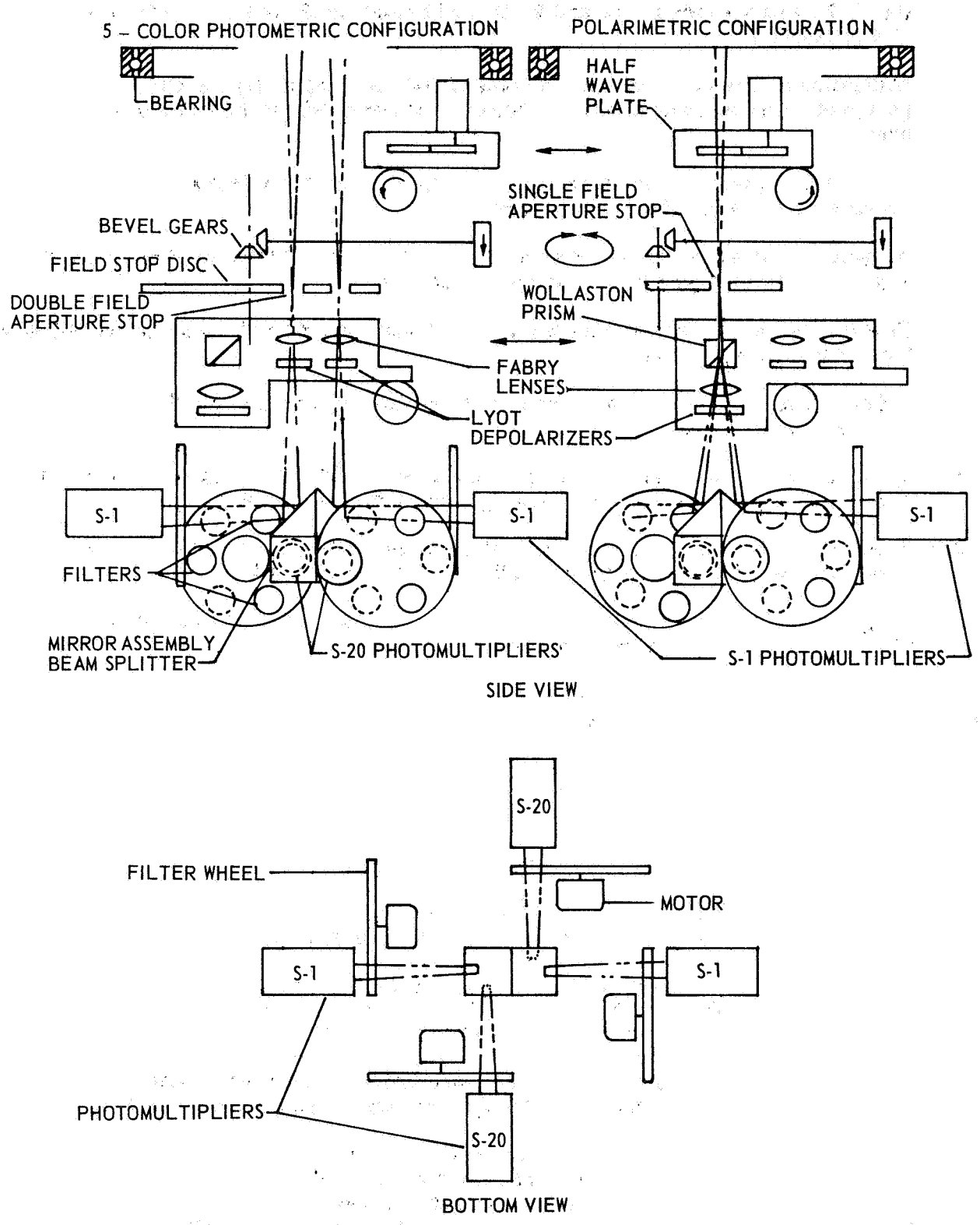

Figure 1. - Schematic diagram of photometric and polarimetric configurations

well only over a relatively narrow wavelength band. However, Yerkes Observatory had located and received an achromatic type of half-wave plate from Halle-Nachte of Berlin (Germany). Measurements of the NASA plate were made at GAC and, as shown in Figure 2, demonstrated an unusually wide bandwidth for a half-wave plate; covering the V and B and a good portion of the U-band with a reasonable degree of uniformity which should therefore not degrade polarimetric accuracy.

An alternate way of accomplishing this would be to provide for rotation of the entire instrumentation head (the prism, beam splitters, filters, sensors and all) with respect to the telescope and the incoming light. This would require either manual rotation of the head during operation, or motorizing the rotation of the head during operation, but would be uniformly effective over all wavelengths the system would handle. This would therefore take care of the V, R, and I bands, the full U-band, and any other band that might later be utilized. Another way to handle the V, R, and I band would be to obtain additional achromatic half wave plates covering these regions (which Halle-Nachte advised they could supply), and provide a means for interchanging them.

Since this latter requirement proved somewhat cumbersome, and since we were unable to immediately evaluate V-R-I half-wave plates (since none had yet been furnished to American customers), and to provide maximum overall flexibility and versatility it was decided to incorporate provisions for both a rotating half-wave plate and a manually rotatable total head that could later be motorized if desired. Both the half-wave plate and the rotating head would incorporate position control and signal pickup provisions for monitoring and recording in the instrument room.

The following items were required to obtain maximum performance and sensitivity from the optics:

(1) An efficient photomultiplier cathode with the light uniformly focused over a fair sized area

(2) A cooled cathode, with effective thermally isolating, nondewing window

(3) A highly efficient optical train leading to the window

Some of these factors were handled by proper attention during the preliminary design phase, but the optical efficiency was a main factor during the conceptual design phase. The concept finally derived ensured maximum optical performance by providing means, when operating at maximum sensitivity, for directing all the light to either photometer pair (U-B-V or V-R-I) sequentially, and the total number of optical surfaces was reduced from an original 13, with a 65 percent transmission loss to 6 with a transmission loss of only 36 percent. Alternatively when maximum sensitivity is not required, the light can be split and directed into all four photomultipliers simultaneously for maximum data gathering speed capability. Thus, the operator can select the mode and performance capability required to fit the circumstances of any particular mission measurement.

Also during the conceptual phase, it was decided to incorporate provisions in the electronic signal processing system to include both differencing amplifiers for subtracting out sky background and much of the sky noise as well as integrating amplifiers. The integrating amplifiers (with variable intervals) would further reduce the effect of noise and should greatly enhance data reduction, digitizing, or automation. The differencing amplifiers could also be used on the orthogonal polarization components.

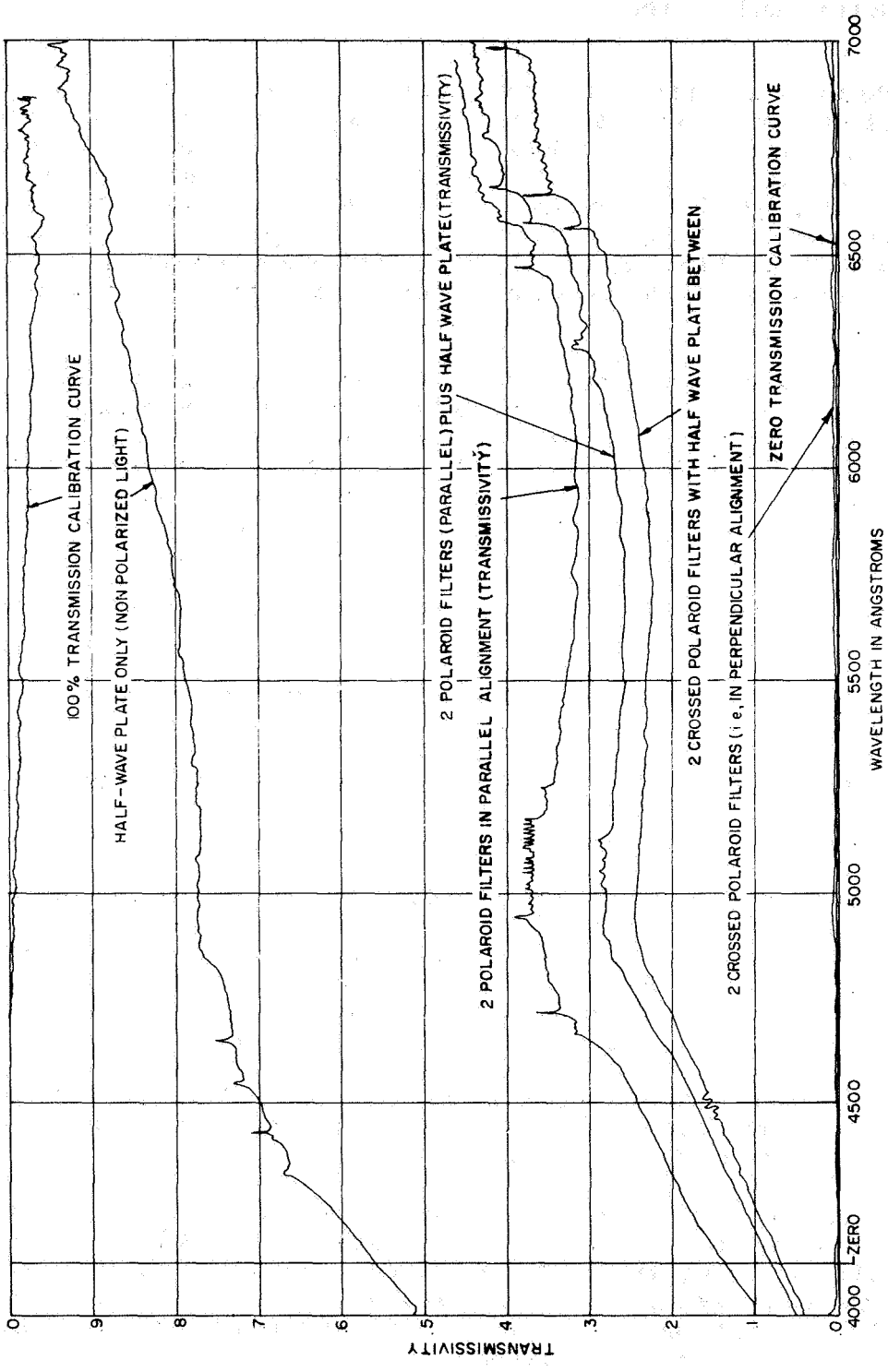

Figure 2. - Response curves for achromatic half-wave plate

Preliminary Design

Based on the design concept established, preliminary design of the system was undertaken with the accomplishment of the following:

(1) Photomultipliers were selected.

(2) Physical arrangement was established.

(3) Dewars and cooling system concept and elements were established and selected.

(4) Optical elements were selected.

(5) Filter criteria were finalized.

(6) Electronic system criteria and functional block diagrams were established.

(7) Equipment configuration and installation concept in instrument room was established.

(8) Installation interface concept for telescope mounted instrumentation equipment elements of the system was established.

(9) Electronic and electrical interface and interconnection cabling concept was established.

(10) Power supply and other observatory interface requirements were derived.

This required the completion of the layout drawings, functional diagrams, preliminary performance analyses, and equipment listing and criteria which formed the basis for the design and fabrication phases.

A primary goal during this preliminary design phase was to provide as much operational flexibility for the system as was possible. Ways and means were worked out for changing from the photometric to the polarimetric configuration in a few seconds by manual settings that could be made without opening the unit and which could easily be done in the dark. Provisions were devised for remote controlling and monitoring, from the instrument room console, the beam splitter, synchronized filter insertions, half-wave plate rotation, preamplifier and differencing amplifier gain settings, and photomultiplier temperature.

Much of the operational flexibility finally achieved for the system was incorporated during this phase.

Design Phase

After the preliminary design of the complete system was established, the detail design and analysis and equipment specifications establishment was carried out. The former was necessary as a means for getting drawings to the shop for fabrication and the latter to initiate procurement of purchased materials, parts, and equipment.

To establish the filters, an analysis was carried out to determine filter characteristics which would provide overall system response as shown in Figure 3. This afforded a basis for filter specification. The response functions presented in Figure 3 were developed by H. L. Johnson et al (Reference 13), for the U, B, V, R, I photometric system.

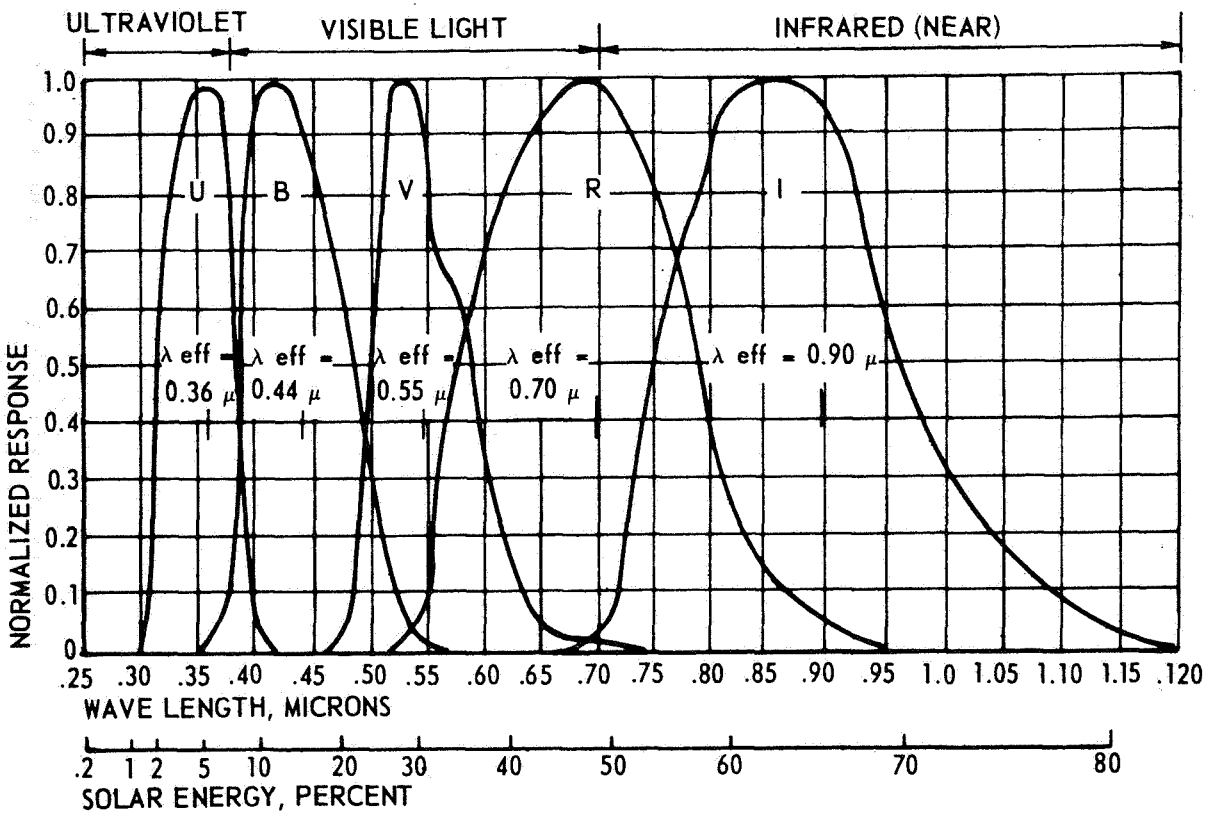

Figure 3. - Normalized response functions for the UBVRI spectral regions

The optical system design and analysis permitted definition and specification for the half-wave plate size, Wollaston prism, Fabry lenses, filter sizes, depolarizers, beam-splitter mirrors, eye pieces, etc.

The design of the photomultiplier cathode cooling system was based on the previously selected dewars as developed and furnished by Electro Optical Associates for the selected EMI photomultipliers. These did not prove adequate however, and later had to be extensively revised.

The reason for the deficiency of the original cooling system is traceable to the assumption that the units offered by the Dewar manufacturer, Electro Optic Associates, for the EMI 9558QA and 9684A photomultipliers, would cool them satisfactorily to their optimum operating temperature, and that this represented state-of-the-art photomultiplier usage. It was discovered, however, that this was not the case, and to achieve the performance potential of which these photomultipliers were capable was beyond the then-existing state of the art. This meant that additional development was necessary to provide a satisfactory operating environment for the photomultiplier which would permit them to operate in the manner intended. (Electronic voltage divider breakdown, tube breakage, and other deficiencies were also encountered.)

Accordingly, the photomultipliers were tested in the GAC cryogenics laboratory and various systems devised and evaluated until safe, satisfactory operation was obtained. It was found that for proper performance the EMI 9684A with the S-1 (V-R-I) photocathode should be operated at 155 $^{\circ}$K (-180 $^{\circ}$F), where the dark current output was approximately 10^{-12} amp. The EMI 9558QA with the S-20 (U-B-V) photocathode operated best at 227 $^{\circ}$K (-50 $^{\circ}$F), where the corresponding dark current was around 10^{-10} amp. Eventually a satisfactory dewar housing, window heater, and associated components were developed and tested which operated properly, held stable temperatures, and avoiding icing or dewing problems. This formed the basis for the final design (see Figure 4).

In addition, a new cryogenic regulating system was designed to match the new dewar design and duplicate its laboratory performance, and provide adequate safeguards for all parts of the system (see Figure 5). An under-temperature alarm and emergency shut-down system was also designed to provide more complete safety against any cryogenic malfunction (see Figures 6 and 7). Fail-safe principles were employed.

The installation design was developed in such a manner as to retain full interchangeability with the original 3-color single-channel instrumentation (which does not require cooling). This included interchangeability of the telescope-mounted units and interconnecting cabling provisions to the instrument room equipment. The instrument room equipment for both systems is permanently installed, including the photometers, monitoring and control consoles, power supplies, etc. (see Figure 8). Thus, to change from the 3-color to 5-color system, it is only necessary to change the equipment mounted on the back of the telescope and make associated connections (electrical, cryogenic - see Figure 9). The units not being used can be carried on the observatory as spare backup equipment, or stored. Added storage space is available on the left-hand side of the forward compartment (see Figure 10).

Connections at the telescope use the same electrical panel on the upper left side of the telescope mirror cell support (see Figure 11), and reconnection in the instrument room are made at the terminal panels inside the lower racks.

The 5-color, 4-channel instrumentation head, mounted on the back of the telescope, is thus located at the Cassegrain focus of the main 24-inch telescope such that the light path is as shown in Figure 1. The six position (three are used at present) filter wheels are advanced

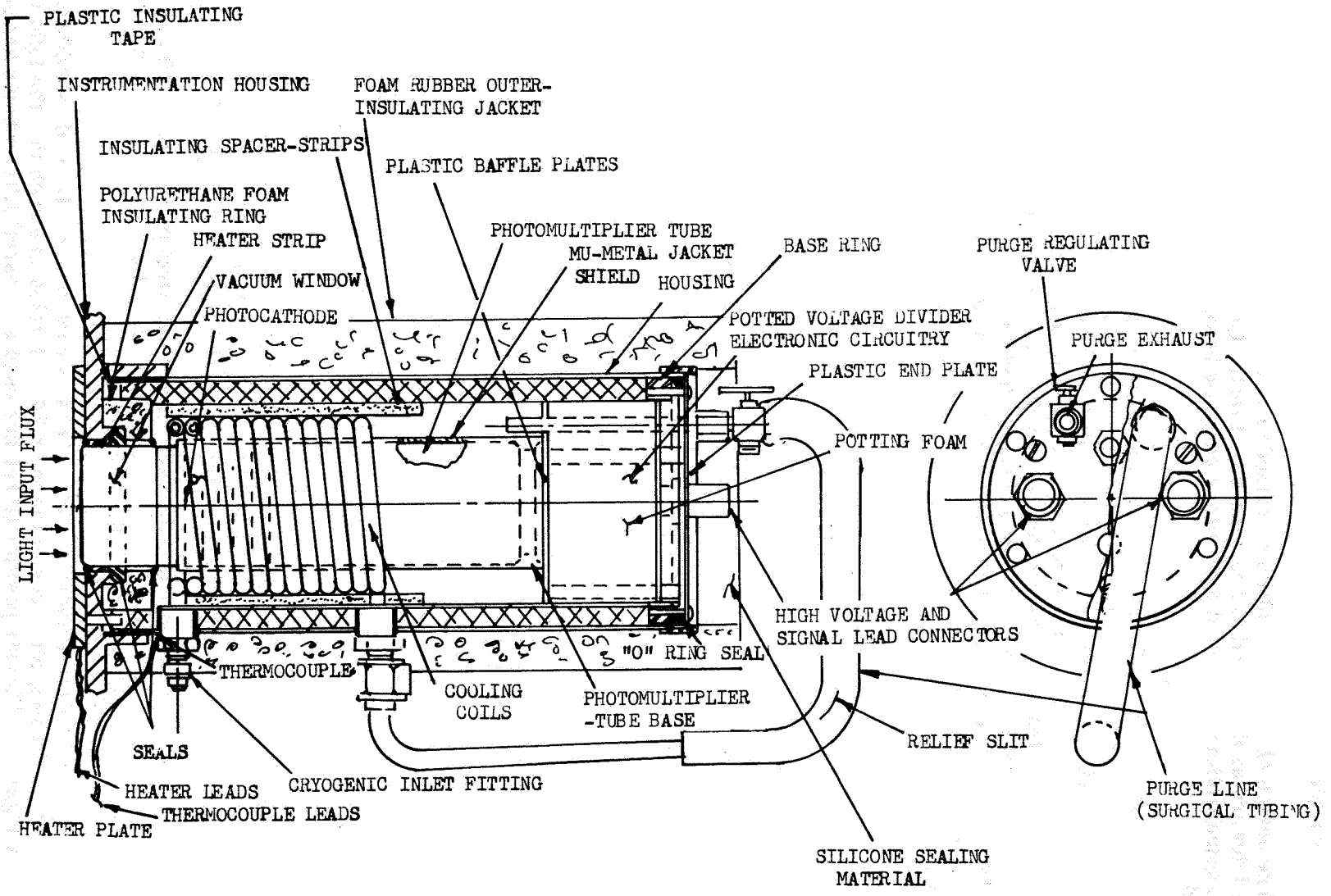

Figure 4. - Photomultiplier and cryogenic housing

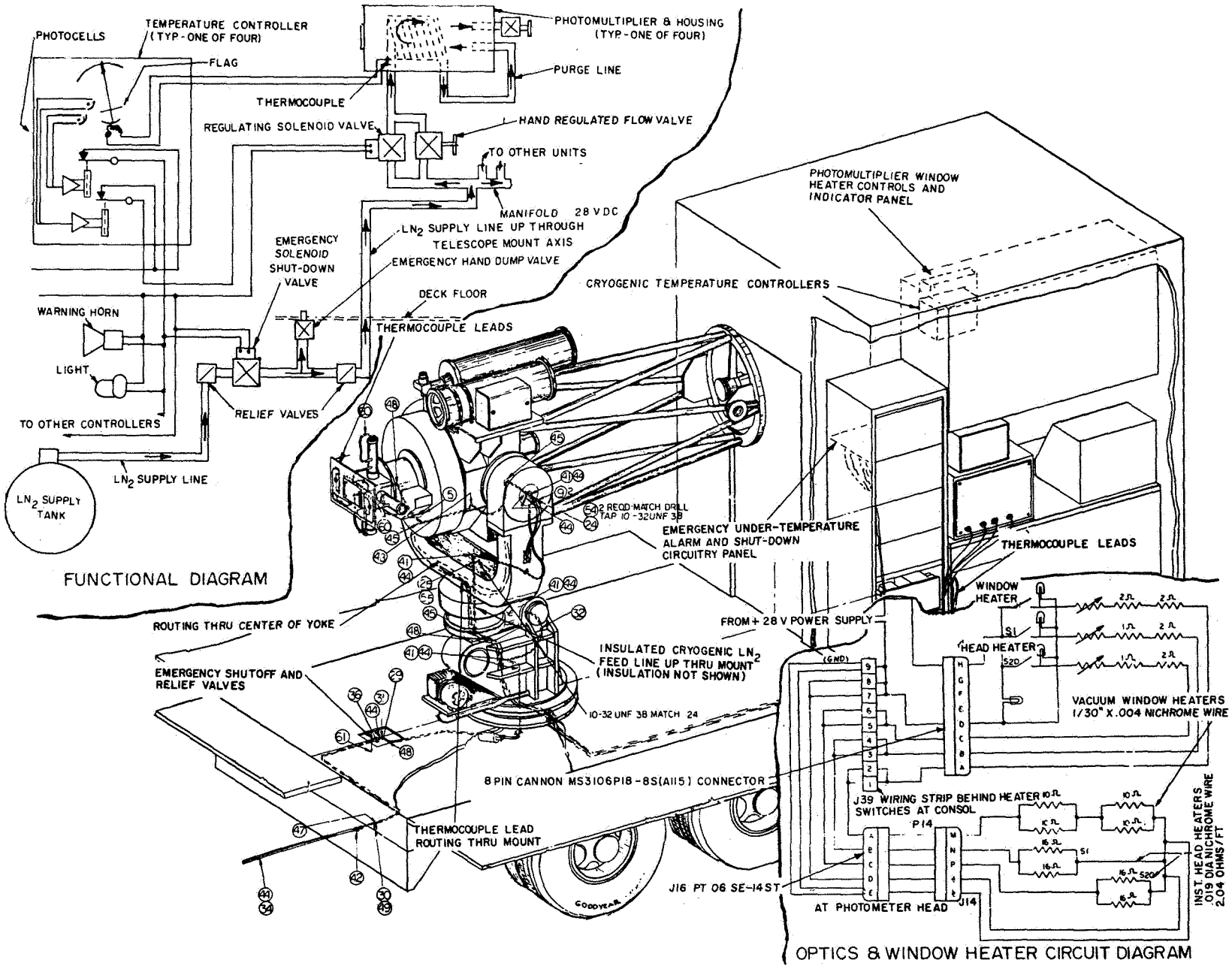

Figure 5. Cryogenic system installation

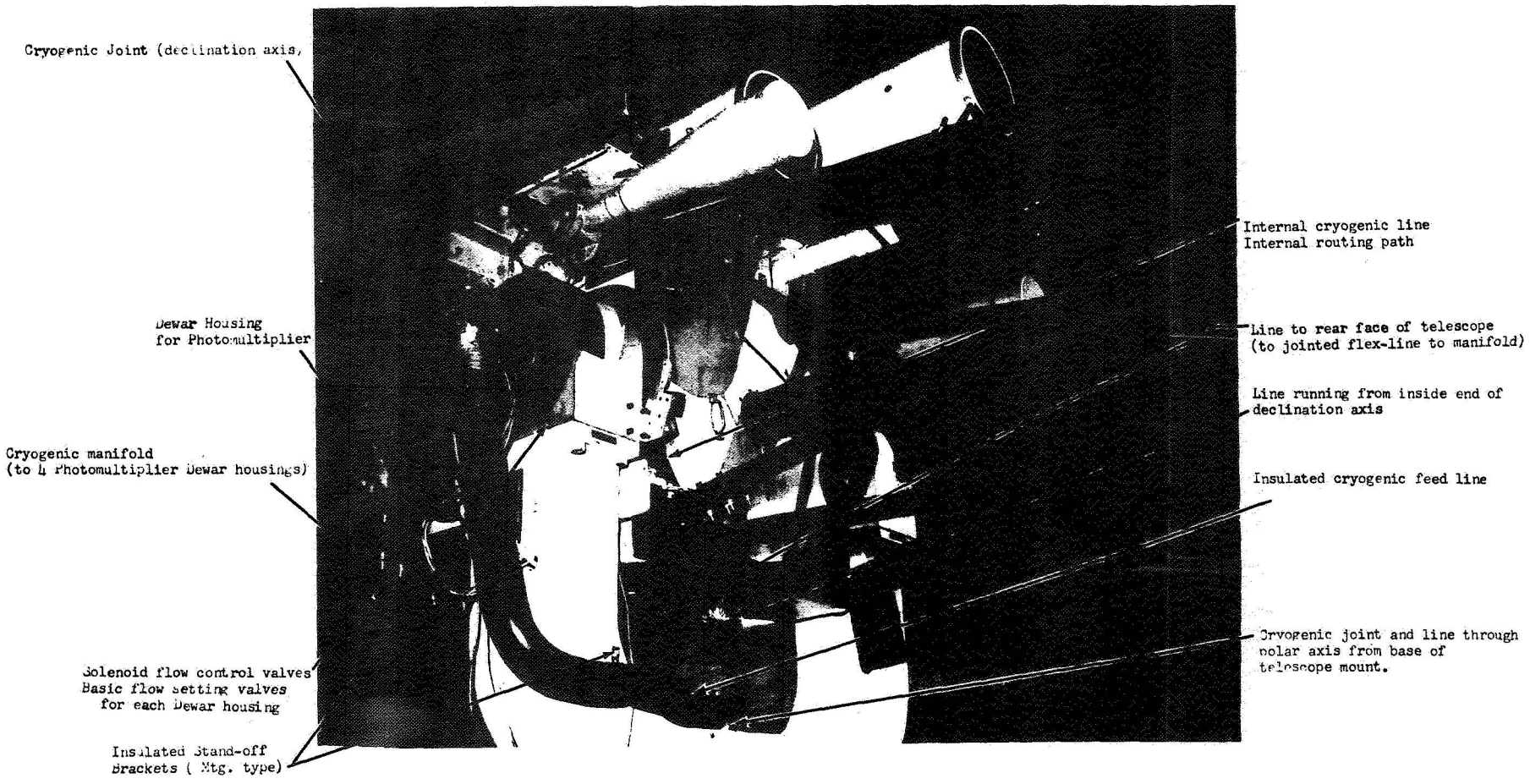

Figure 6. - Insulated feed line routing of the cryogenic system

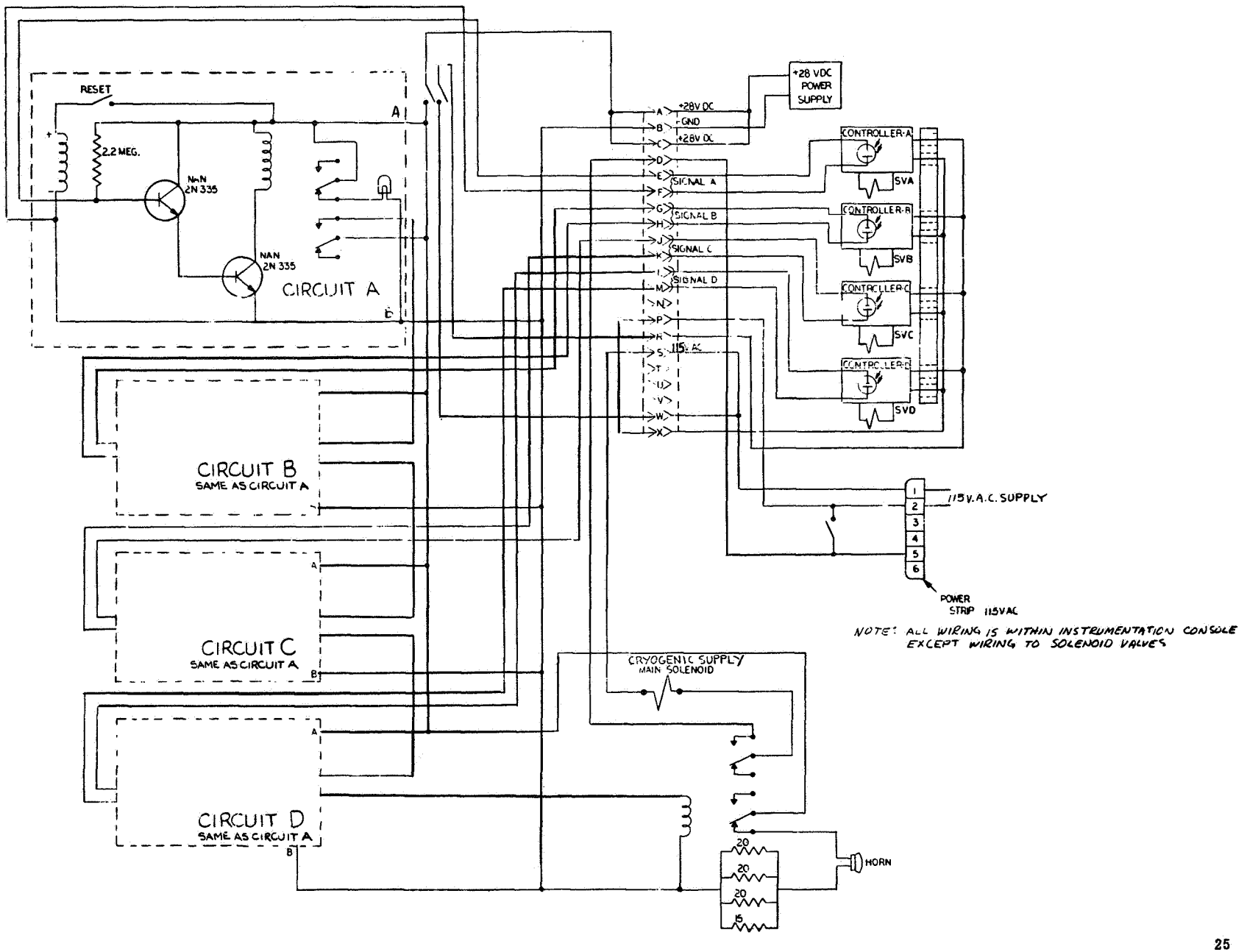

Figure 7. - Under temperature alarm and cryogenic schematic diagram

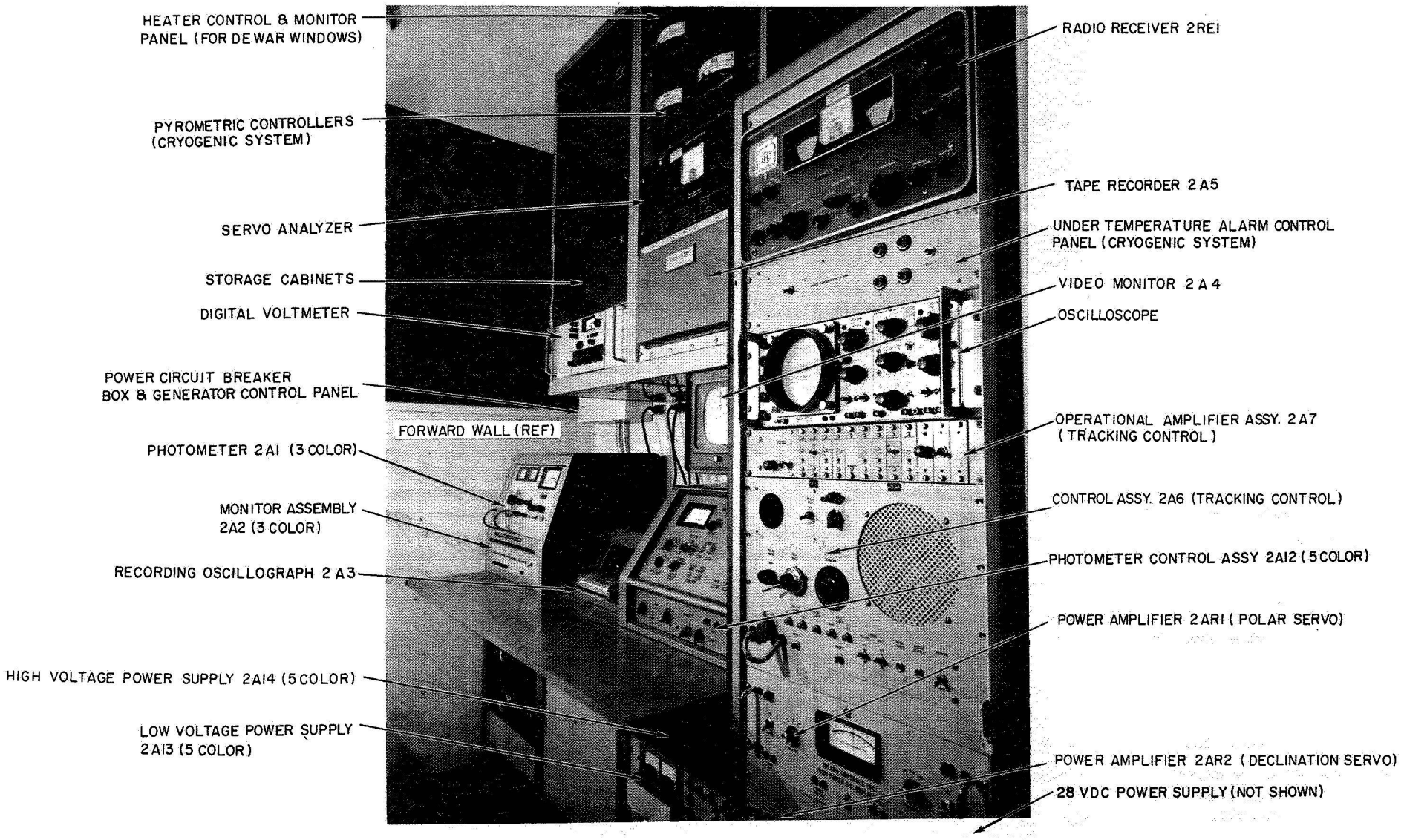

Figure 8. - Curbside wall of forward compartment

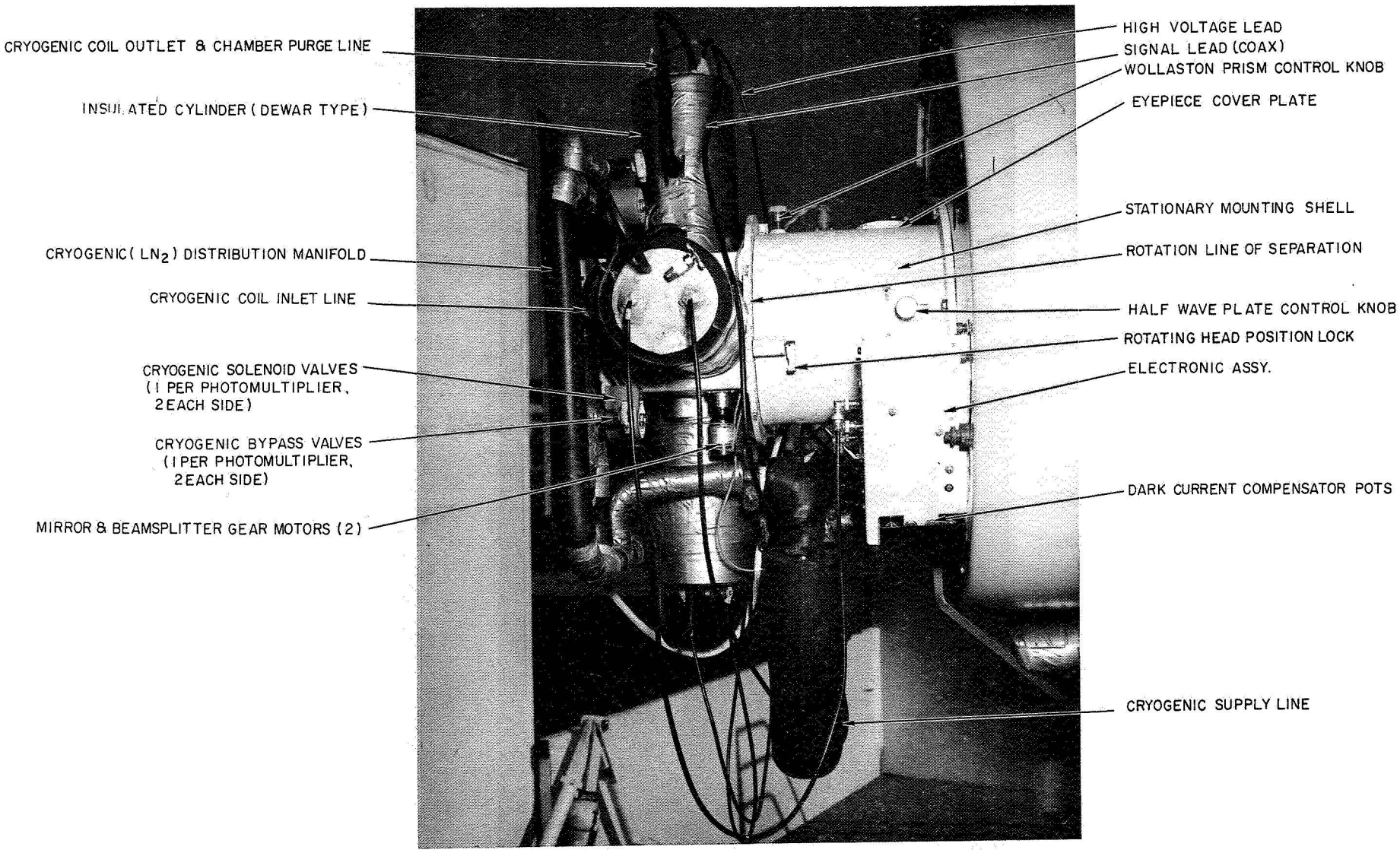

Figure 9. - Five-color photometer head - Right Side

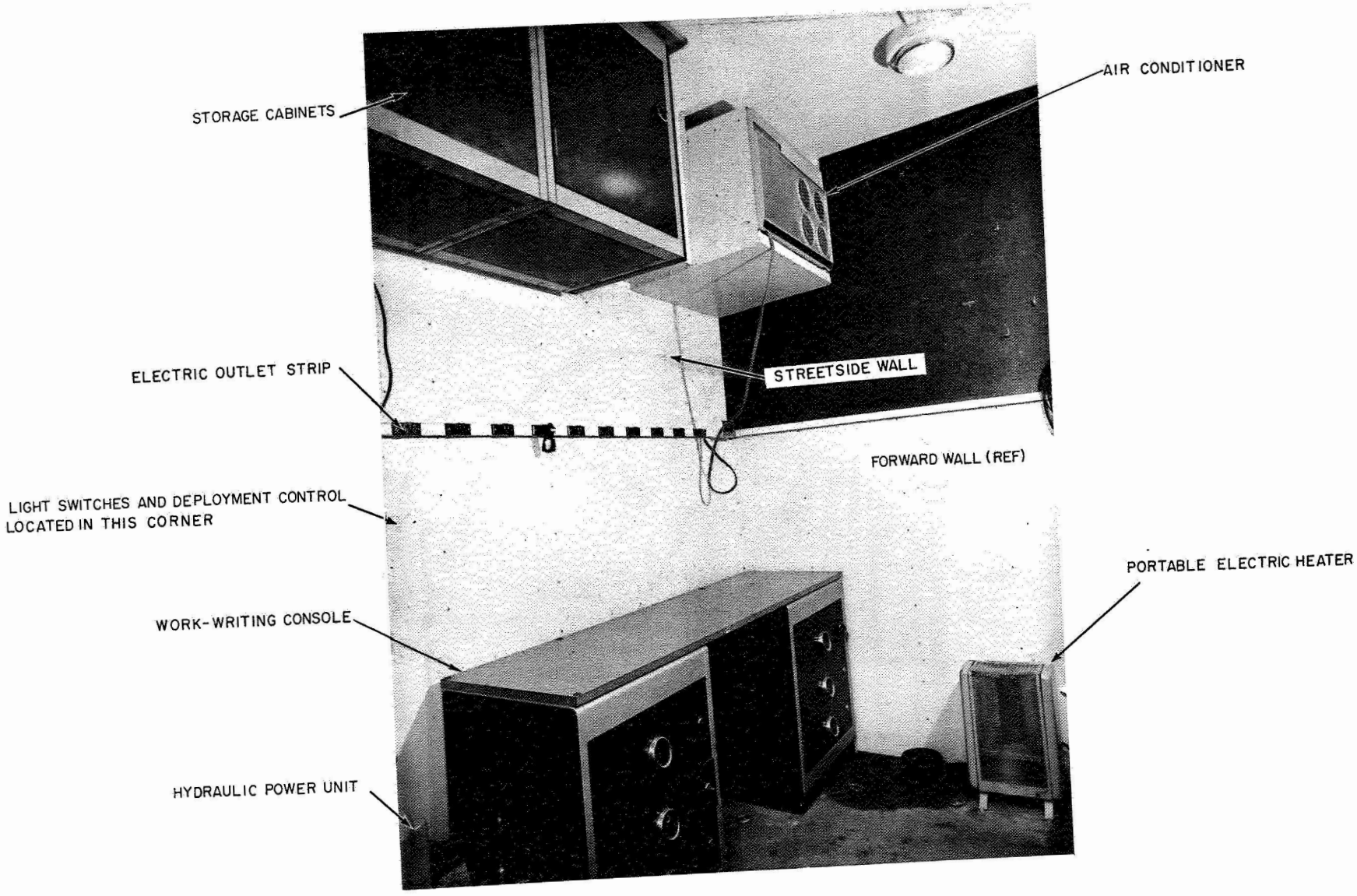

Figure 10. - Streetside wall of forward compartment

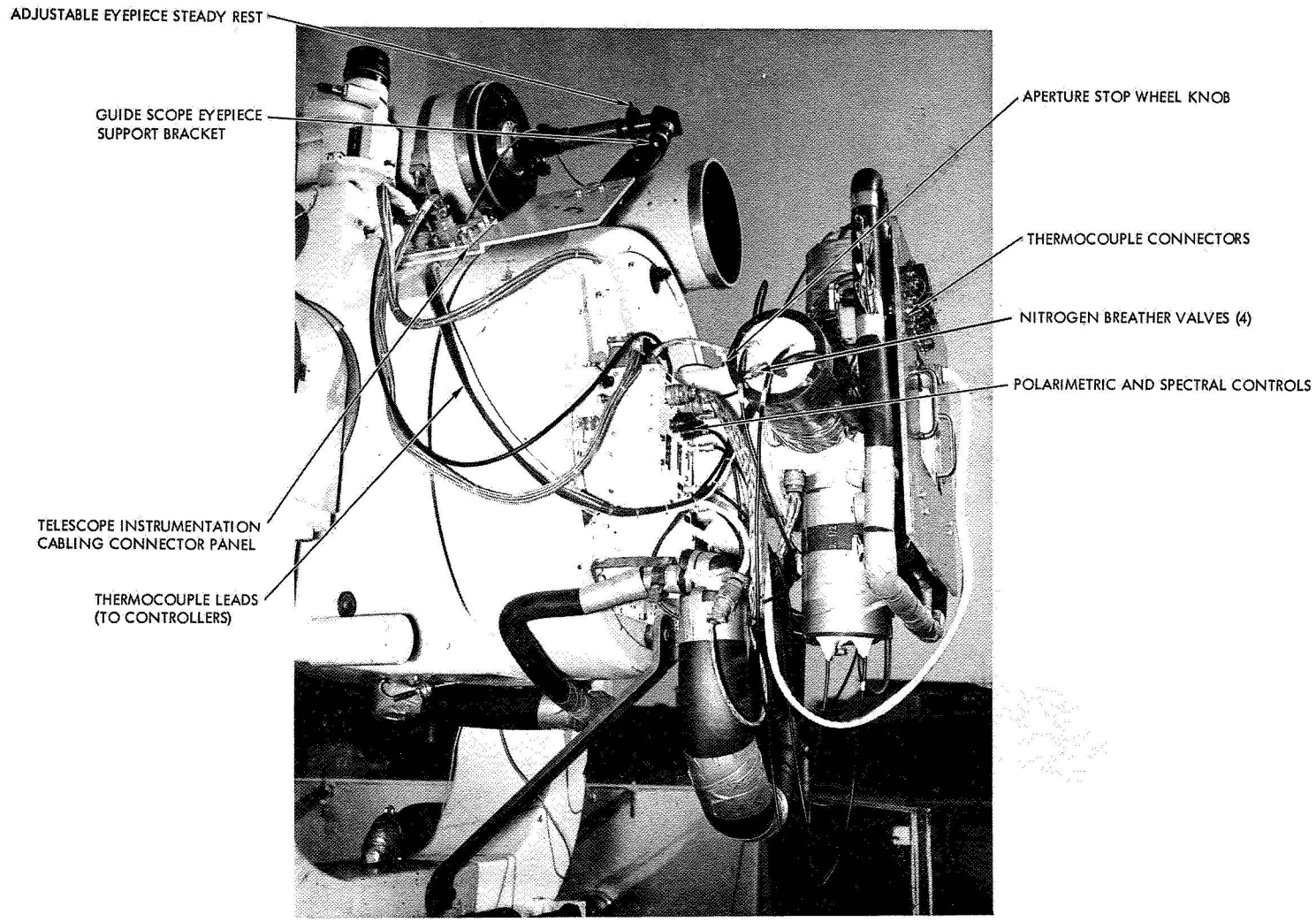

Figure 11. - Five-color photometer head - Left Side

sequentially by stepping switches, as is the rotation of the half-wave plate in the polarimetric mode. These steps can be controlled manually or are automatically sequenced from the control units in the instrumentation room. The sequencing rate or time of integration per color per data point is also controllable. The instrumentation provides for a variety of operating modes with respect to the multicolor beam sharing techniques. These modes are as follows:

(1) A pair of full-silvered mirrors reflect the sky-only and sky-plus-object light beams into matched S-20 photomultiplier tubes (U-B-V).

(2) A pair of half-silvered mirrors reflects half of the light into the S-20 photomultipliers, while the remainder of the signal is transmitted and then reflected into the S-1 photomultipliers (V-R-I).

(3) By moving both the full-silvered and half-silvered mirrors out of the light path, all the light passes to the lower mirrors and is reflected directly into the S-1 photomultipliers.

For determining linear polarization, two methods are utilized:

(1) By use of a ten position half-wave plate and a Wollaston prism, orthogonal component beams are split and directed similarly either into the S-20 (U-B-V) or S-1 (V-R-I) photomultipliers, or into both. (Since the presently installed achromatic type half-wave plate operates in the U-B-V region, only the S-20 mode is used.)

(2) By moving the half-wave plate out of the light path and rotating the photometer head, orthogonal polarization component beams may also be directed into either photomultiplier combination so that degree of linear polarization in all five colors may be measured.

The system response functions for the U-B-V-R-I spectral regions are shown in Figure 3. The response functions are defined by filter transmission; photomultiplier spectral response; atmospheric transmission; and reflectance and transmittance of the various optical components of the primary telescope and associated mirrors and lenses.

The term effective wavelength is defined by:

$$\lambda_{eff} = \frac{\int \lambda \phi(\lambda)\, d\lambda}{\int \phi(\lambda)\, d\lambda} \tag{18}$$

where $\phi(\lambda)$ is the response of the system at a wavelength λ. The integrals are evaluated by summing the area under the plotted curves of wavelength times response function and the area of the response function. The true 5-color system effective wavelengths are shown in Table I.

The optical elements of the instrumentation head are described below in the sequence in which they are located along the optical path leading to the photomultiplier windows.

The eyepiece assembly is used to adjust the focus of the 24-inch telescope. With the photometer head set at the zero rotation position the eyepiece cover plate can be removed and the eyepiece assembly can be inserted and secured with three screws. The assembly contains a mirror positioned on the optical axis at a 45-degree angle to the axis, thus reflecting the image to the objective plane of the eyepiece. This plane contains an illuminated taut wire cross hair which is viewed through a 25-mm orthoscopic eyepiece. The eyepiece must be removed and the cover plate replaced to obtain photometric data.

TABLE I. - FIVE COLOR (U-B-V-R-I) PHOTOMULTIPLIER SYSTEM CHARACTERISTICS

Band	Type of filters	System effective wavelength	λ_{eff}-standard system	Photomultiplier
U	Schott BG-38 UG-11	3560 Å	3600 Å	EMI 9558 QA (S-20)
B	Schott BG-13 BG-37	4470 Å	4400 Å	
V	Corning C-3384 Schott BG-18	5420 Å	5500 Å	
V	Schott CG-14 BG-18	5590 Å	5500 Å	EMI 9684 A (S-1)
R	Corning C-4600 Schott RG-1	6980 Å	7000 Å	
I	Schott RG-780 BG-3	8930 Å	9000 Å	

The half-wave plate assembly is located immediately behind the eyepiece position but ahead of the image plane. The half-wave plate is supported on a slide assembly so that it can be placed (by rotation of an external hand knob) on the optical axis when used for polarimetric data or moved to the side, out of the optical path for straight photometric data. The half-wave plate is supported in a ring that can be rotated in 36-degree increments by a step servo motor. Coupled to the half-wave plate drive is a 1 K continuous rotation servo potentiometer to provide a voltage to monitor and record the position angle in the instrument room. The half-wave plate (an achromatic type made by the method of Pancharatnam) is useable for polarimetric measurements in the B (blue-photographic) and V (yellow-green) (visual) bands and a good portion of the U band of the spectrum. For polarimetric measurements in the R and I regions, the half-wave plate can be moved to the side (with the hand knob) and data obtained by rotation of the head in 36 degree increments (this method can also be used for the U as well as the B and V bands if desired).

The field stop assembly is the next element along the optical path. Light is gathered by the telescope and focused on the plane of the field stop. The field stop assembly contains a disc that may be rotated by an external hand knob to select any one of five positions. Four of these positions contain a dual aperture for non-polarized photometric measurements of simultaneous sky and sky plus subject. The size of these aperture pairs are 0.5, 1.0, 2.0, and 4.0

minutes of arc in diameter. The fifth position contains a single 2.0 minutes aperture on axis for the polarimetric measurements.

The lens assembly is located immediately behind the field stop and contains three lenses (two for photometric and one for polarimetric measurements). These are Fabry-type lenses, the purpose of which is to direct all the light collected by the main telescope aperture which passes through the field stop on the desired area of the photocathode. In order to accomplish this the focal length and position of these lenses is set to focus the image of the 24-inch primary mirror on the photocathode producing a well diffused spot slightly less than 0.5-inch in diameter. The two lenses for nonpolarized photometric measurements are 22 mm diameter double convex lenses made of Homosil. Their focal length is 240 mm at 3000 and 259 mm at 11,000 angstroms. Immediately behind the lenses are Lyot depolarizers made of calcite. These lenses are as close to the field stop as mechanical clearances allow in order to provide sharp cut off as the target object moves out of the field stop area.

The polarimetric lens is a 31 mm diameter, double convex lens also made of Homosil. Its focal length is 215 mm at 3,000 angstroms and 232 mm at 11,000 angstroms. This lens is placed behind a Wollaston prism which is positioned as close to the field stop as mechanical clearances allow. The Wollaston prism is a three-element type made of calcite. Deviation of each ray falls within the limits of 7 and 9 degrees from 3,000 to 11,000 angstroms. Behind the lens is a Lyot depolarizer 31 mm in diameter and made of calcite. The three lenses, depolarizers, and Wollaston prism are mounted on a knob controlled slide assembly allowing the transition from the (nonpolarized) photometric to the polarimetric mode by means of an external hand knob.

The 45-degree mirror and beamsplitter (half-silvered mirror) assembly is mounted behind the lens assembly and contains two aluminized mirrors and two inconel beamsplitters mounted on a slide assembly aligned with the level of the S1 photomultiplier pair (see Figure 12). The mirrors and beamsplitters are independently driven in and out of position by 115 VAC reversible motors. Micro switches determine the drive limits and provide an interlock so that neither motor can drive its component into position unless the other is all the way out.

With the upper mirrors and beamsplitters both out of the optical path, the light is reflected by another pair of mirrors located at the level of the S-20 photomultipliers, as described in the next paragraph, and thereby impinges on the S-20 photocathodes. With the upper mirrors shifted into the light path position the light is reflected on the S-1 photocathodes for VRI data only. With the beamsplitters in the light path position the light is split striking the S-1 and S-20 photocathodes for simultaneous U-B-V, V-R-I data acquisition.

The color filter and fixed mirror assembly consists of four-color filter wheels and two fixed mirrors (the pair aligned with the S-20 phototubes) mounted on the photometer head back cover plate. The two fixed mirrors reflect the light onto the S-20 phototubes. Two of the four color filter wheels are associated with the S-1 photocathodes and contain three glass absorption filters in three of the six available positions providing system effective wavelengths of 5590, 6980, and 8930 angstroms. They are so located that each filter position is sequentially centered on the light path. The other two wheels are associated with the S-20 photocathodes and contain three glass absorption filters providing system effective wavelengths of 3560, 4470, and 5420 angstroms. Each color filter wheel is rotated by a digimotor and its position is read out with a rotary wafer switch to permit synchronization of the wheels in pairs to be maintained, and to provide a position indicating signal to the photometric control unit (and to the recorder).

The entire photometer head, with the exception of the shell that is bolted to the telescope, can be rotated clockwise or counterclockwise 108 degrees in increments of 36 degrees.

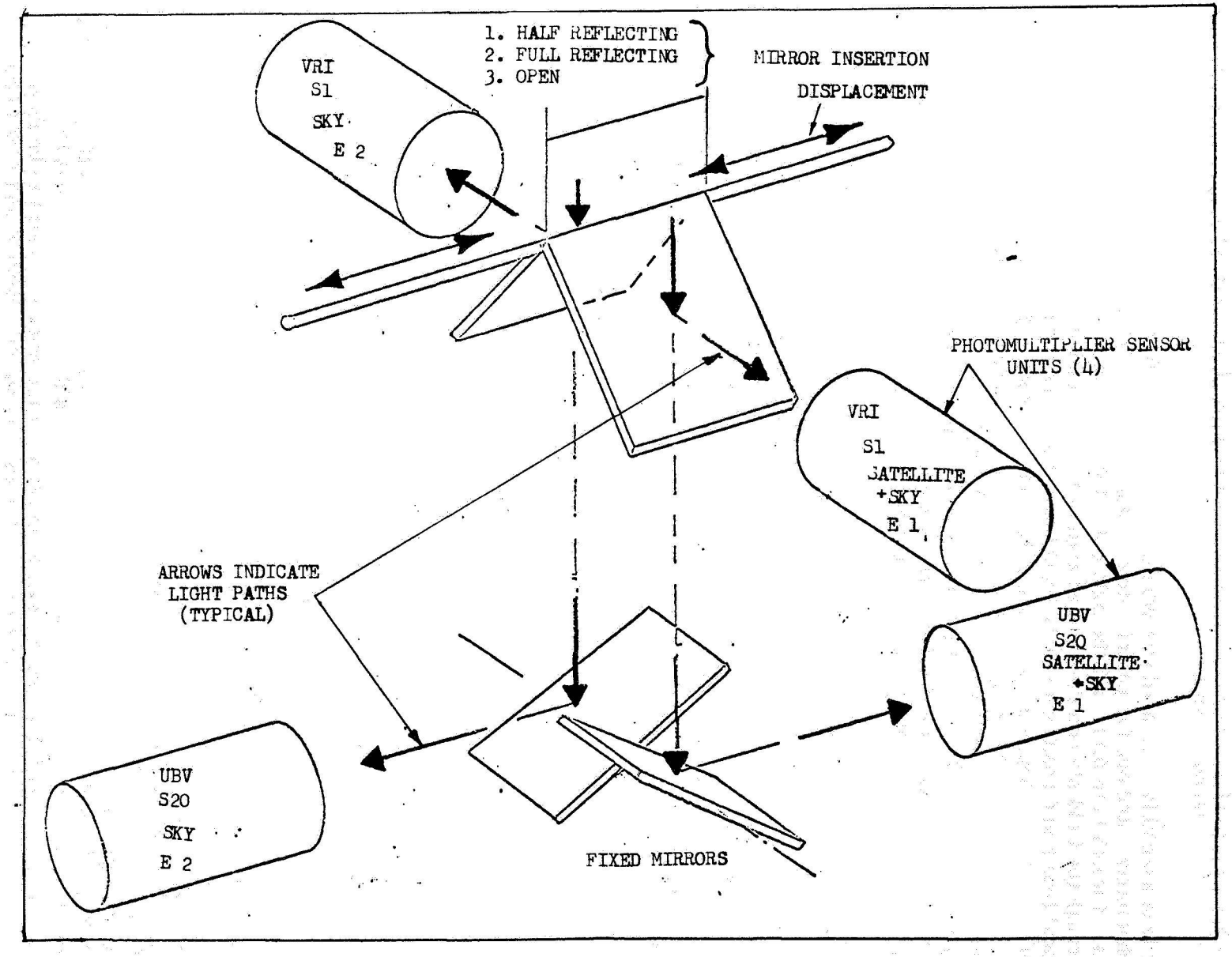

Figure 12. - Schematic diagram of mirrors and beam splitters

This causes the complete optical system beyond the telescope to be rotated accordingly, thus providing an alternate method of obtaining polarization data to that of using the half-wave plate.

In addition to the optical head, directly below it on the back of the telescope is also mounted the mating electronic assembly unit. This electronic assembly contains four preamplifiers, one for each photomultiplier. They are Analog Devices, type 301, high impedance solid state amplifiers. Six different gain levels can be selected by a bi-directional stepping switch controlled from the control console. The anode of each photomultiplier is connected directly to its respective amplifier input. The feedback resistor on the amplifier establishes the current to voltage conversion with the amplifier serving only as an impedance transforming device. The six resistance values are spaced two magnitudes apart, namely 15.81K, 100K, 631K, 4M, 25.12M, and 158M. There is one stepping switch for the V-R-I pair of preamplifiers and another for the U-B-V pair. Wafer switches attached also provide means for monitoring and recording of gain levels.

The output of the preamplifiers can be metered or recorded at the control console or connected to the inputs of two differential amplifiers. These amplifiers are Analog Devices, Model 101/c. The feedback resistor is fixed at 100K but the input resistor is selectable from 1K to 158K in half magnitude steps. These input resistors are selectable in pairs by a twelve position bi-directional stepping switch controlled at the control console, and equipped with wafer switches to provide means for monitoring and recording of gain level in use.

Although the S-1 and S-20 photomultipliers are each matched pairs, they are not identical in gain and spectral response. Also, differences in the filters or optical system in general will result in unequal gains. Since a differential system is employed for elimination of sky background and for polarimetric ratios the photomultiplier gains must be equalized for each color in both modes of operation, spectral and polarimetric. Equalization of the gains is accomplished by controlling the overall voltage applied to the photomultipliers. The negative high voltage is connected to the center arm of a potentiometer. The ends of the potentiometer are connected to the cathodes of the photomultiplier tubes, by means of a twelve position stepping switch, either directly or through a resistor to obtain the necessary voltage drop to equalize the gains. Six potentiometers are used for V-R-I and six for U-B-V. The V-R-I and U-B-V photomultiplier gain stepping switches are independently controlled by the logic circuits in the control assembly. These potentiometers provide a means of matching the photomultiplier pairs in each color. In addition, four potentiometers are provided, one for each photomultiplier, as a means of balancing out the circuits for minimum dark current output.

The photomultiplier units mounted on the instrumentation head on the back of the telescope are cryogenically cooled by a system which feeds regulated liquid nitrogen to them through a manifold fed by an insulated line which passes through the telescope axes from beneath the floor. The purpose of the cryogenic cooling system is to reduce the photomultiplier cathode temperatures to a level at which a very low dark current occurs, so that very low signal levels and their corresponding low light levels can be measured. This is necessary because of the photocathode characteristics of the photomultipliers used in this system, especially those with the red sensitive (S-1) photocathodes. The blue sensitive (S-20) photocathodes are normally regulated at an operating temperature of -50 degrees F, and the red sensitive (S-1) photocathodes are regulated at -180 degrees F. This is accomplished by allowing the cathodes to drift toward a thermal radiation balance with the metallic μ-metal shield which is directly outside the glass envelope enclosing the cathode and other parts of the photomultiplier (see Figure 4). The μ-metal shield, in turn, is in conduction contact with a tubular copper coil wound around it. It is through this coil that the liquid nitrogen is passed to hold it down to the desired temperature despite thermal losses to the surrounding media at higher temperatures. The regulating sensor (thermocouple) is on the inlet side of the coil, and the

entire assembly is enclosed in an insulating jacket to keep heat transfer losses to a minimum. The regulator turns the flow of liquid nitrogen on and off as necessary to maintain the sensor temperature within ±2 degrees F. The cryogenic system consists of the following elements:

(1) The insulated cryogenic supply line runs from a connector fitting on the back of the truck under the floor to the bottom of the telescope pedestal. The line is then routed up through the telescope mount axes to the back of the mirror cell and on to the distribution manifold. Two safety relief valves on either side of the emergency shut down solenoid valve and a shut off system dump valve are located under the aft access plate in the floor of the observation deck (see Figure 13).

(2) The distribution manifold is mounted on the panel attached to the rear of the instrumentation head and leads to each of the four photomultiplier dewar cylinders. Load regulating flow control valves and solenoids are provided for each cylinder (see Figure 9).

(3) The four insulated (dewar type) cylinders mounted on the rear of the instrumentation head, house the photomultipliers and associated electronic components (see Figure 11).

(4) The cryogenic temperature regulating system with its 4 precision regulators are mounted in the instrument room (see Figure 8). The cryogenic control consists of four modified West Instrument controllers (one for each photomultiplier). Each controller is connected to the thermocouple in the corresponding photomultiplier housing, and activates the solenoid valve controlling cryogenic flow to that photomultiplier which holds its temperature at the pre-set level. An auxiliary photocell in each controller activates an alarm and causes emergency shut-down of the complete cryogenic cooling system if the temperature of any unit falls more than a few degrees below the pre-set level.

(5) The window and optical heater-defroster system is mounted at the base of each dewar type cylinder and is controlled and monitored from the instrument control room. A control and monitor indicating panel for the photomultiplier window heaters and adjacent optics of the instrument head is located above the cryogenic control panel.

(6) An under temperature and emergency shutdown safety system is provided which includes warning lights and a horn. It also activates the emergency shutdown selenoid valves which shuts down the complete cryogenic system.

In operation, an insulated hose is connected between the fitting on the rear of the truck and a liquid nitrogen supply tank. The supply line from the rear truck fitting is insulated throughout the truck, telescope and manifold. Carefully aligned cryogenic rotary joints are provided in the supply line at each telescope axis to reduce friction to an acceptable level.

The panel on the back of the instrumentation head provides facilities for mounting the manifold, control valves and thermocouple connectors. Continuous thermocouple leads run down through the telescope and its mount where they enter conduits leading to the instrument console and the four controllers (see Figure 8). Each controller regulates the temperature of one photomultiplier.

The window heater system is designed to keep the outside of the glass, where it is in contact with ambient air, sufficiently warm to prevent dew or frost formation despite the coldness of the nearby cathode and other elements. The heating system also prevents thermal condensation on other optical surfaces in the instrumentation head. Operation is controlled by switches and indicator lights on the control console.

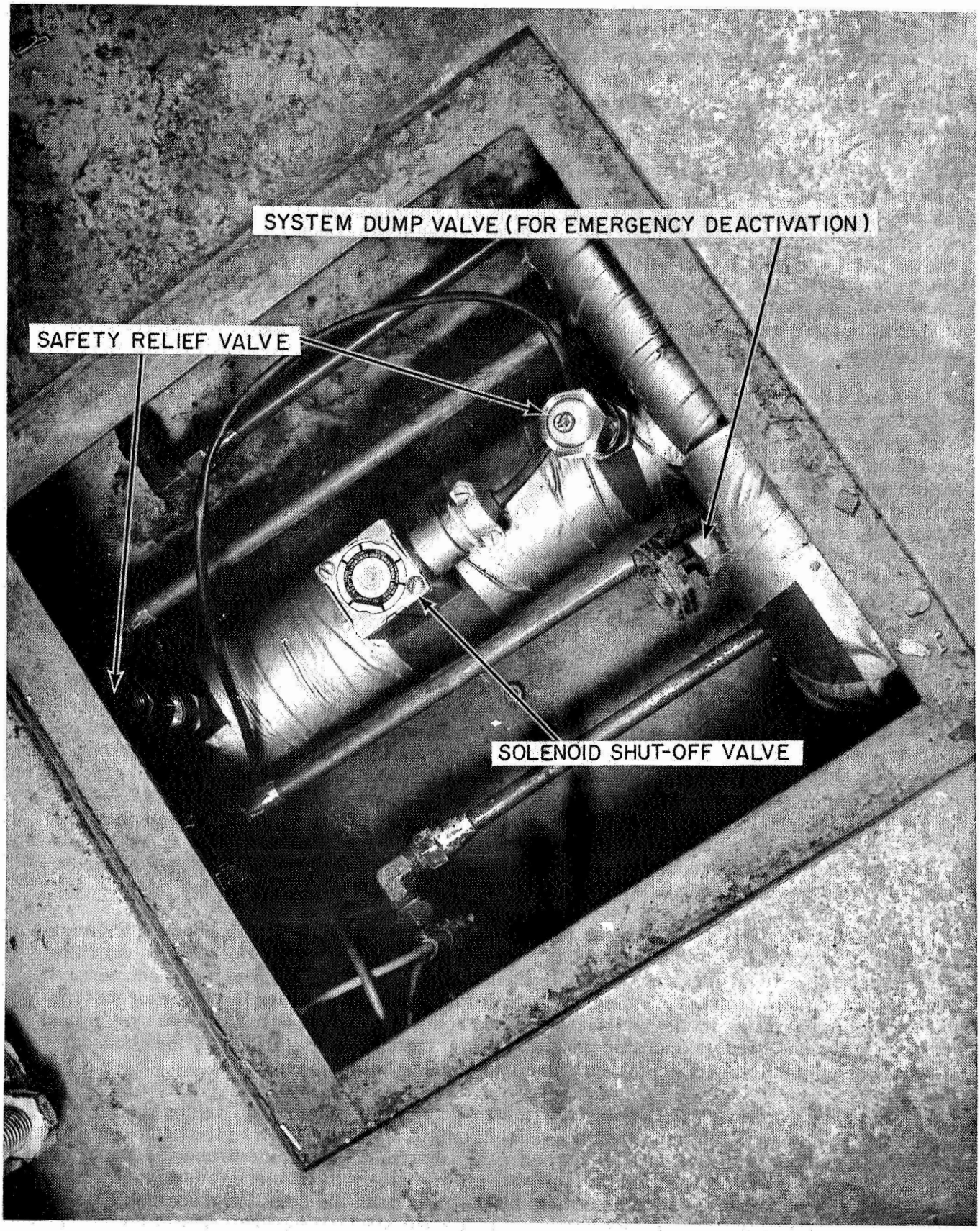

Figure 13. - Cryogenic system and emergency shut down valves

The under temperature safety system is activated by a photocell mounted on the temperature controller so that any sensor dropping more than 10 to 15 degrees below the temperature setting will activate the alarm (horn and warning lights). This also closes the solenoid valve in the liquid nitrogen supply line (see Figure 13) thereby shutting down the complete cryogenic system.

The four insulated (dewar type) cylinders enclosing the photomultipliers are of a special design to meet the stringent requirements of their application. They operate satisfactorily in any position or attitude, permit ready access to the photomultiplier tubes, and provide a suitable operating environment for the critical requirements of these tubes. The cylinders also provide the necessary voltage divider net and associated components, electrical connections and protection for the photomultipliers as well as affording a light tight enclosure to exclude all light except that entering the telescope. The cryogenic exhaust is bled through the dewar to keep it purged free of ambient air, thus ensuring completely dry gas in the dewar chamber at all times.

As can be seen in Figure 14, the operator's control console in the instrument room provides for monitoring and controlling all the functions of the instrumentation system. The meter at the upper left (plus the two selector switches below and the one to the right of the meter) are for indicating settings (left-hand switch), monitoring signals (right-hand switch), and setting scale ranges (upper switch to right of meter). The four lights at upper right, and the row of four lights at the right end of the lower panel are also for indicating operating configuration of labeled elements of the instrumentation head. The other switches are for controlling the system in the various modes and are grouped according to function, as indicated by the labeling. Note that the entire right side of the main panel controls the various data sequencing modes available. Figure 15 shows much of the circuitry and general arrangement of this unit, and Figure 16 shows the meter readings indicating the various corresponding settings of the system.

The photometric output signals (as well as monitoring voltages indicating gain settings, filter wheel positions, and angular position of half-wave plate or rotating head, see Figure 16) from the control assembly is fed directly to the recorders, where it (along with the demodulated WWV radio time signal output) is used to activate 11 of the 18 available recording channels. In addition, the selected photometric channel signal output is coupled to the relay circuits controlling the tone generator which is fed to the speaker on the observatory deck to assist the tracker by indicating when the satellite (or star) is within the field stop aperture.

High quality components were selected and specified throughout the system design as needed to ensure required operating stability and precision and reasonable service life.

Functionally, this photometer control assembly serves as the "switchboard" and monitoring control panel for the entire photometric system. It enables the operator to vary the system operation in any desired manner, depending on the circumstances being encountered, and objectives, to obtain optimum data. In addition, the control assembly incorporates the capability of generating the logically constrained routine control functions of the system and doing so with considerable operator controllable variations. It also supplies the necessary interlocks; and incorporates signal processing and distribution circuitry.

The signal processing circuitry and controls include provisions for taking the direct (pre-amplified) signal, or the differenced signal originating from each of the photomultiplier pairs (with selected gain level applied), and either distributing it to the proper recorder channel or routing it to the integrator. The purpose of the differencing mode for the matched photomultipliers is to use the signal generated by the light from the satellite and its sky background in one and that from an equal portion of adjacent sky in the other. Thus, the difference

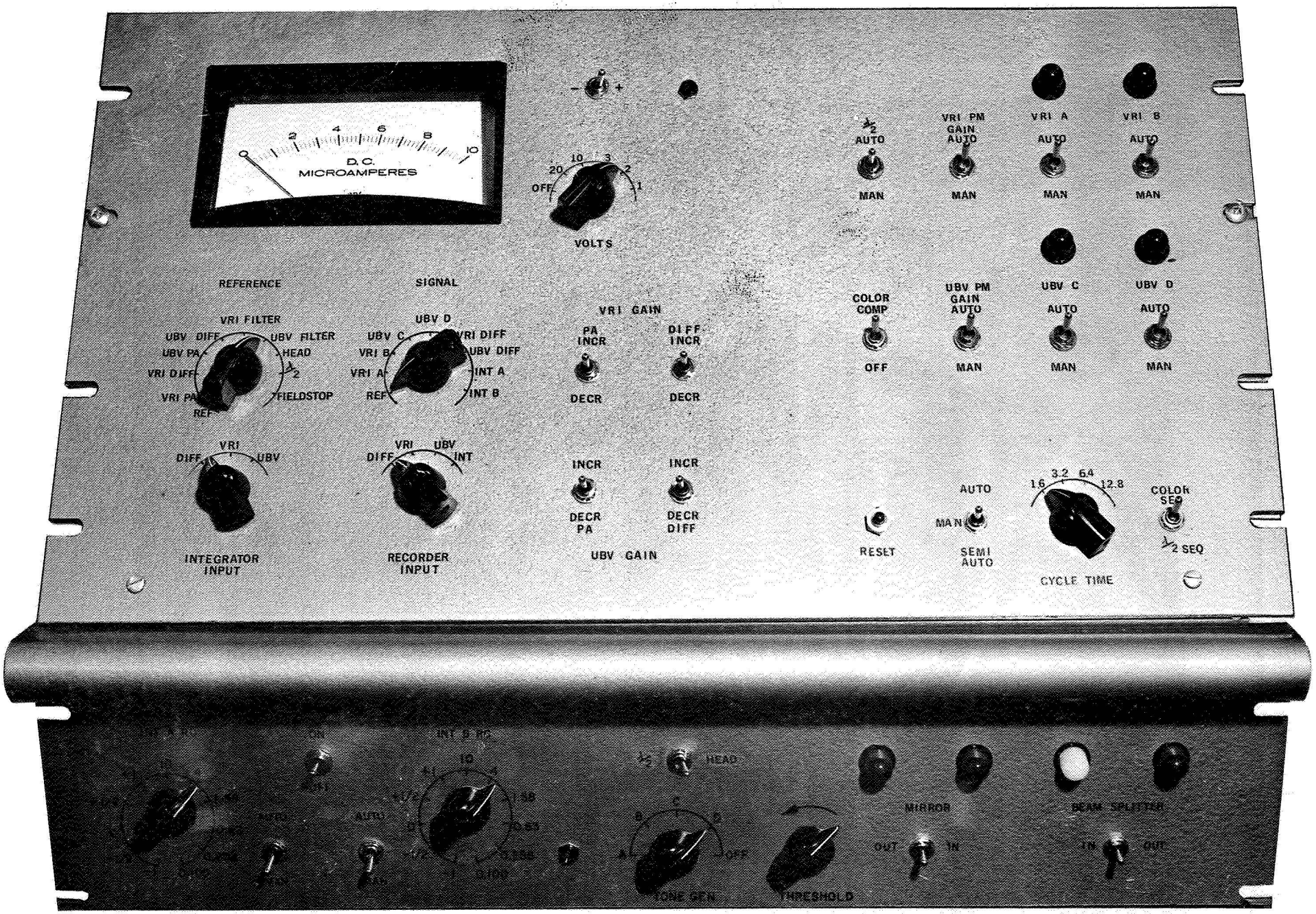
D.C.
MICROAMPERES
VOLTS
REFERENCE
SIGNAL
VRI FILTER
UBV FILTER
HEAD
FIELDSTOP
UBV DIFF
UBV PA
VRI DIFF
VRI PA
REF
UBV D
UBV C
VRI B
VRI A
VRI DIFF
UBV DIFF
INT A
INT B
VRI GAIN
PA INCR
DIFF INCR
DECR
INCR
DECR PA
DECR DIFF
UBV GAIN
COLOR COMP
OFF
RESET
VRI PM GAIN AUTO
UBV PM GAIN AUTO
VRI A
VRI B
UBV C
UBV D
AUTO
MAN
SEMI AUTO
CYCLE TIME
COLOR SEQ
SEQ
INTEGRATOR INPUT
RECORDER INPUT
VRI
UBV
DIFF
INT
INT B RC
HEAD
TONE GEN
THRESHOLD
MIRROR
BEAM SPLITTER
IN
OUT

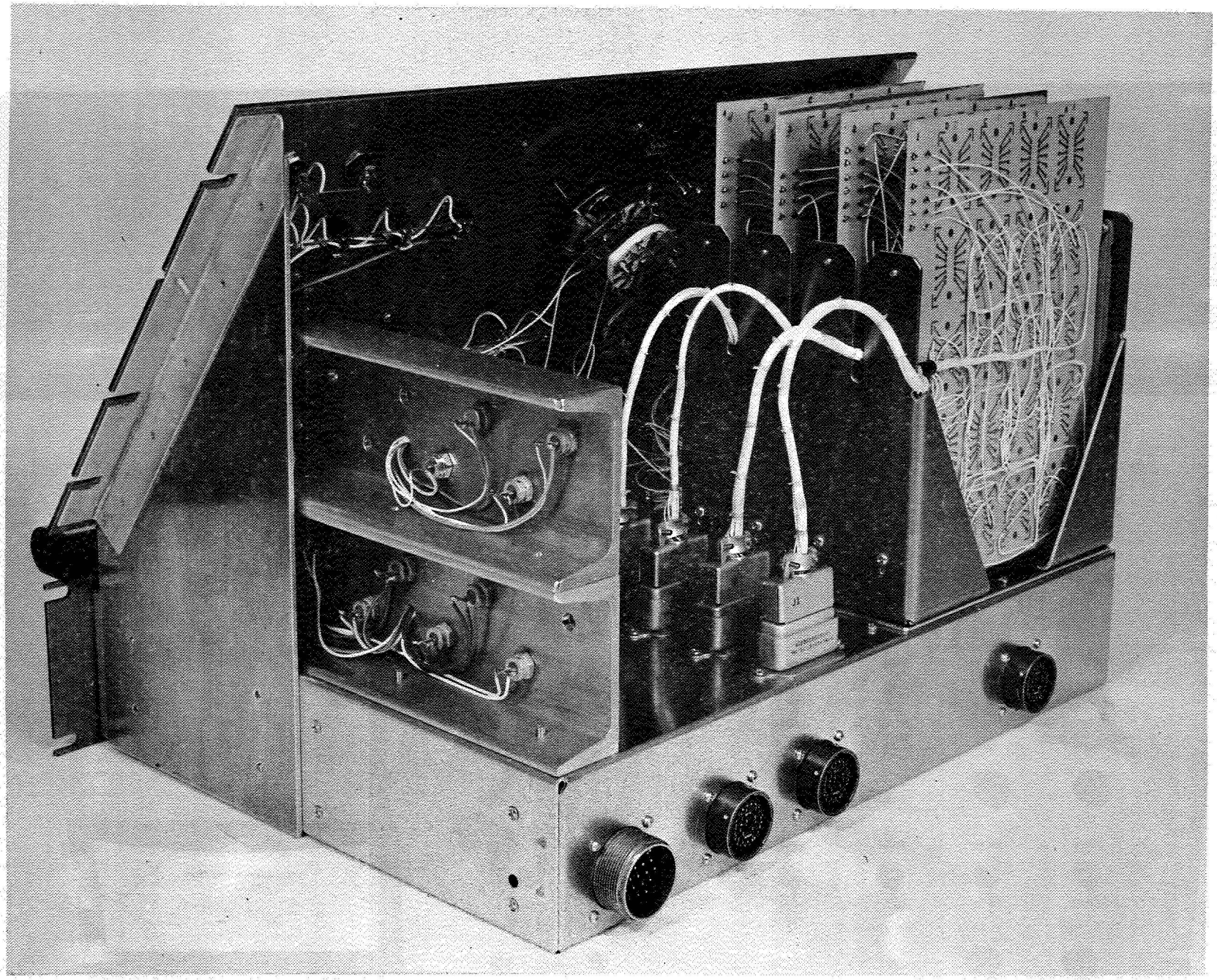

Figure 15. - Logic boards in rear of photometer control assembly

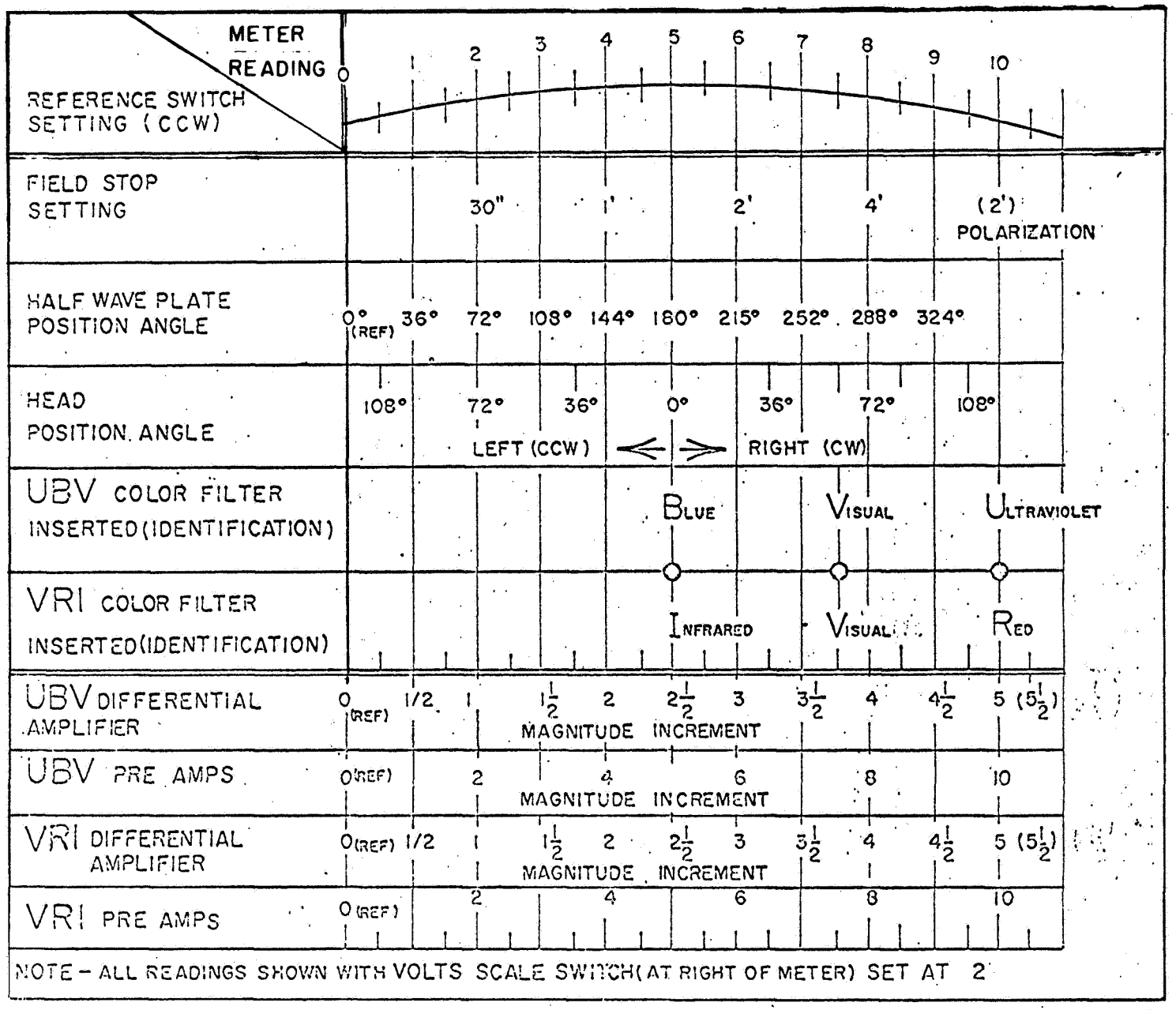

Figure 16. - Legend for monitor panel meter readings

obtained will be satellite (or star) alone. The same technique is employed for polarization by differencing the signal caused by the two orthogonally polarized components falling on each of the photomultiplier cathodes of the matched pair. Thus, equal signals (no polarization) will give a difference of zero. The adjustments for balancing these outputs are on the right side of the electronic unit mounted on the back of the telescope (see Figure 9).

The control signals which are internally generated for automatic sequencing, timing, and integrator control are developed in 4 plug-in logic boards listed below:

(1) Timer

(2) VRI/UBV Control

(3) $\lambda/2$ Control

(4) Integrator Control

The logic boards are printed circuit boards mounted vertically in the photometer control assembly as shown in Figure 14. They are easily accessible and removable by sliding the control assembly panel forward. The boards and their functions are described in the following paragraphs.

The Control Logic consists of the following four boards: Timer, VRI/UBV Control, $\lambda/2$ Control, and the Integrator Control. The Timer Board consists of a counter and logic to control the mode of operation. The counter converts the 60 Hz line frequency to 3.75 Hz which is used as the clock frequency to step the digi-motors of the color wheels, $\lambda/2$ plate and gain switches. The counter also provides frequencies with periods of 2.13, 4.27, 8.53, and 17.1 seconds which control the time for each cycle of operation. The VRI/UBV Control Board controls the digi-motors for the VRI PM GAIN, UBV PM GAIN, and the four color wheels (VRI A, VRI B, UBV C, and UBV D). The $\lambda/2$ Control Board controls the digi-motors for the half-wave ($\lambda/2$) plate, enables the Integrator Control circuit and inhibits the Color Wheels from stepping during the first through tenth steps of the $\lambda/2$ plate. The Integrator Control Board controls the set and reset of the integrator relays and provides the reset pulse to reset the control circuit Flip-Flops at the end of each cycle of operation.

At the beginning of each cycle of operation in the Auto Mode and Color Seq., the color wheels will step to the next color filter and remain until the beginning of the next cycle of operation. The time for one cycle of operation is determined by the position of the CYCLE TIME switch on the Control Panel. The Mirror and Beam Splitter will determine which color wheels change position. The following conditions can exist:

Mirror	Beam splitter	Color wheels stepped
In	Out	VRI
Out	Out	UVB
Out	In	VRI, UBV

After the color wheels have been stepped, the integrator relays will set to start the integrators. The integrator relays will be reset at the end of each cycle to turn off the integrators.

In the AUTO Mode and $\lambda/2$ SEQ, the first cycle of operation will step the color wheels as described above, then the $\lambda/2$ plate (only) will step one position each cycle until ten steps have been completed. This completes one $\lambda/2$ sequence which will automatically repeat with the next color. 400 ms after each $\lambda/2$ cycle begins, the Integrator Relays will set to start the Integrators. The relays are reset at the end of the cycle to turn off the integrators.

With the Mode switch in the MAN position, each digi-motor operates independently and will step one position each time its corresponding switch is momentarily placed in the MAN position. Four steps are necessary to advance from one color filter to the next one.

The added power supply requirements for this system were met by a regulated low voltage unit and a regulated high voltage unit, both installed in the rack below the control console (Figure 8).

The low voltage power supply contains a power switch that disconnects all power to the 5 color photometric units. It contains fuses for the 115 VAC, 28 VDC, and 6.0 VDC. Mounted in this unit are three purchased components listed below:

(1) Power Supply TW5005, Power Designs Inc. which supplies ±15 VDC for signal amplification and reference voltages.

(2) Power Supply M 6.6 - 3.0A, Technipower, which supplies power to the logic circuitry and tone generator.

(3) Variable Transformer, Superior Electric Q 117 U, which supplies 55 VAC 60 Hz to pulse the digimotors and rotary solenoids.

The high voltage power supply is a Power Design, model 1544 which supplies 1500 VDC to the photomultipliers.

The junction panel adapts some of the original cabling of the 3-color system for use with the 5-color system. It also provides the junction between cables from the telescope complex to the photometer control assembly. It is located in the bottom of the right-hand rack.

The cryogenic control consists of four modified West Instrument controllers (one for each photomultiplier). Each controller is connected to the thermocouple in the corresponding photomultiplier housing, and activates the solenoid valve controlling cryogenic flow to that photomultiplier which holds its temperature at the pre-set level. An auxiliary photocell in each controller activates an alarm and causes emergency shut-down of the complete cryogenic cooling system if the temperature of any unit falls more than a few degrees below the pre-set level.

A control and monitor indicating panel for the photomultiplier window heaters and adjacent optics of the instrument head is located above the cryogenic control panel.

Fabrication

As the advanced material requisitions and design drawings were released, parts procurement and fabrication were initiated in parallel on a tightly planned schedule to meet the requirements for use in the second observation interval (scheduled for midwinter, January, February, early March 1967 period). The most critical aspect, as expected, was the delivery of purchased parts and components.

Accordingly, a rigorous expediting program was set up whereby delivery date requirements, lead time requirements of the supplier, and purchase date were adjusted to a common schedule which identified long lead time items and pin-pointed the problem areas. Expedited ordering, special arrangements with the supplier, and special pick-up arrangements were utilized to resolve the problem areas; and a follow-up was then set up to ensure maintenance of the schedule and otherwise resolve problems and expedite deliveries as required.

Under this program, the European items (half-wave plates and photomultipliers) were ordered first, by telephone and cable. The other long lead-time critical items proved to be the filters, Wollaston prism, and power supply units; although many other items required alert followup and vigorous expediting to avoid problems. Despite the tight schedule, this program resulted in the delivery of all items in time to permit completion of the system by mid January, thus making it possible to use the new system for the second observation interval as planned.

The fabricated units were adjusted and checked out and installation accomplished to permit system checkout and field verification. The fabricated units (including instrumentation unit and electronic unit for the telescope, control units and power supplies for the instrument room, cabling, and cryogenic system) are shown near completion in Figures 17, 18, 19, 20, and 21.

After initial checkout (reported in the next section) they were mounted in their proper locations (on the telescope and in the instrument room, see Figure 21 and Figure 8). The new cabling was installed through the conduits of the observatory and connections made to the equipment. The cryogenic lines and other system elements were installed and insulated, and connected to the distribution manifold for supplying the photomultipliers. (Later this was repeated to provide the improved cryogenic system, as described above under Design.) The system was then aligned and adjusted, and prepared for final system checkout and field verification and acceptance trials.

Checkout and Acceptance Testing

Equipment checkout was conducted at several levels:

(1) Bench checkout of individual units, cabling, etc.

(2) System checkout.

(3) Field verification trials and acceptance testing.

These checkout operations were interlaced with the necessary fabrication adjustments and alignments, installation and operations as described separately, but the complete checkout sequence will be treated here.

System component checkout. - The component checkout involved physical and electrical continuity checks followed by functional checkout of each unit as follows:

(1) Optical Instrumentation Head Unit

Following mechanical and circuit checks, the unit was mounted on the optical bench for alignment. The following checks were made:

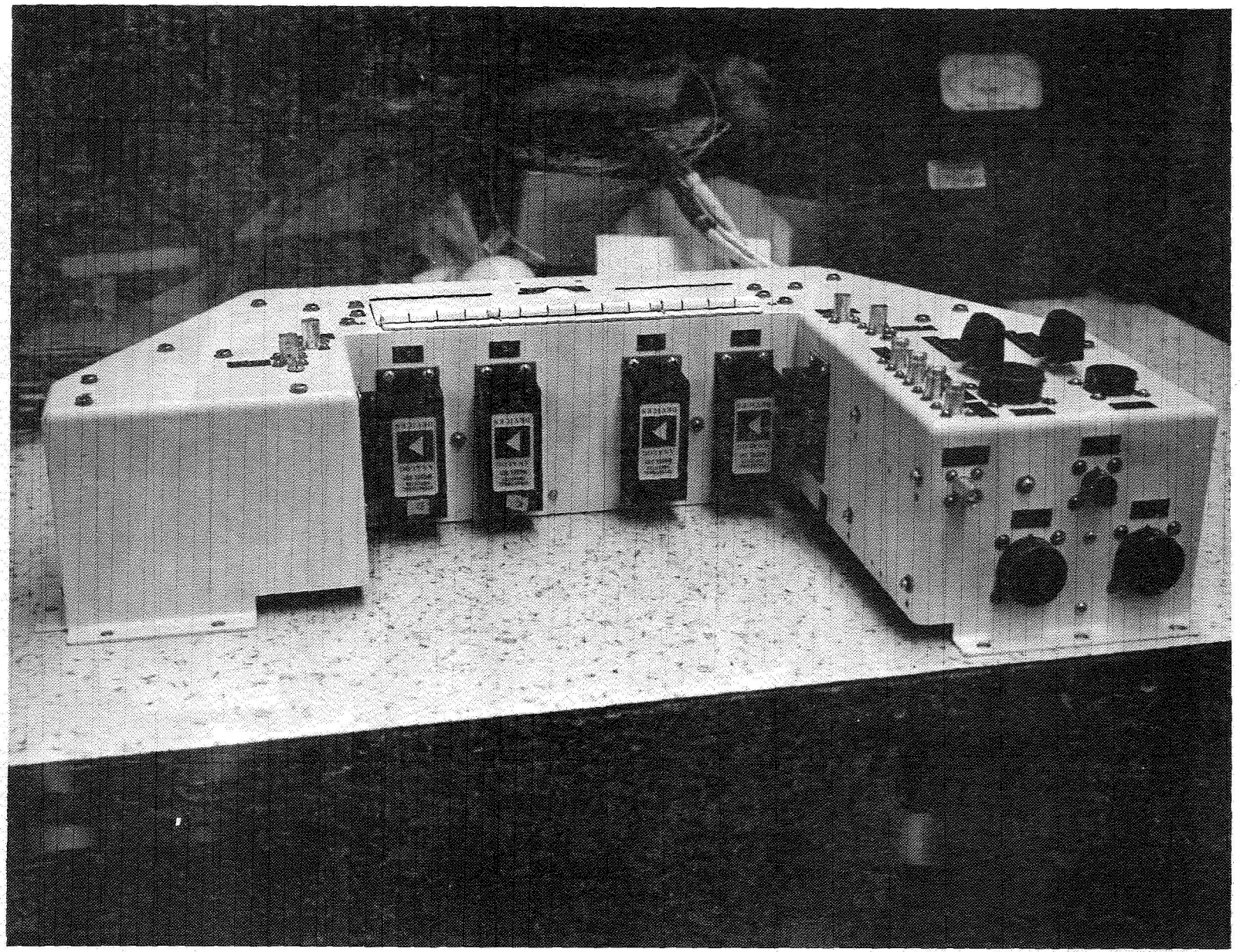

Figure 17. - Electronic unit - Exterior View

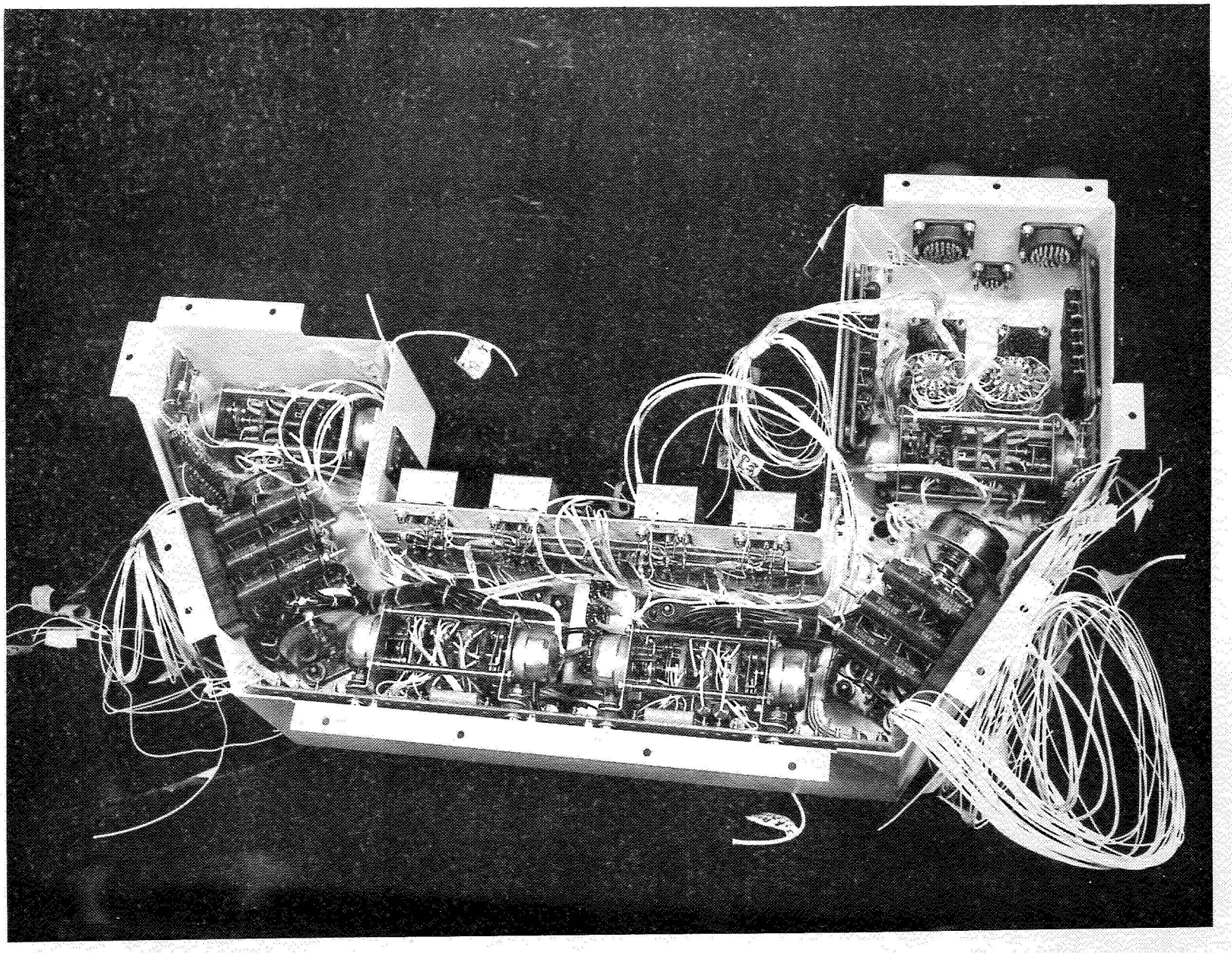

Figure 18. - Electronic unit - Interior view, nearing completion

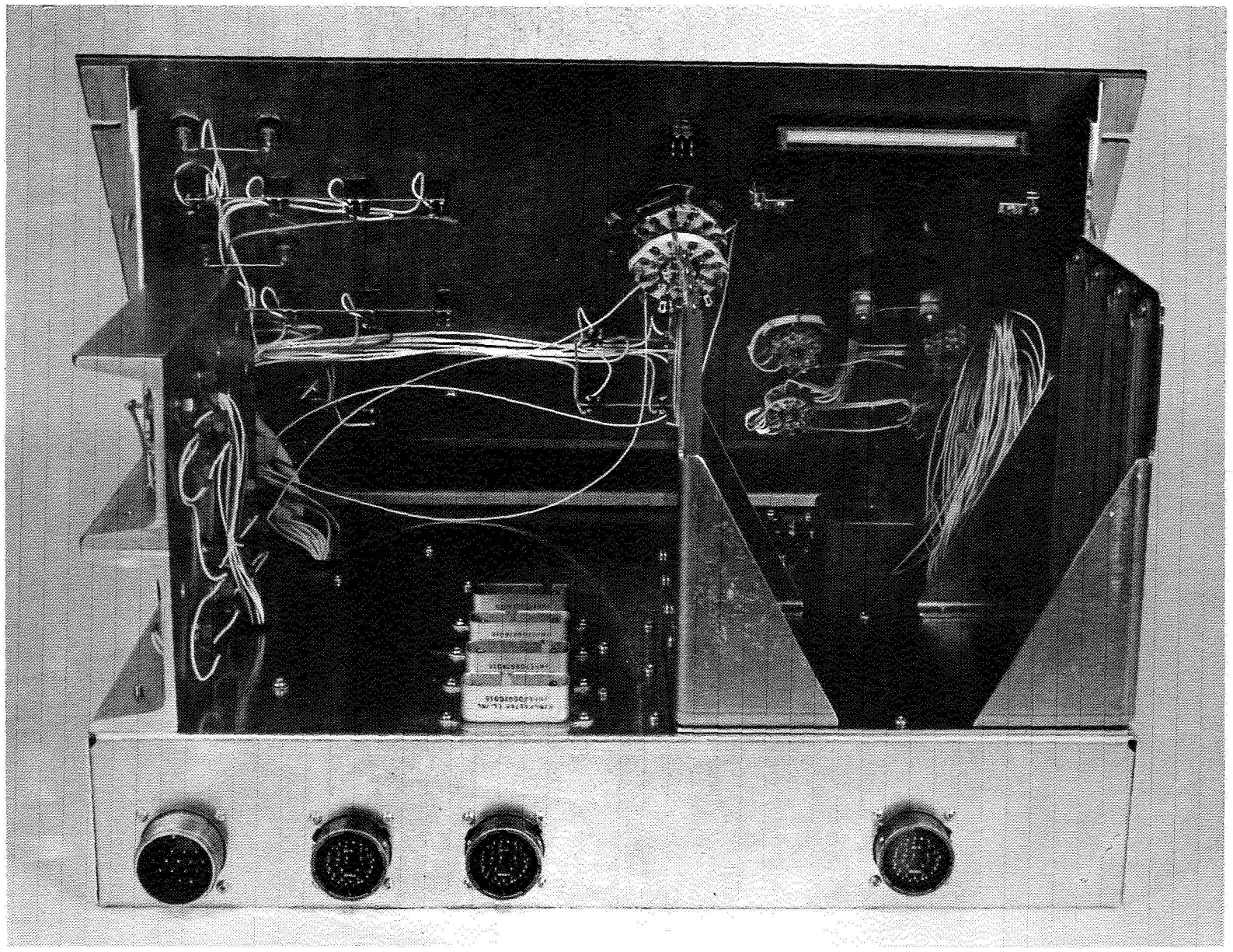

Figure 19. - Photometer control assembly, nearing completion

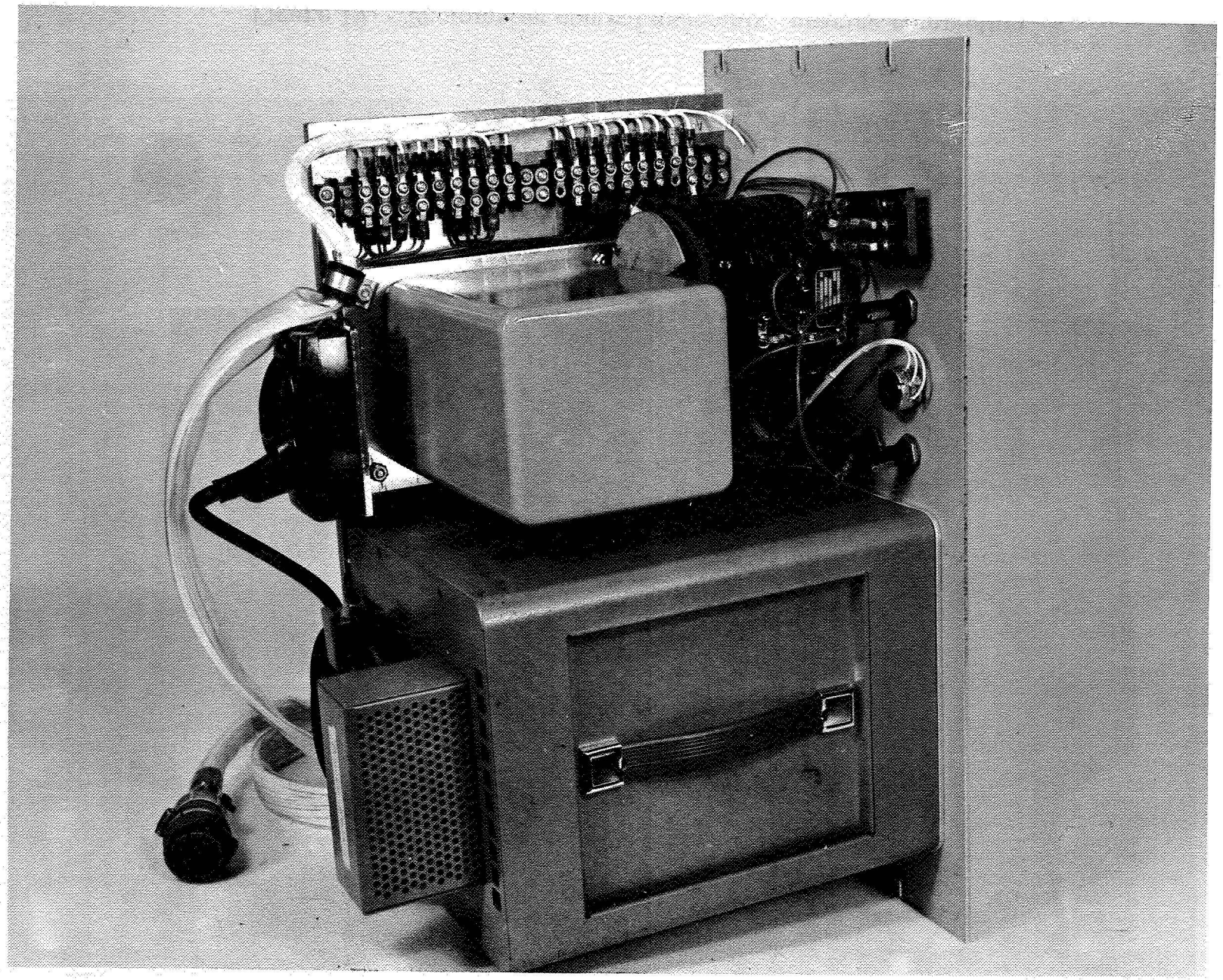

Figure 20. - Power unit assembly

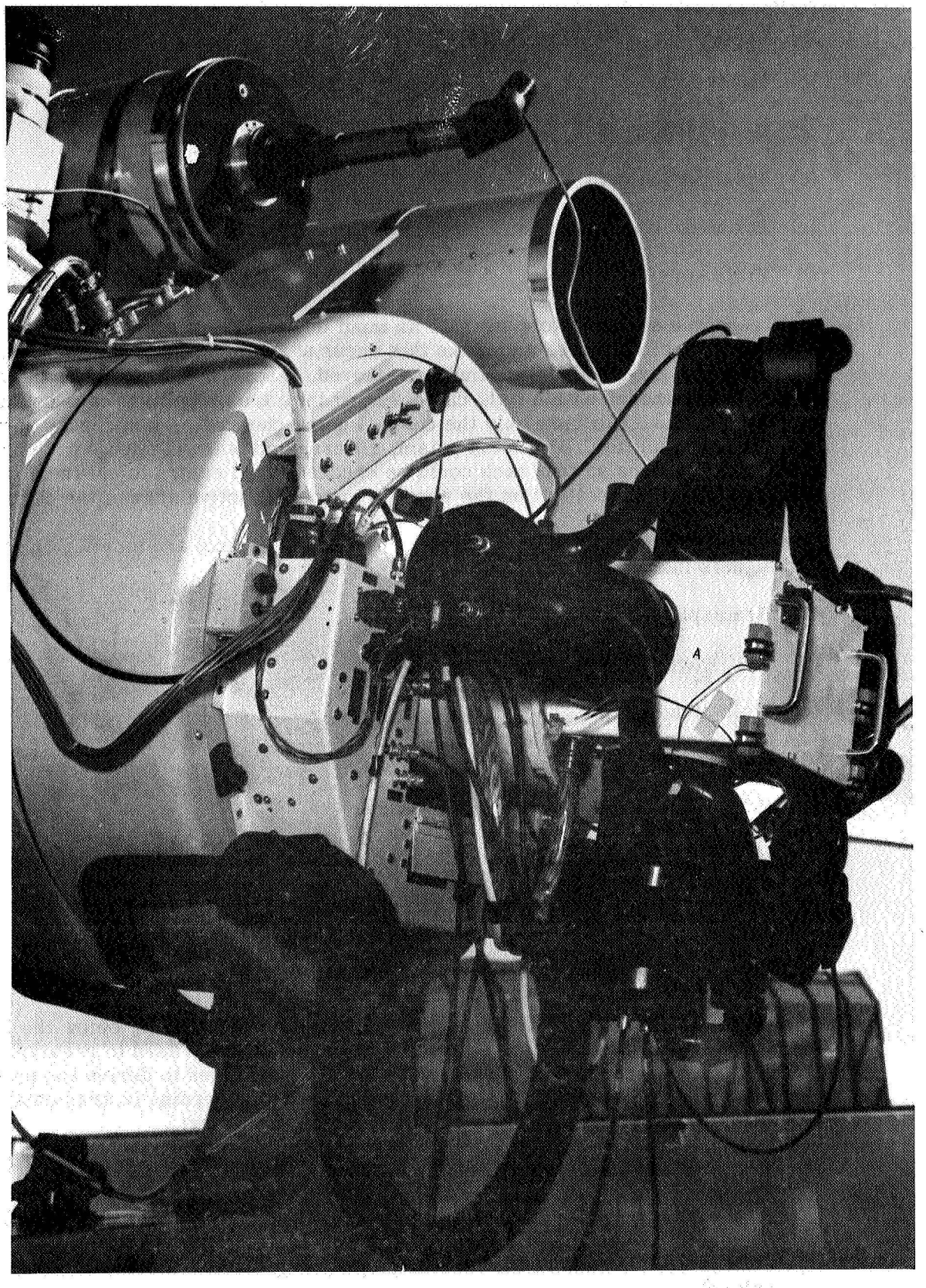

Figure 21. - New five-color instrumentation - Telescope Installation

(a) Optical ray path through system

(b) Fabry focus

(c) Beamsplitter, S-1, S-20 paths

(d) Polarization path

(e) Eyepiece alignment and focus conformity

(f) Field stop focus

The technique used was to culminate an input beam to correspond to that of the telescope at the prime focus, and make this occur at the location of the field-stop plane. Then with the photomultiplier housing removed, a screen was placed at the position of the photocathode, with a light cap covering this; thus, the light caps could be removed individually to view only the channel being checked. Then checks were made with the beamsplitter, Wollaston prism, filters, and other elements in their various operating positions so that each could be checked in all colors to ensure alignment such that the light spot fell on the screens inside the active area of the photocathodes.

Functional checks were also made of all the active control and monitoring actions and signals including:

(a) Beamsplitter drive

(b) Half-wave plate rotation

(c) Wollaston prism

(d) Color filter wheels

(e) Head rotation position monitoring signal

The photomultiplier housings were then installed and the complete unit checked.

This checkout and alignment was made simultaneously. When all alignments were completed, the above check showed the unit to be entirely satisfactory.

(2) Electronic Assembly

The electronic assembly, which mounts on the telescope directly below the instrumentation assembly unit, and is directly connected to it, is used to preamplify and process the photomultiplier signals and control its voltages to derive the proper photometric output signals to the control console and recording instrumentation circuits. Bench checkout of this unit included the following:

(a) Preamplifier gain stepping switch action (check action both directions).

(b) Differential amplifier gain stepping switch action (check both directions).

(c) Gain levels for each of the various steps (for precise conformance to design values).

Note: preamplifier gains are in six 2-magnitude steps; differential amplifier gains are in twelve 1/2-magnitude steps (see Table II).

TABLE II. - AMPLIFIER GAINS

PREAMPLIFIER (A) GAINS

Gain position	Gain (magnitudes)			Gain position	Gain (magnitudes)		
	B, V (S-20) R, I	U	V (S-1)		B, V (S-20) R, I	U	V (S-1)
1	0.0	0	0	4	6.0	5.994	5.984
2	2.0	1.995	1.986	5	8.0	7.994	7.984
3	4.0	3.994	3.984	6	10.0	9.994	9.984

DIFFERENTIAL AMPLIFIER (B) GAINS (ALL COLORS)

Gain position	Gain magnitudes	Gain position	Gain magnitudes
1	-0.497	7	+2.500
2	0.000	8	+2.995
3	+0.495	9	+3.489
4	+0.995	10	+4.005
5	+1.505	11	+4.503
6	+2.003	12	+5.000

OPERATIONAL AMPLIFIER (C) GAIN (ALL COLORS)

Mode	Gain position	Switch	Gain magnitudes
Nonintegrating	1	-1	-0.991
	2	-1/2	-0.497
	3	0	0.000
	4	+1/2	+0.495
	5	+1	+0.989
Integrating	6	10 meg-ohms	-2.500
	7	4 meg-ohms	-1.505
	8	1.54 meg-ohms	-0.469
	9	0.630 meg-ohms	+0.502
	10	0.249 meg-ohms	+1.509
	11	0.100 meg-ohms	+2.500

(d) Adjustment range of each of the four dark current compensation potentiometer circuits.

(e) Adjustment range of each of the six U-B-V and six V-R-I color compensation potentiometer circuits.

When these checks were satisfactorily completed (including all necessary alignments) the photomultiplier units of the instrumentation head were connected by their proper cabling to permit interface and functional checks. (Later, after completion of the next two units, they too were connected to the electronic unit and complete functional interface checks made.)

(3) Photometer Control Assembly

This assembly is the means for controlling and monitoring the functions of the above two assemblies, and its bench checkout was carried out as follows:

First, since many of the control functions and sequencing operations are generated by the logic boards, a checkout of each of them was carried out separately before installation in the control assembly. These boards are shown in Figure 22, and their checkout consisted of checking through electrically each circuit function of each board. Then they were installed in the control assembly, and their function checked out while installed. The functional checks of the control console included:

(a) Mode selection

1. Photometric or polarimetric
2. Automatic or manual
3. Color compensation (in or out)

(b) Control functions

1. Photomultiplier amplifier gain control
2. Filter position advance
3. Mirror/beamsplitter position control
4. Output signal control

(c) Monitor functions

1. Meter reference
2. Gain level indications
3. Filter identification
4. Half-wave plate position indication
5. Head rotation angle position indication
6. Mirror/beamsplitter configuration indication

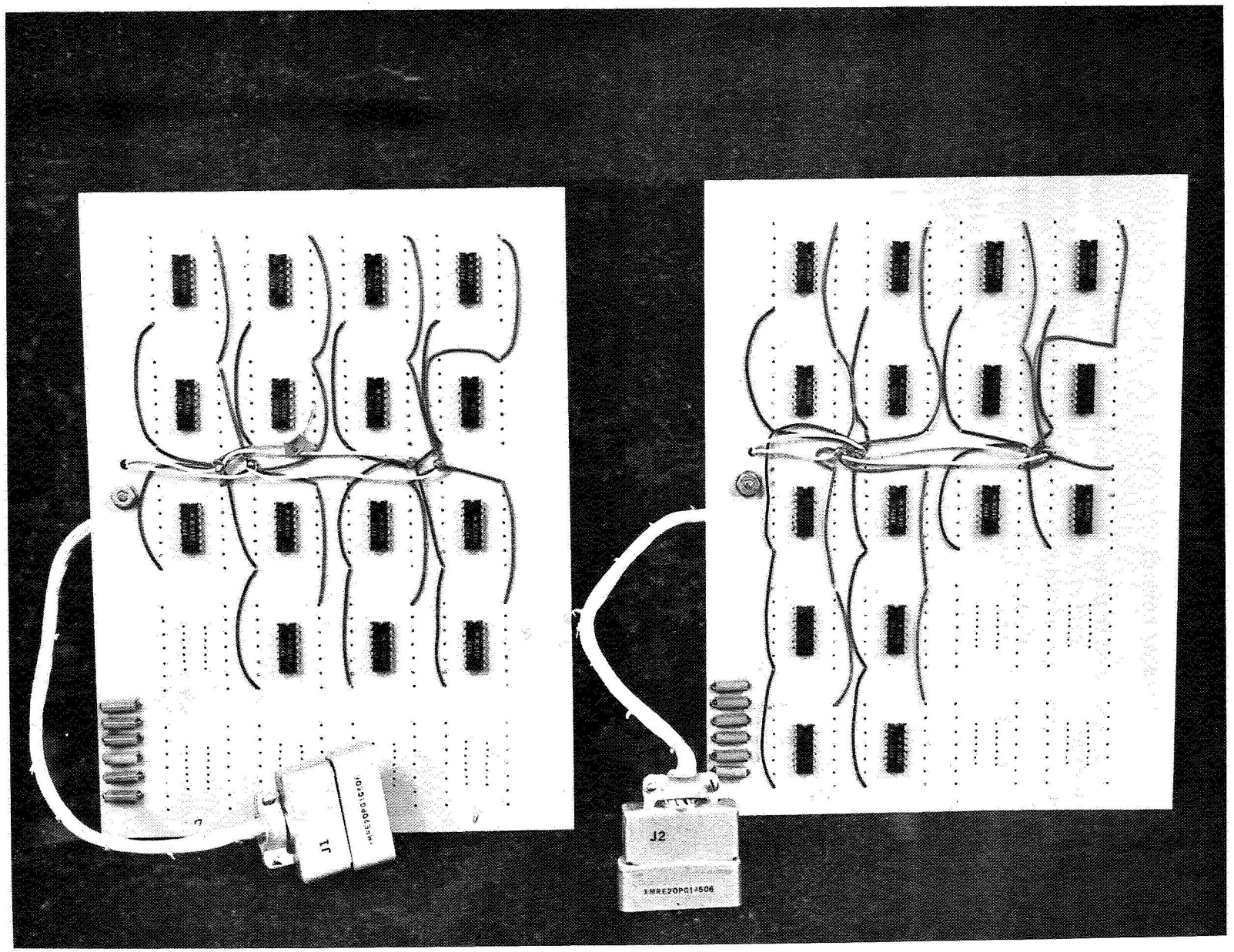

Figure 22. - Pair of logic boards

(d) Integration functions

(e) Sequence time generator (timer)

(f) Tone generator control

The technique used in these checks was to set the various modes sequentially, and for each apply the various control functions and verify the output signal at the proper connector pin. The monitor functions were checked in a similar way by applying the input signal to the proper connector pin and verifying the corresponding indication on the panel. The integrator function was observed on the meter with an input signal voltage level applied at the various RC time constant settings. The recorder outputs, (as well as the tone generator control) could also be checked with these input signals applied. The sequence generator was operated over its range and observed on the meter and at the outputs. The quality of the logic functions generated were also observed on an oscilloscope.

(4) Power Supply Checkout

The power supply for this system includes a low voltage power supply and a high voltage power supply. The low voltage supply actually provides three output voltages, and the checkout included:

(a) Check of the regulated 15-volt DC output reference and signal amplifier voltage.

(b) Check of the 6-volt DC logic circuit (and tone generator) supply voltage.

(c) Check of the adjustable 55-volt, 60-cycle AC solenoid actuator pulse supply voltage.

The voltage outputs and regulations were checked by both varying the line voltage from 105 to 125 volts and varying the load from zero load to full load and measuring the corresponding output voltage variation to ascertain that design values were not exceeded. The low voltage supply met all performance specifications.

The high voltage supply provides the regulated 1500 volts DC to the photomultiplier, and checkout of this unit consisted of monitoring the output voltage as the load was varied from no-load to full and the line voltage was varied from 105 to 125 volts. The unit performed in accordance with specifications.

(5) Interconnecting Cabling Checkout

All interconnecting cables were checked out for proper connections, continuity, and absence of shorts prior to use in the system.

(6) Cryogenic System

The following checks were made on component elements of the cryogenic system:

(a) Photomultiplier assemblies (including complete housings) were each bench checked in the lab by applying proper anode voltage to the photomultiplier, covering the windows with opaque material (aluminum foil), and applying liquid nitrogen through a solenoid valve controlled by a regulator connected

to the thermocouples in the housing. The photomultiplier output was fed to a Schoeffel M600 photometer unit, and both the photometer output and temperature recorded. The the test was activated with the regulator set to the control temperature and the photometer output (dark current) observed from ambient through cooldown and until stable operating temperature was reached (1/2 hour or more) to verify that satisfactory low and stable dark current were reached. In the final version (which was tested and incorporated after the initial mission was completed, as stated previously) the regulated operating temperature for the S-20 units used in these tests was - 50° F (although they were checked to lower temperatures), while that for the S-1 units was -180° F. Dark currents obtained under these tests were 10^{-10} amps and 10^{-12} amps, respectively, for the S-20's and the S-1's.

(b) The window heaters were also operated during these tests to verify their capability to prevent frost or dew. This was checked by opening the covering at the end of the tests with the cryogenic system continuing to operate, allowing some dew or frost formation to accumulate and checking on the ability of the heater to reduce it and clear the window.

(c) The temperature controllers were functionally checked.

(d) The cryogenic lines and joints were checked for leakage, and the solenoid valve action checked both ambient and cold.

System checkout. - The system electro-optical units were interconnected on the bench for interface verification, installed on the observatory, then given a complete system checkout. This system checkout was carried out, after making proper final alignment and adjustments, in the following manner.

For light input the telescope was aimed at either a distant light source (as an artificial "star" where a full-point source was not critical) or an actual star. The electronic and cryogenic systems were turned on, the cryogenic "Under Temperature" alarm system checked and reset, and the recorder used to record system outputs. The system was then checked as follows:

(1) Dark current balance (light tube covered) check for all four channels.

(2) Color compensation match - check both photometric and polarimetric for the three colors in each of the two pairs (12 adjustments in all)

(3) Control and monitoring functions

(a) Beamsplitter/mirror assembly

1. Set controls for each configuration, note corresponding light indication.

2. Check interlock (neither mirror will go "in" when the other is "in").

(b) Amplifier gains

1. Set signal switch (below meter) on "reference"

2. Set reference switch to "VRI PA" (first position)

3. Using VRI gain switches in center of panel run through all 12 steps both ways. Note meter and recorder identification trace indication of each step, and note gain ratio conformance to design values (see Table II) as indicated on intensity trace.

4. Repeat above steps for differential amplifier gains "VRI DIFF"; all 6 steps both ways.

5. Repeat above steps for UBV gains, both pre amp ("PA") and differential amplifier ("DIFF"), (control switches located below VRI switches).

(c) Cycle timer (sequence generator)

Note: This will also verify the half-wave plate operation in UBV

1. Set reference switch to "$\lambda/2$", and set switch at lower right side of upper panel to "$\lambda/2$ SEQ".

2. Put polaroid filter cap over light tube, and put three hand knobs on instrumentation assembly to the "polarization" settings.

3. With switches immediately to the left of the latter switch, operate cycle timer in manual, automatic, and semiautomatic mode at various cycle time values.

4. Verify action by meter indication advance for each step.

(d) Color band filters

1. Set the reference switch to the "UBV" and "VRI Filter" positions and note filter indicated (see Figure 16).

2. Using controls and indicator lights on right side of panel, operate and check filter advance.

3. Put one filter wheel only a step ahead (out of synch with its mate). Actuate filter to verify synch system.

4. Operate in all combinations (manual, automatic, etc.) for both filter sets (monitoring with reference meter and recorder), and with cycle timer.

5. Check "re-set" action.

(e) Color compensation

With a red or blue filter, turn color compensation switch off and on, noting effect on corresponding intensity signal.

(f) Integrator

1. Set signal switch to "INT A"

2. Set input switches below it to right-hand positions

3. Set "INT A RC" switch (lower left) to mid-range.

4. Note integrator action by saw-tooth output on meter and recorder intensity trace.

5. Vary "INT A RC" values, and note response.

6. Repeat above steps, using Integrator B.

7. Change Integrator Input Switch to "DIFF", and note response to changing differential amplifier gains.

(g) Rotating head

1. With head in polarization configuration for two hand knobs (field stop position and Wollaston prism) but $\lambda/2$ plate out, set reference switch to "HEAD" (Signal switch on "REF"). (Have polaroid filter cap on light tube.)

2. Set recorder input switch to "DIFF".

3. Rotate head to next 36° position and lock. Note meter and recorder head position trace indication, and note response in intensity channel recording traces.

4. Repeat, resetting head to each of the other positions, then back to zero.

(h) Field stop monitoring indication

1. Set reference switch to "FIELDSTOP" position.

2. Set all three instrumentation unit knobs in photometric configuration.

3. Rotate field stop knob successively to each of the positions.

4. Note position indication on meter, and note response of intensity trace proportional to the various field stop areas with telescope using bright sky or diffuse field input only (no star).

5. Verify "adjacent sky" stop by having star in first one stop (tracking orientation) then in neither, then in the other - with UBV recorder input setting. Note intensity trace response on recorder.

6. Repeat step 5 with recorder input switch on "DIFF". Note intensity trace.

(i) Tone generator

1. Set signal switch at "UBV C".

2. Point telescope at star or light source so it is centered in field stop area.

3. Advance or decrease UBV gain until meter reading is around half scale.

4. Set tone generator switch (bottom center) to "C".

5. Advance threshold switch (immediate right) to give solid tone.

6. Verify that reduction of signal to low level will cut off tone, and increase will restore it. (Swing telescope to take star in and out of field stop area.)

(4) Tracking Operation

With the tracking control system activated, a star (or satellite) was acquired and instrument controls at console operated to record photometric signals such as to verify compatibility of new instrumentation system with the tracking and other elements of the observatory and their operation together. Operation was then switched from shore power to the motor generator system to verify complete system interface and operational compatibility.

During these checkout operations and subsequent field verification trials many discrepancies and problems were encountered and remedied in order to complete the checkout satisfactorily and obtain an acceptable system operation in accordance with design performance and objectives. The eventual corrections of all difficulties and subsequent satisfactory operation of the system verified the soundness of the design and of the general concept developed for the new five color U-B-V-R-I system.

It had originally been planned to complete the system checkout and brief field verification operating trials before dispatching the system to Yuma in late January to begin its first deployed assignment on the second observation interval of the contract. To complete the final aspects of the system checkout and to conduct the field operating trials, clear skies were required to demonstrate calibration star and satellite tracking and measurement capability of the system.

Fortunately, as checkout progressed during the middle and third week of January (expecially the latter), an unusually good percentage of cloudless nights prevailed. However, in the final steps of system checkout where stars were needed, and before field verification trials could be conducted, bad weather prevailed with at least a week of stormy, cloudy weather forecast, thus seriously disrupting the planned schedule. If it had been possible to get the observatory completed and on the road by then, weather would not have been a problem.

In view of the weather, observing schedule, and satellite visibility windows, a conference was held with NASA participating, to review the situation and decide on the best course of action. One suggested plan was that, since weather was the main problem, this might be circumvented by transferring operations to the Goodyear Aerospace plant west of Phoenix, Arizona. There the balance of the checkout and any required debugging could be carried out while tracking stars and satellites, and the data obtained in this process could constitute the initial observations (since they would simply be made from Phoenix rather than the even more ideal conditions at Yuma). Then as soon as the system checkout and acceptance trials were complete, operations could be moved to Yuma (a distance of only about 175 miles), and the photometric observation continued according to the original plan.

This plan seemed to offer considerable advantage over any others. Arrangements were checked out with GAC Phoenix plant personnel in corresponding disciplines (electronics, physics, astronomy, plant operations, and management) and found satisfactory for all needed technical support, etc. Some final additional work on some of the units was deemed advisable as a result of checkout operations, and this could be accomplished without undue rush or loss of time by retaining these units only. The rest of the system could be dispatched (the observatory, with the new system installation and all mission support equipment and supplies) immediately, so that it would be in transit during the bad weather here. Then the revised units, which could

be completed and checked out in three days, could be carried by the engineer involved and arrive by commercial airline at Phoenix in time to install in the observatory upon its arrival (transit time 4-1/2 days).

After careful consideration, this plan, which seemed to entail the least risk and virtually eliminated schedule slippage, was considered most advisable. It offered no disadvantages which were considered serious, whereas the alternatives had to contend with the problems of a period of bad weather which was developing at Akron. Accordingly, it was decided to adopt this plan and arrange for immediate departure of the observatory. It was loaded, secured, and made ready for transit in approximately 18 hours and started on its way. The field crew was also dispatched according to the original plan, so that they arrived in Phoenix at nearly the same time as the observatory.

Everything worked out quite well in accordance with the revised plan and therefore very little schedule time was lost. The balance of the equipment was installed in the observatory right after its arrival in Phoenix, and the now combined program of completing system checkout and making satellite photometric measurements proceeded. Approximately 12 days later, the operations were moved to the planned site near Yuma and the mission carried on as originally planned.

All parts of the system proved quite satisfactory after the initial shakedown period except for the liquid nitrogen cryogenic system. Because of problems encountered with it in the original version it was elected to go to dry ice cooling, and this was used for the balance of that observation mission. The system was then returned to Akron and the cryogenic system revised to its current satisfactory configuration as described previously. The system was shown in a subsequent test demonstration and in the subsequent observation intervals to be entirely satisfactory.

All the operations and data covered in this report (except for that taken at Palomar during the first observation interval) was taken with this new extended range five color instrumentation system. It represents one of the most advanced photometric data gathering capabilities which exists today.

Field verification tests. - The field verification tests were carried out at the Goodyear Aerospace Phoenix, Arizona plant and at Yuma in combination with the other operations as described above. This included a demonstration of proper overall operating capability as well as specific tests in each of the principle operating modes. These were as follows:

(1) System Gain Factor Calibration

The system gains, when using the various amplifiers (pre-amp, diff-amp, etc.) are a very important part of every measurement taken, and are entered into the basic computer program for reduction of the star calibration and satellite data. They must also be stable (and are established in this system by precision resistors) to give consistent results such as those demonstrated by star measurements and their "goodness of fit," which was checked as described below (next paragraph) under calibration stars.

Accordingly, checks were made to verify and precisely measure the exact gain values. The method was to measure, while tracking a constant light source (star), the output voltage ratio when gains are switched from one to the other. The results obtained are tabulated in Table II above.

(2) Star Calibration Measurements

The observatory was set up for operation in the normal manner. Second order extinction coefficients and system scale factor data were obtained for a preselected list of appropriate calibration stars, using the techniques described in the "Star Calibration Mission" section of the Operations and Maintenance Manual.

The resulting data was later reduced to determine its validity and to fully demonstrate the operational capability of the system to make accurate and valid calibration measurements. The coefficients obtained and related star measurements were checked for goodness of fit. The results are reported on page 102 of this report.

(3) Five-Color Photometric Operation

The system is designed to carry out photometric operations involving measurements in the U, B, and V bands (with the S-20 photomultipliers) and in the V, R, and I bands (with the S-1 photomultipliers) simultaneously. It is able to electronically difference the outputs of the two photomultipliers in each pair (S-20 or S-1 pair) and thus eliminate sky background reading from the signal. It is also able to integrate the photometric signal obtained to reduce the effects of scintillation and other noise source and simplify the reading of a true average data value. Accordingly, the system was operated in these various modes while tracking a single source (star) to verify such operating capabilities. Figure 23 shows an example of the recording obtained, with the left portion showing a straight (nonintegrated) signal output, and the right-hand portion showing the recording with the signal integrated (labelled "integrating mode").

Note the filter identification traces on the lower part of the chart (labelled "U," "B," and "V" - for upper trace, and "V," "R," and "I" - for lower trace); and note the change in the corresponding signal level traces (as labelled) in the upper part of the chart for the nonintegrating portion, and the center portion for the integrating portion. The typical gain level identification traces (4) are also labelled in this sample data record.

Photometric data taken on stars in this part of the test and field operations were later reduced and examined for accuracy and validity, as previously stated above, and presented on page 102 of this report.

(4) Polarimetric Operation

The system is also designed to make similar polarization measurement in various modes and color bands, and this was also checked by operating the system in each mode using a star as a target. Figure 24 shows data taken on a nonpolarized star (B.S. 5340, Arcturus) showing both the plain and integrated signals. Introduction of a polarizing filter results in the strong polarization indications shown in Figure 25.

These recordings were made in the V-band, and are typical of those obtained in other bands. However, for the R and I bands the half-wave plate installed does not function, and the rotating head is used for these bands. It gave analogous results, operating over a range of ±108° (again in 36-degree steps). It should be noted that 180° (±90°) is sufficient to cover the full range, and this is what causes the duplication shown in the 10 steps of Figure 25 (which total 360°).

Notice that Figure 24 shows no variation in signal value for either polarization

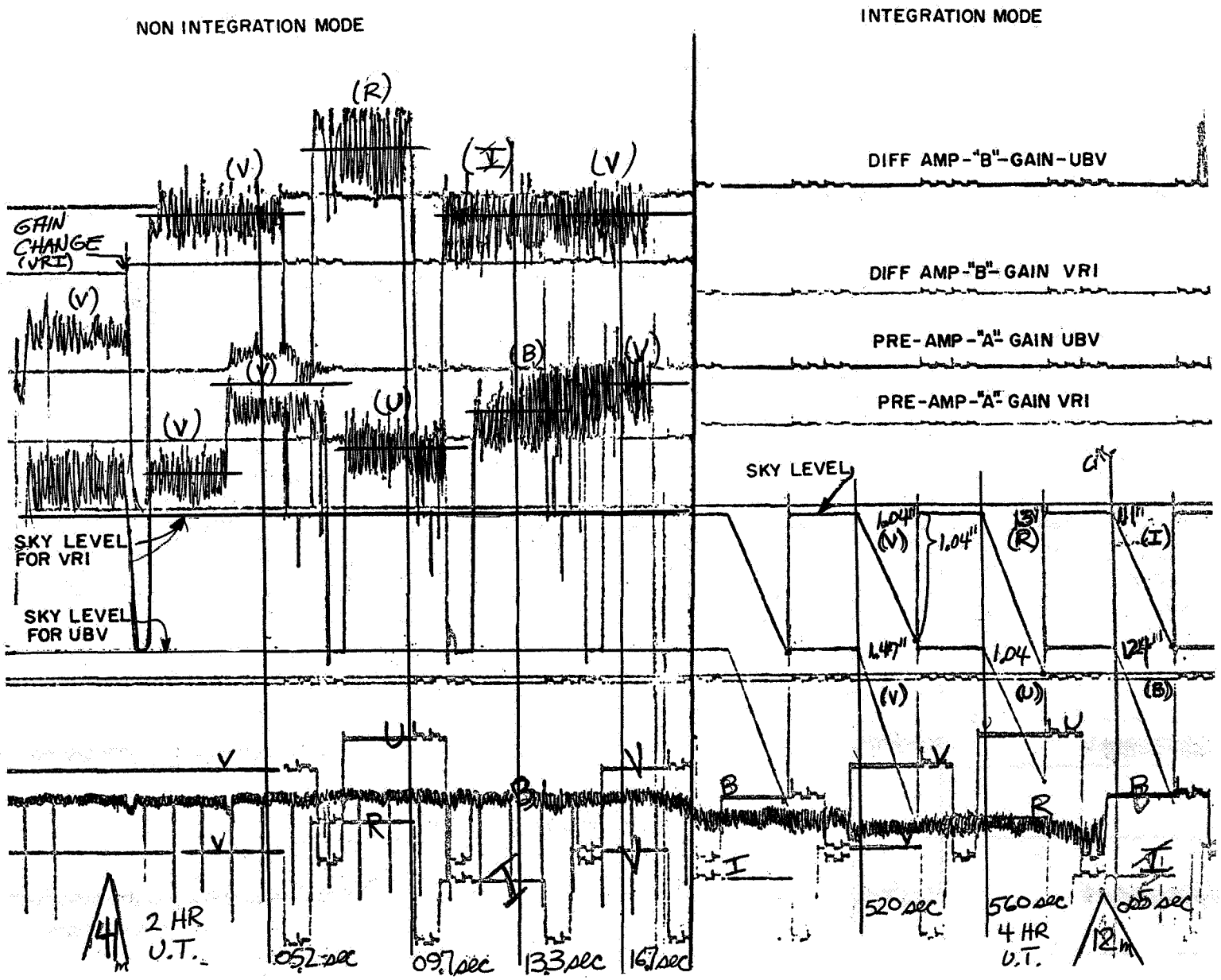

Figure 23. - Photometric intensity values in UBVRI

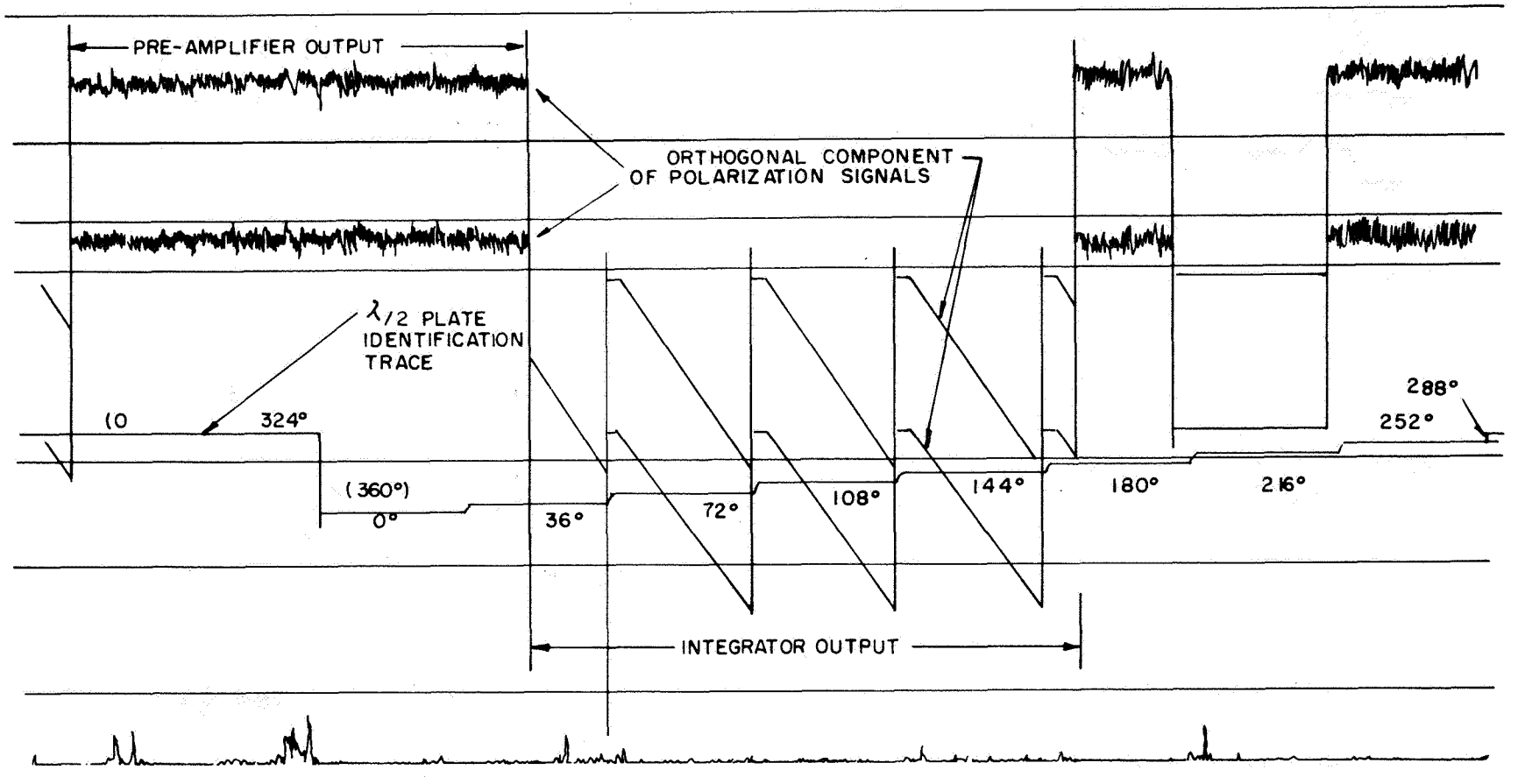

Figure 24. - Comparison of integrated and non-integrated polarimetric signal for Arcturus

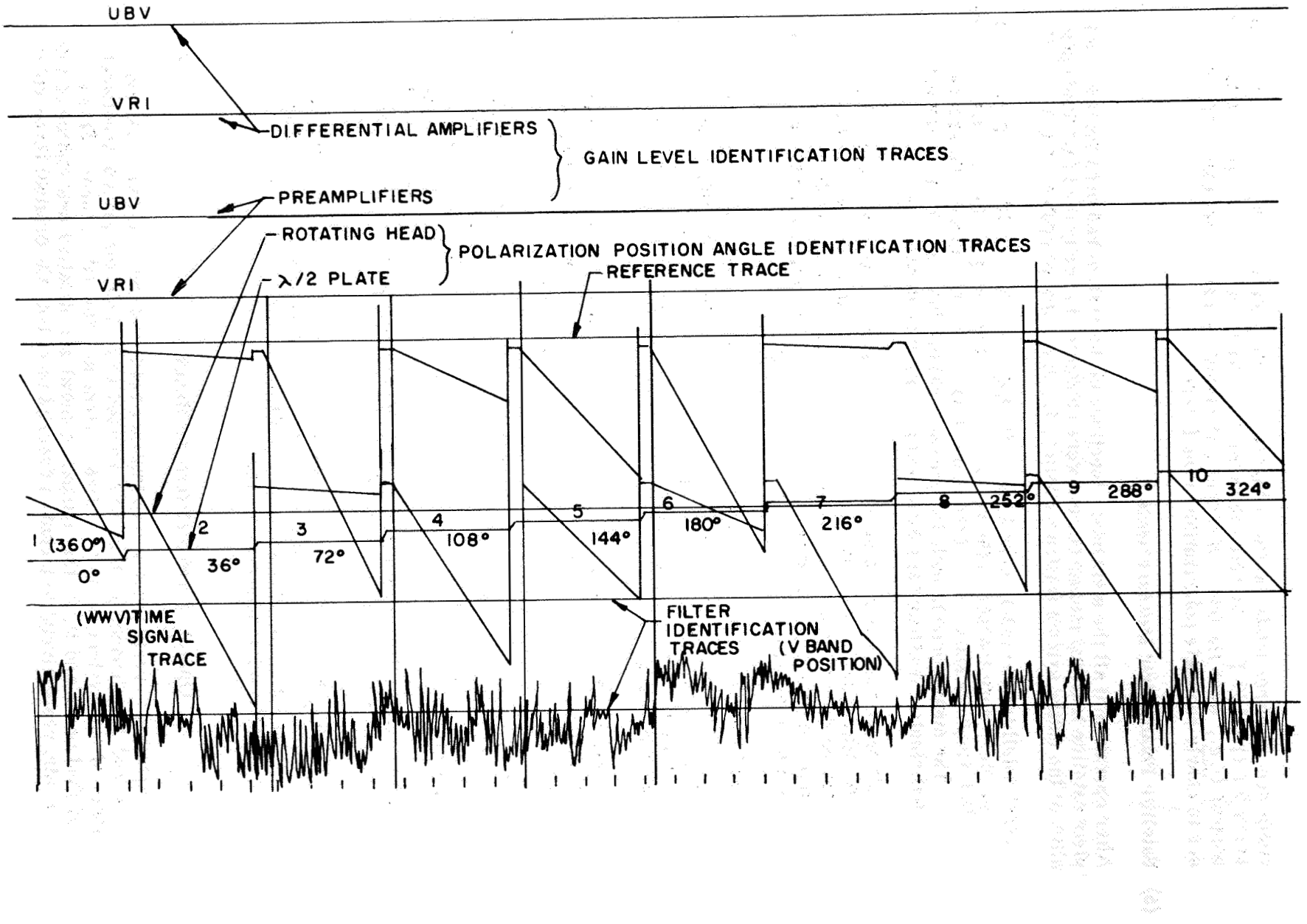

Figure 25. - Polarimetric signature of Arcturus with polaroid parallel to the declination axis

component in either mode, while in Figure 25 a complete cycle of values occurs for every 5 steps (180°). Also note the reciprocal character of the two polarization components (i. e., when the one is strongest, the other is least; practically zero here, due to nearly complete polarization of the filter).

(5) Satellite Photometric Measurements

After operation of all the elementary functions of the system had been verified, complete satellite tracking measurements were conducted to verify the integrated operation of the entire system (instrumentation, tracking control system, etc.).

Several satellites (including Echo I, Echo II, Explorer XIX, PAGEOS, Agena launch vehicle, etc.) were tracked in the various photometric and polarimetric modes. Figures 26 through 29 show some of the more interesting recordings of these measurements. The measurements included pre-pass calibration data (for primary extinction coefficients), satellite pass data, and post-pass calibration data.

These data were reduced and analyzed to determine their validity and provide required satellite measurement data. The results, described on pages 103 and 104, demonstrated the operational measurement capability of the complete mobile observatory equipment with the revised instrumentation system (a memorandum of joint acceptance was included in progress report number 6).

Two exceptions to the fully satisfactory operation were noted in the initial tests and operations. One concerned the capability for obtaining the polarization data by means of the rotating head method for the R and I (and back-up U) bands. This was later resolved to the satisfaction of all concerned, following reduction and analysis of the data, reported on pages 98, 99, and 106.

The second item was more serious, having to do with shortcomings of the original cryogenic system. The liquid nitrogen system was subsequently modified in order to meet the performance specifications originally conceived.

After the system was revised (as reported above on page 35), field tests with the NASA representative present were carried out (following checkout) to demonstrate the full capability of the entire system with the final cryogenic system in operation. This was done in Akron as a part of the third observation period. The system was shown to be entirely satisfactory, Figures 27 and 32 show data obtained with this final configuration. This data was reduced and analyzed, and found to be valid. The results are included on pages 83, 85, and 91.

A significant amount of field operations with this system followed the verification testing and operations reported above. These operations (along with the data obtained) have served to fully confirm the capabilities of the complete five-color extended range photometric observatory system.

Operation and Maintenance Manual

Following completion of verification and acceptance testing of the final five-color system, the Operation and Maintenance Manual was revised to include the proper treatment of the new elements of the system, and the entire system as effected by them. This included revision of Sections I and II, of the manual (general and detailed description of the system and components, respectively) to include a description of both the original three-color

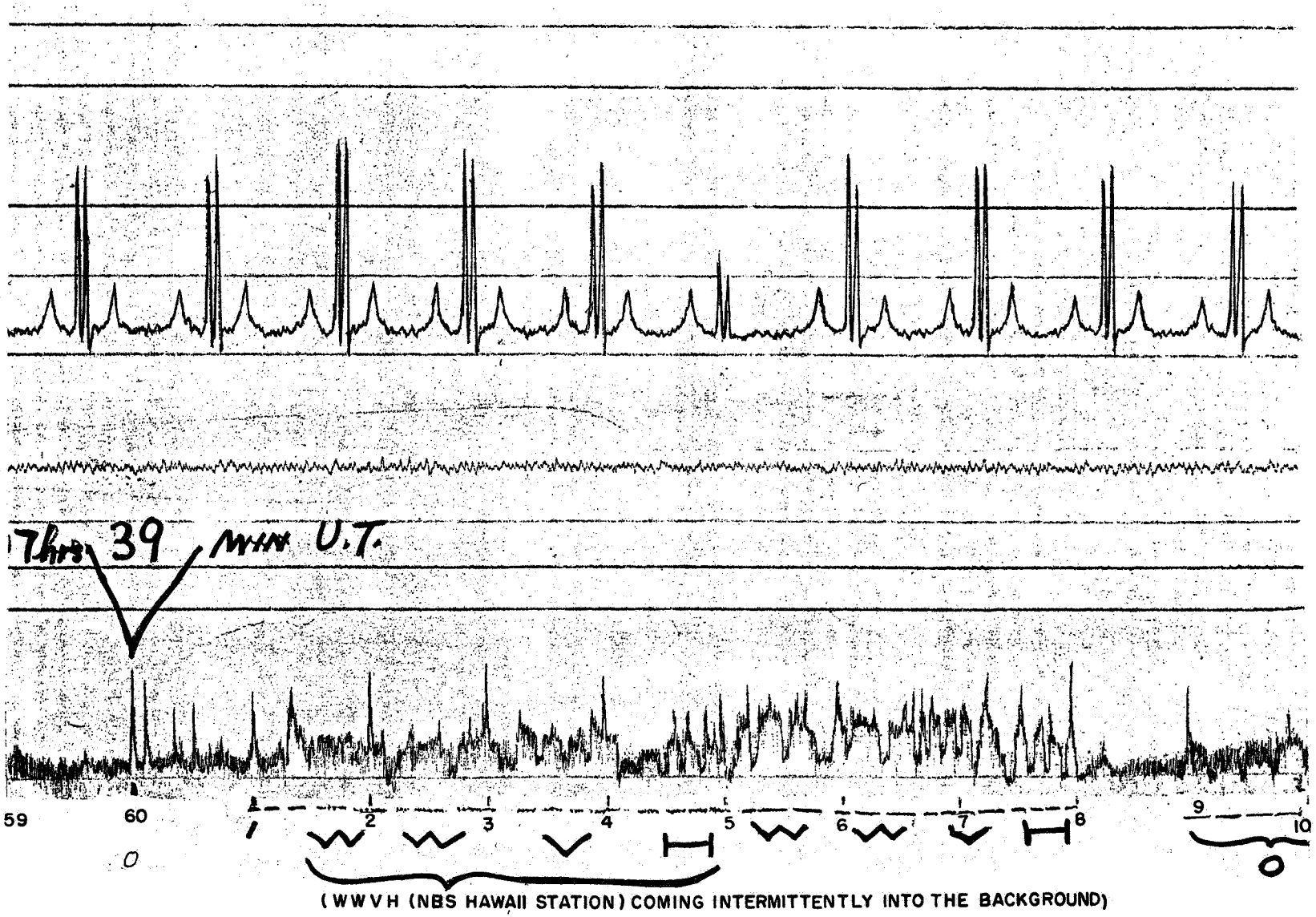

Figure 26. - Photometric signature of the PAGEOS rocket body

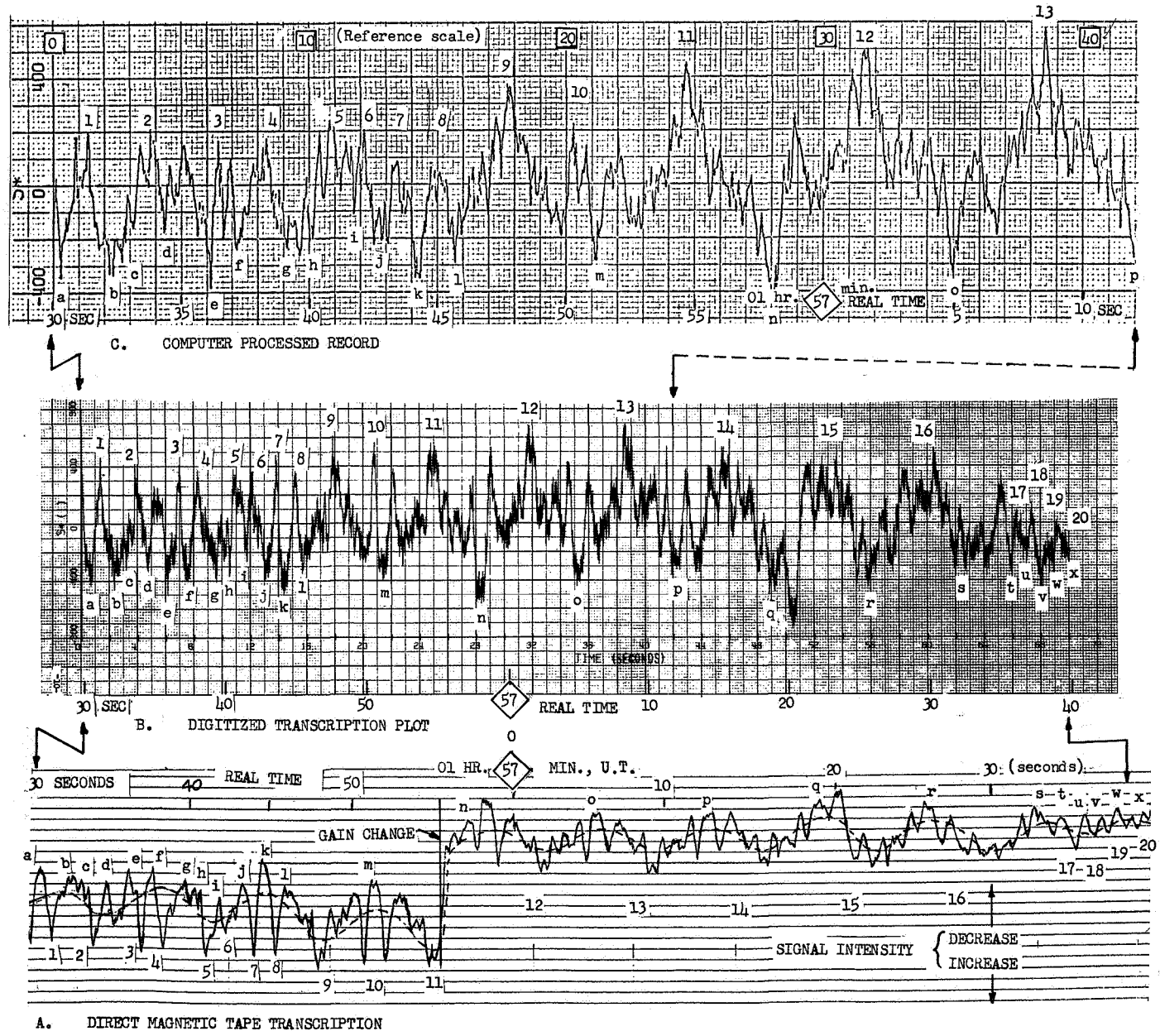

Figure 27. - Photometric signature of Explorer XIX

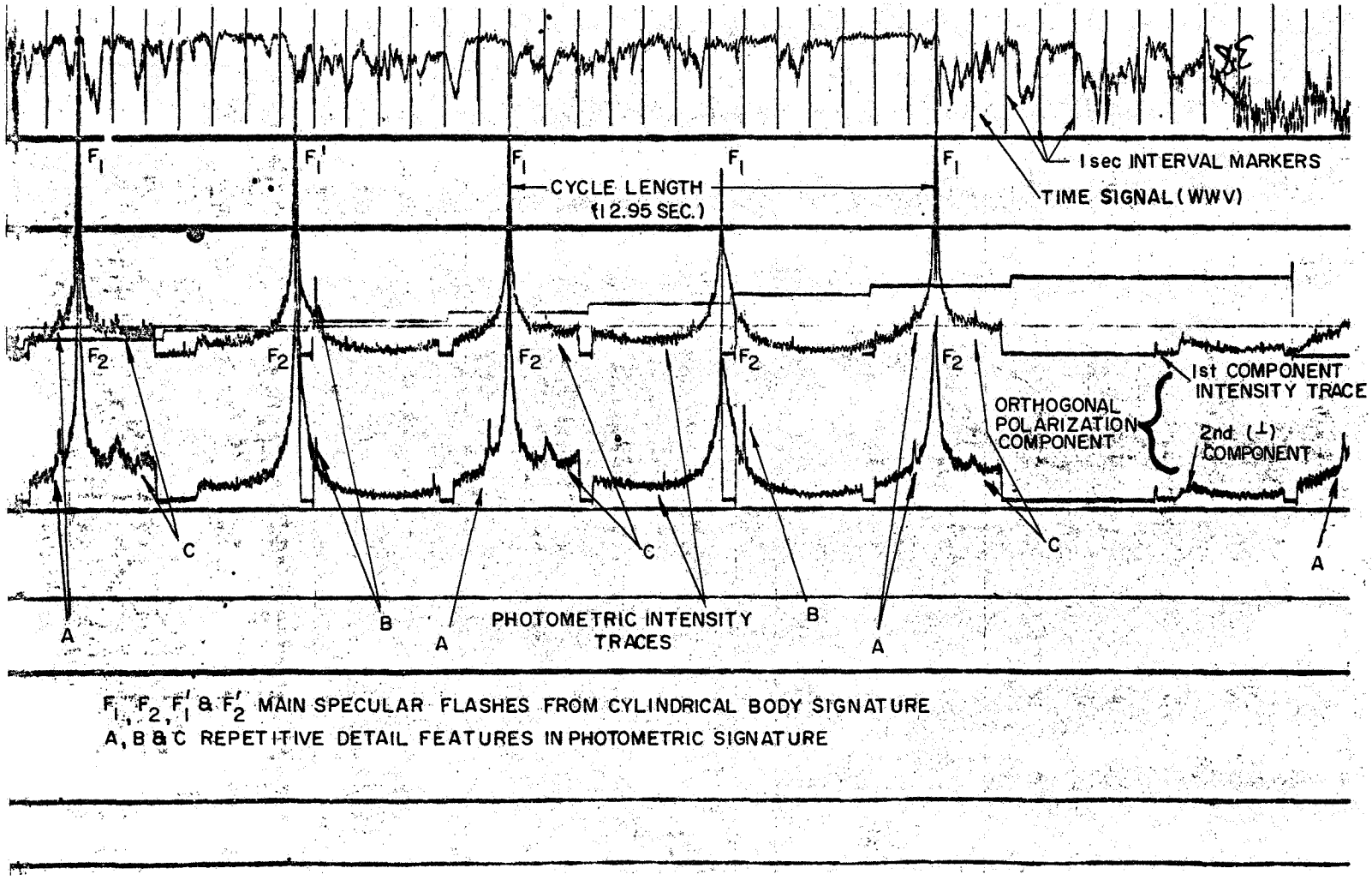

Figure 28. - Photometric signature of an Agena rocket body

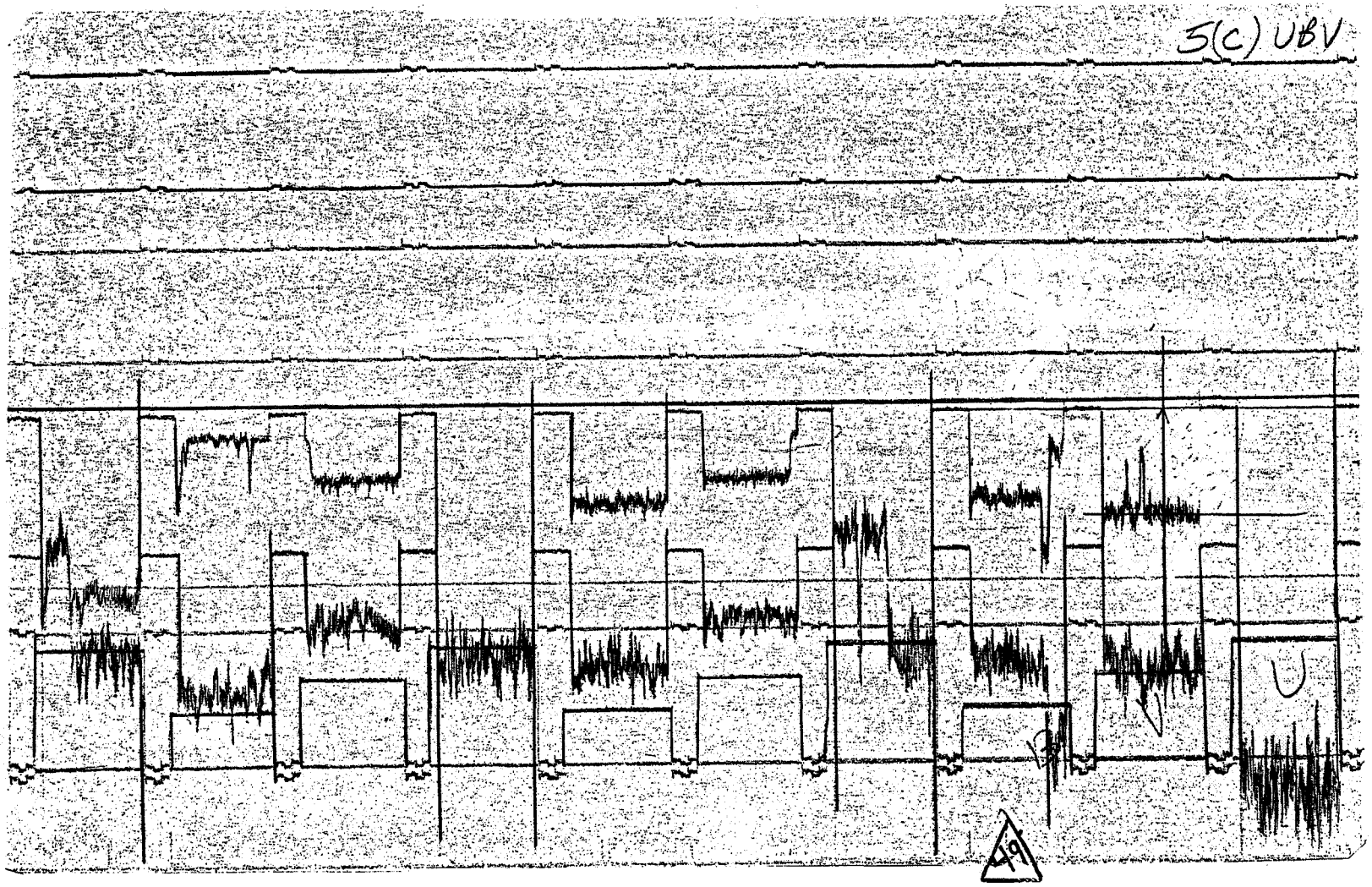

Figure 29. - Photometric signature of the star Sidus Ludoviciana

and the new four-channel extended range five-color system as optional interchangeable alternatives available to the operator.

Section III of the manual was similarly expanded to include the theoretical principles involved in the extended color band (R and I - red and infrared) regions - to about one micron - of the new extended range system.

In a corresponding manner, Section IV of the manual (Operations) was similarly expanded to explain how to operate the system in making photometric measurements with the new five-color system as well as with the original three color instrumentation. Section V (Data Reduction) was likewise expanded to cover data reduction in the new bands and modes of operation (e.g., integration) provided by the new system.

Section VI, covering maintenance, probably required the most expansion of all since it was expanded to fully cover all aspects of maintaining the new and much more complex instrumentation, along with its new regulated power supplies, cryogenic system, etc. New auxiliary manuals had to be provided to cover the new system components involved, and new drawings and diagrams for the manual (in addition to the new figures and illustrations) were provided as needed to cover the new equipment involved.

As a result of this revision to the manual, it now gives the same degree of coverage to all the new elements and aspects of the system as the original manual gave to the original system. Furthermore, the philosophy adhered to throughout was to fully retain the original system capability (since it can still serve as a simpler, highly sensitive, noncryogenic system, wherever appropriate, and as a back-up capability) and treatment of all aspects covered in the manual; while giving a similarly thorough treatment of the more complex new extended range system developed under this contract. It also fully explains what is necessary to interchange the two systems.

The new revised manual therefore represents full coverage of both the original and new configuration in a manner designed to provide the operators with all the essential information needed to properly operate and maintain the system.

SATELLITE PHOTOMETRIC/POLARIMETRIC MEASUREMENTS

Field Preparation

Before field observations could be performed, the observing site was selected and prepared, the mobile observatory was made ready, and transportation for the observatory and crew was arranged.

Site selection and preparation. - In selecting the remote sites for the photometric observations, several items were taken into consideration: excellence of transparency and seeing during the planned observing period, logistics, installation of power lines, transceiver instrumentation, etc., if required, security and observatory safety practices, latitude, altitude, and longitude determinations of the site (for satellite predictions and data reduction) ease of acquiring supplies, etc.

After the recommended site received NASA-LRC's approval, rental arrangements were finalized with the land owner. At Palomar Mountain the site preparation included the necessity of spreading a dust inhibitor. Provisions for "shore" power were found feasible and were made at all of the sites used. All selected sites had existing high security fences except on Palomar

Mountain, where the crew members were quartered on the same property and, in effect, provided a continuous watch over the equipment.

Table III lists the various sites from which the observations reported herein were made, together with the time periods.

TABLE III. - OBSERVING SITES

Date	Site	West longitude (deg)	North latitude (deg)	Altitude above mean sea level (ft)
Jul-Aug 1966	Palomar Mountain, Calif.	116.849	33.310	5640
Jan 1967	Phoenix, Arizona	112.361	33.434	970
Feb-Mar 1967	Yuma, Arizona	114.646	32.550	165
Jun-Jul 1967	Wingfoot Lake Knoll Site Akron, Ohio	81.378	41.024	1275
Sep-Dec 1967	Wingfoot Lake Knoll Site Akron, Ohio	81.378	41.024	1275

Principal reasons for operating out of the various sites were:

(1) Palomar

(a) Near-ideal transparency and seeing expectancy during the planned (summer) observation period

(b) Easy accessibility and logistic support

(2) Phoenix-Yuma

(a) Good transparency and seeing expectancy during the planned (winter) observation period

(b) Easy accessibility and logistic support

(c) Crew efficiency during winter

(3) Akron

(a) Expected economy

(b) Convenience to main plant

(c) New cooling system shakedown period

Observatory readiness and shipment. - Before the NASA mobile satellite photometric observatory was transported to each of the selected remote sites, the observatory was checked for any difficulties in performance of optical and/or electronic instrumentation, and the truck

was checked and lubricated to assure its road readiness. Finally, all needed auxiliary supplies and paraphernalia were put on-board and tied down. The truck was then turned over to the commercial truck driver who had been thoroughly briefed (verbally and in writing) on the truck handling, destination, route and communication checkpoints.

Satellite Predictions and Orbital Geometry

The observing missions were scheduled in accordance with satellite "visibility windows" forecast in advance from a projection of the local orbit sweep times. During the mission, discrete local pass predictions were generated by GAC's E1215 computer program in terms of culmination times, conventional altitude - azimuth and right-ascension-declination coordinates, and also four axis coordinates, from the latest orbital elements received from the Smithsonian Astrophysical Observatory and Norad. "Moonwatch"-type positional fixes on the satellites were used to keep track of the ephemeris time residuals (corrections) until new orbital elements were received.

To compute the time-correlated altitude, slant range, and phase angle geometric circumstances of the satellite for the purposes of photometric data reduction and analysis, the observed ephemeris time correction was used with the instantaneous anomalistic period to compute the satellite's effective mean anomaly at the epoch of the orbital elements.

Observation Procedure

This section describes the tasks of the observatory crew while on field missions. The crew usually consisted of three persons; crew chief, field astronomer, and technician. This section describes a few of the duties and responsibilities of the console operator and telescope operators.

On deck tasks. - Approximately two hours before the expected satellite acquisition time, the van was opened and the telescope uncovered except for the dark cap over the central light baffle. The cryogenic and high voltage systems were then turned on in order to allow ample time for the photomultiplier tubes to cool and stabilize. Meanwhile all auxiliary needed equipments and reference materials were assembled; binoculars, stop watch, star charts, computer predictions, observer support ladders, etc. The antenna was deployed and WWV time signals received. The plan for the night's operation was reviewed by several members of the observing crew.

About one hour prior to the satellite acquisition time, the dark currents were monitored and, if necessary, compensated, and (when the sky is sufficiently dark), the dark cap is removed. If, as is generally true, all the planned pre-pass calibration stars were accessible in the four-axis satellite acquisition mode, the mounting was then moved and clamped in azimuth and elevation to the computer-predicted settings that align the polar axis to the effective pole of the satellite's trajectory. If some of the calibration stars were not accessible in this polar attitude, they were generally reached by temporarily offsetting the polar elevation.

The first pre-pass calibration star observed served to confirm or adjust boresighting of all auxiliary telescopes. The primary calibration stars were observed and recorded in the same mode in which the satellite data was taken.

Approximately ten minutes before the expected satellite acquisition time, the telescope was clamped to the predicted satellite cross-track setting, and swung on the polar axis to

determine and provide for all observer-support requirements. The telescope was then moved to the satellite acquisition field by setting the predicted track (hour) angle, and confirmed in the three-inch acquisition telescope against the general star field by comparison with star charts and the predicted corresponding right ascension and declination. Since satellites are often a few minutes early, set up for acquisition was begun about five minutes before the expected time.

As soon as the satellite was acquired, the observer adjusted the tracking rate potentiometer to pace the satellite, making it appear stationary in his field. He then used the stiff-stick control in the same manner as when observing calibration stars to push the field's center (marked by illuminated reticle) to the satellite. The audio tone generator was then energized by the photometric signal being received in the main 24-inch telescope. Meanwhile the tracking observer visually acquired the satellite in one of the more powerful boresighted auxiliary telescopes and the stiff-stick tracking control was transferred to him. His objective was to maintain the audio tone by precise tracking until the satellite became too low for useful data, or until the satellite enters eclipse.

The acquisition observer served several functions during the tracking period:

(1) He was responsible for quick re-acquisition when the tracking observer lost track of the satellite

(2) He provided for any change in observer-support (e.g., ladder) requirements

(3) With binoculars and stop-watch he obtained a timed position of the satellite ("Moonwatch Point") for subsequent up-dating of the orbital elements and determining the geometric circumstances of each photometric data point by time correlation; and

(4) He advised the instrumentation room if the satellite was subject to vignetting, if it "sideswiped" a bright star or passed through a region of thin haze, enabling the oscillograph recording to be so marked.

He was, of course, also available to replace the tracking observer. During certain polarimetrically-observed passes, he manually rotated the photometric head.

Immediately following the pass, the primary calibration stars were re-observed. On several nights during the observing mission, special calibration programs were observed to determine the system transformation scale factors and second-order extinction coefficients. Generally these programs were conducted with the telescope mount in the conventional sidereal mode, except when the declination of the chosen program stars were in excess of 40 degrees.

Console tasks. - The console operator was responsible for the following tasks before a series of stellar or satellite observation.

(1) Loading the oscillograph with chart paper and assuring that the paper did not run out while a satellite pass was being observed.

(2) Switching gain steps through all positions on the chart paper and manually marking the pre-amp and diff-amp UBV and VRI positions.

During observations, the console operator tasks consisted of (1) selection of the mode of operation: photometric or polarimetric, and (2) continuous controlling and/or monitoring of the following

(1) Photomultiplier gains

(2) Filters

(3) Position of the mirrors within the photometer head

(4) Intensity output

(5) Reference meter

(6) Quality of time signals.

The complete description of the operational procedure of the photometer console is presented in the Operations and Maintenance Manual.

Field Operations

Administration of field operations. - The field crew chief at the Palomar Mountain and Arizona remote sites, Mr. C. L. Rogers, was in daily telephone contact with the home office in Akron, Ohio, to maintain complete coordination and reporting. His responsibilities included observation scheduling, field personnel work assignments and provisions for required transportation, instrumentation security and maintenance, supplies, records, data quality control and data return (by airmail). At the Ohio sites, Mr. Ed Kalasky performed the above functions of the crew chief, as modified by the proximity of these sites to the home office.

Astronomer-observer. - The tasks of the field astronomer-observer included the following:

(1) Tabulating the useful satellite passes for observation scheduling and plotting the trajectories of the various satellites on star charts.

(2) Selection of well positioned standard stars to determine the various calibration and extinction coefficients for the stellar calibration computer programs.

(3) Location of the stars and aiding the telescope operator in obtaining photometric observations of the stars.

(4) Locating the satellite at some predetermined altitude and aiding the telescope operator in acquiring and maintaining the satellite in the photometer field of view.

(5) Obtaining a "Moonwatch" point for the satellite pass in order to update the mean anomaly of the orbital elements.

Technician. - The duties and responsibilities of the field technician were as follows:

(1) Orientating the observatory at a given azimuth for a given pass or series of passes.

(2) Setting up the jacks and leveling the observatory through use of spirit levels.

(3) Setting the correct azimuth, elevation, and declination drives on the telescope from the four-axis predictions.

(4) Performance of tasks at the telescope during the satellite pass or at the console as directed by the crew chief.

(5) General mechanical or electronic maintenance, etc.

It should be stated that the foregoing description of the tasks of the field crew is not comprehensive, but merely to be illustrative of the various tasks on deck or at the console.

Data Reduction and Analysis

The following steps were employed to prepare the photometric and polarimetric data for analysis:

(1) Analog-to-digital conversion of the photometric and polarimetric data

(2) Placing the digitized data on forms, keypunching, and listing the data

(3) Application of the stellar calibration programs

(4) Application of the satellite data reduction programs to determine orbit geometry, and optical and physical properties

(5) Data analysis and establishment of data accuracy levels

The method of analog-to-digital conversion is slightly different for the two photometer systems used during this contract period because of different amplifiers. The U-B-V photometer system data reduction methodology is described in Reference 3. The method of data reduction for both photometric and polarimetric modes using the U-B-V-R-I system are as follows:

After receipt of the oscillograph charts from the field crew, the analog-to-digital conversion for the stars and satellite of interest was performed. Because this task was performed manually, each photometric point required the following information: filter color, time, intensity height in inches and two or three gain factors. In addition, each star was identified by its Yale Catalog Bright Star (B.S.) number, and pair number if the second-order extinction coefficient program was used.

After the analog-to-digital conversion was completed, the data points were placed on special forms for key-punching. These forms are shown in the manual along with instructions for their use. The key-punched cards were then submitted to the computer programmer for listing and checking. The stellar transformation and/or calibration programs were first run; plots were then drawn by an automatic X-Y plotter. Printouts and plots were examined for possible errors or unsatisfactory values. In the latter case, the data was analyzed to determine the cause of the discrepancy and reruns performed to obtain satisfactory values.

After the calibration and extinction coefficients had been established for the satellite pass, computer program E-1216, "Satellite Photometer Program: Stellar Magnitudes," was used. This program prints out the satellite extra-atmospheric and normalized magnitudes, slant range, and phase angles, etc., for each data point. These results were then examined for very low altitude points (~10 deg) and clearly spurious magnitude values. These data points were discarded. Computer program E-1214, "Specularity, Radius of Curvature and Reflectance Determinations," was then used for each color. In addition to obtaining these parameters for each pass, combined runs were performed for the satellite in each color. Plots of the specularity were then prepared.

A complete flow diagram for the various photometric computer programs associated with the stellar and satellite data reduction and analysis is presented in Figure 30. The computer programs, represented by the elements of the flow diagram, are described as follows.

Photometric programs. -

(1) Calibration Program I (E 1961 and E 1962)

This program is used to obtain the second order extinction coefficients from successive (two or more) series of photometric observations of three-to-five close pairs of standard stars having widely differing color indices at low altitudes. The subsequent calculation of these k" values are listed in Table IV.

(2) Calibration Program II (E 1971 and E 1972)

Using the parameters determined from Calibration Program I and photometric observations obtained on 10-15 standard stars near the zenith, the scale factors for system transformation (ϵ, μ, ψ, ρ, σ, τ) are calculated.

(3) Calibration Program III (E 1981 and E 1982)

Using the parameters determined in Calibration Programs I and II, and photometric observations on 5-7 standard stars located along or near the satellite path, both before and after the satellite pass, the primary extinction coefficients (k's) and zero point terms (ζ's) for the various spectral regions are determined.

(4) Satellite Data Reduction (E 1216) (UBV and VRI)

This program uses the previously determined stellar calibration and extinction coefficients and the photometric values of intensity and gain for the satellite photometric observations, such parameters as extra-atmospheric and normalized magnitudes as well as orbit geometry parameters (phase angle, slant range, etc.) are determined and printed out.

(5) Satellite Data Analysis (E 1214) (UBV and VRI)

Using the previously determined values of satellite normalized magnitudes and phase angles for each data point, mean normalized magnitude, specularity, radius of curvature, reflectance, figure of merit, etc. are calculated and printed out.

(6) Specularity Plot (EA 852)

This program plots the brightness of each data point ($4E/E_0$) versus 8/3 Russell phase function $[8/3\ f(\psi)]$ and draws a best fit line through the data points.

(7) Data Reduction - Polarimetric

The data recorded on the oscillograph charts are converted from analog-to-digital form by manually measuring the filter, gains, and analyzer (Wollaston prism or half-wave plate) positions, the two intensities (I_1 and I_2) and the time for each star or satellite data point. In addition, the Henry Draper (H.D.) catalog number is recorded for each star. After the analog-to-digital conversion is completed, the data is placed on forms. The data is key-punched, and submitted to the computer programmer for listing and checking.

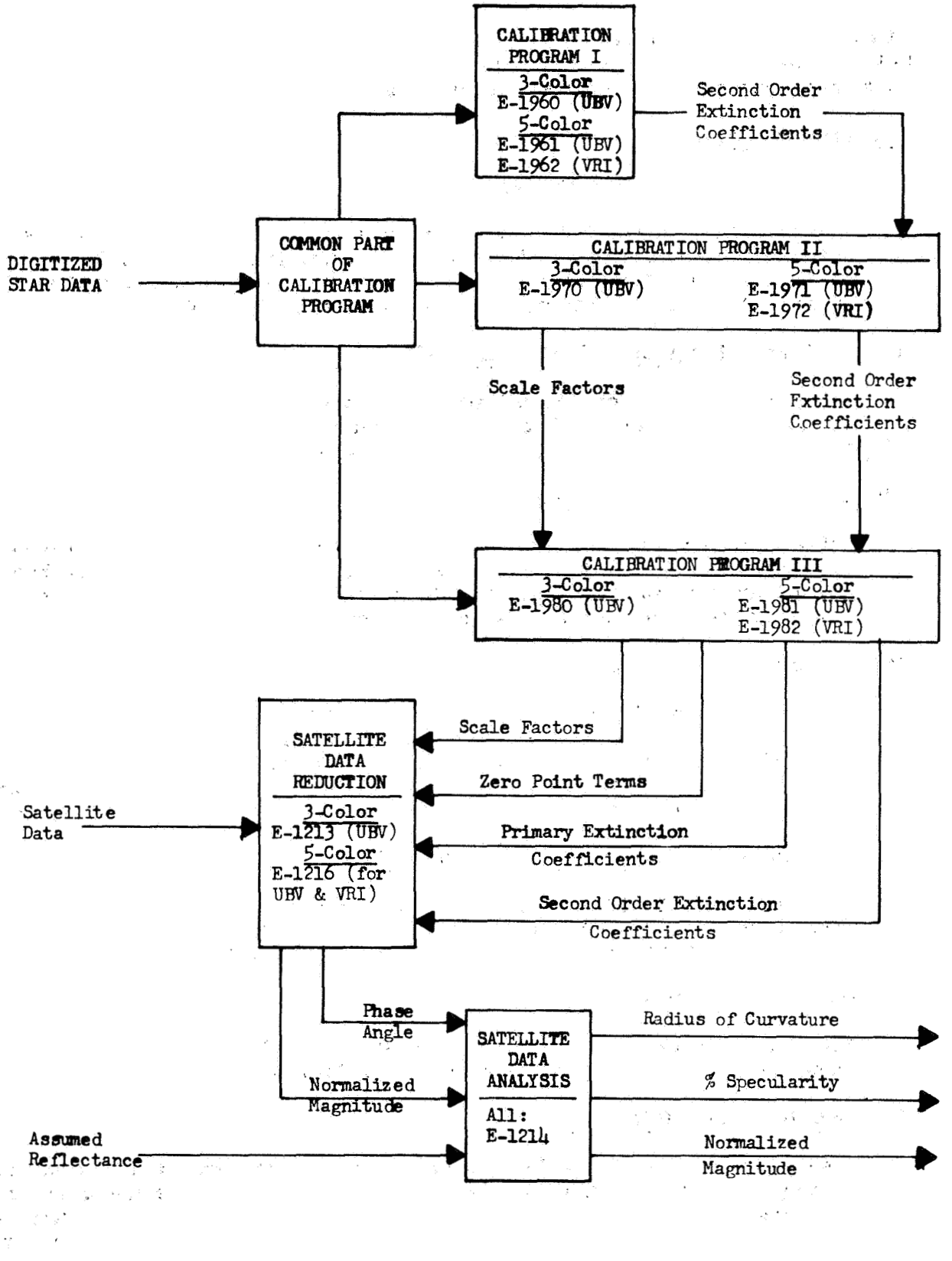

Figure 30. - Block diagram of computer data flow

The various stellar and satellite polarimetric programs are then run. A brief description of the various polarimetric computer programs follows.

(8) System Bias and Calibration Check (EA 580)

The data obtained for polarimetric observations on zero polarized stars, is corrected for any variation between the two intensities I_1 and I_2 for either the rotating Wollaston prism or the rotating half-wave plate.

Using the system bias from zero polarized stars and polarimetric observations on highly polarized stars, the percent polarization calculations for these stars are checked against the Alfred Behr catalog values (Reference 12).

(9) Satellite Polarization and Phase Angles (EA 600)

Using the results from EA 580 and polarimetric observations on the satellites of interest, the percent polarization and phase angle of the satellite is determined.

(10) Plotting of Satellite Percent Polarization and Phase Angle Data (EA 601)

The results from the Satellite Reduction Program, EA 600, are used in the EA 601 program for the combined plotting of satellite data. This program provides a listing of the data cards and plots the percentage polarization versus the phase angle of the satellite.

Analysis, i.e., determination of various optical and physical properties, correlations, etc., are performed for photometric and polarimetric observations and are presented in "Discussion of Results" that follows. Accuracy of results, i.e., performance of stellar photometric and polarimetric checks as well as statistical determination of satellite observation accuracies are discussed in "Accuracy of Results."

Discussion of Results

Calibration. -

Second-order extinction coefficients: Values of the second-order extinction coefficients used in the equations to determine such parameters as transformation scale factors, primary extinction coefficients and zero-point terms, and stellar and satellite magnitudes and color indices are presented in Table IV.

Scale factors: Scale factor observations were performed at least once during each observation period. Values of each parameter are presented in Table V.

Primary extinction coefficients and zero-point terms: Calibration observations for the determination of primary extinction coefficients and zero point terms are usually performed before and after each pass of a given satellite on approximately 5-7 standard stars taken from References 5 and 6. Exceptions to this practice happen at times when a satellite pass occurs near sunrise or sunset, or if passes of two different satellites occur within a short period of time. The pre- and post-pass values of these parameters are combined and effective values of the primary extinction coefficients and zero-point terms are obtained to use in the calculation of satellite extra-atmospheric magnitudes. Mean values for the primary extinction coefficients are plotted versus effective wavelength in Figure 31 for the Palomar Mountain, Yuma, and the two Akron observation periods.

TABLE IV. - SECOND ORDER EXTINCTION COEFFICIENTS

Observation period	No. of star pairs used	k''_{b-v}	k''_{u-b}	k''_{v-r}	k''_{r-i}
Summer, 1966 7/17 - 8/5	4	-0.004	-0.001		
Summer, 1966 8/6 - 8/14	3	-0.047	-0.014		
Summer, 1966 8/15 - 8/22	4	-0.028	-0.041		
Winter, 1967 2/12 - 3/14	4	-0.040	-0.010	0.000	0.000
Summer, 1967 6/13 - 7/6	3	-0.040	-0.010	0.000	0.000
Autumn, 1967 9/26 - 12/17	3	-0.040	-0.010	0.000	0.000

TABLE V. - SCALE FACTORS OBTAINED FROM OBSERVATIONS

Date of observation	No. of stars used	ϵ	μ	ψ	ρ	σ	τ
July 15, 1966	13	0.050	1.021	1.020			
August 6, 1966	13	0.054	0.960	1.043			
August 13, 1966	14	0.046	0.982	1.002			
March 6, 1967	12	-0.046	1.098	1.072	0.037	1.122	1.167
June 26, 1967	10	-0.080	0.994	1.012			
October 3, 1967	13; ϵ, μ, ψ 10; ρ, σ, τ	0.061	1.084	0.998	0.080	0.986	1.548

High primary extinction values are often associated with inhomogeneous atmospheric conditions, resulting in reduced photometric accuracy. The high extinction values encountered at the Akron site during the 1967 Summer observations are the probable cause of the greater scatter in the data from that observing period.

Photometric observations of PAGEOS I, Echo I and Echo II, and Explorer XIX. - There were four separate time periods during which multicolor photometric observations were performed on the various satellites during the present contract.

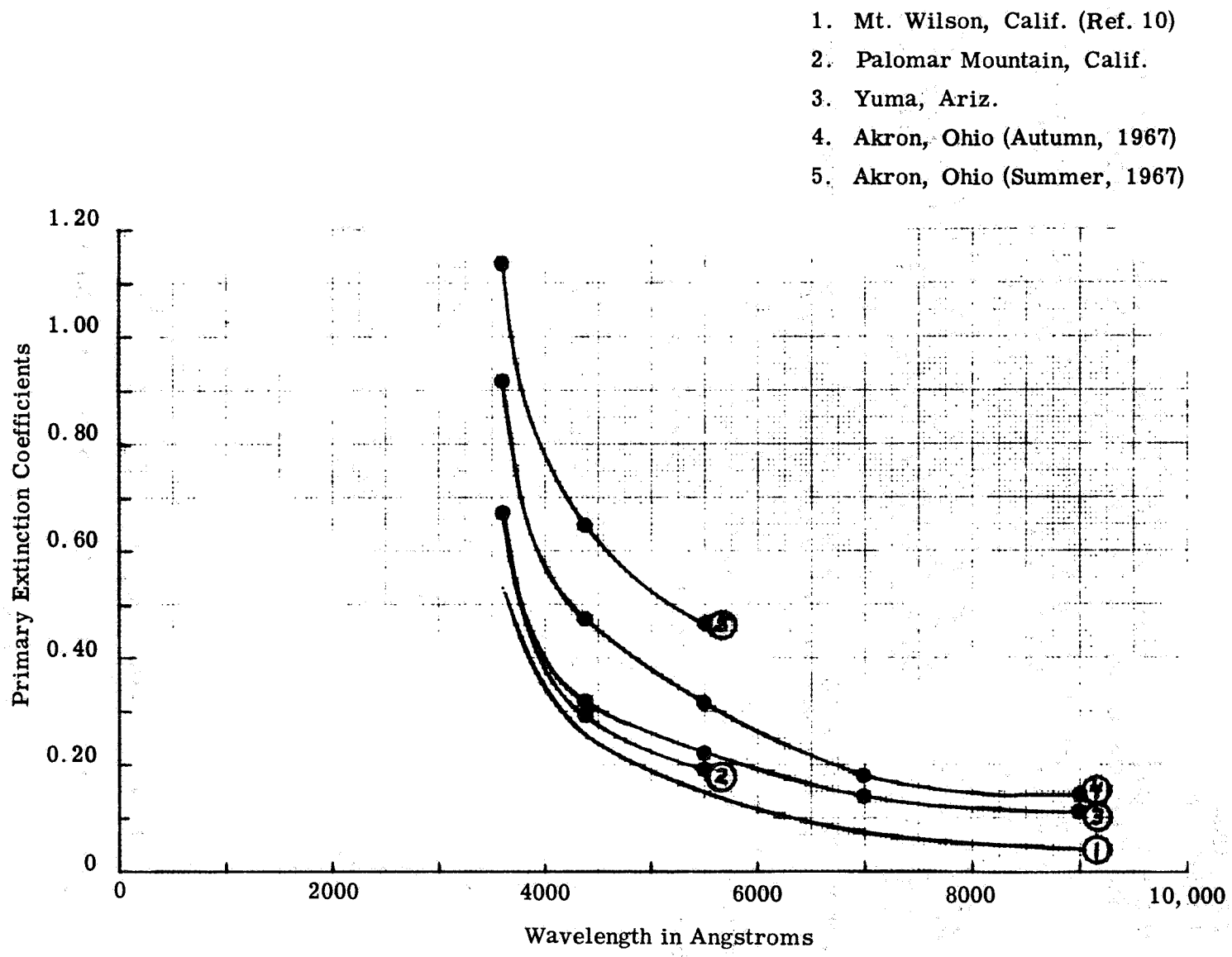

Figure 31. - Primary extinction coefficients

These included:

(1) U-B-V photometric observations performed on Echo I during July and August, 1966, at Palomar Mountain, California

(2) U-B-V-R-I photometric and polarimetric observations were performed on PAGEOS I, Echo I and Echo II during January-March, 1967, at Phoenix and Yuma, Arizona

(3) U-B-V photometric observations were performed on PAGEOS I, Echo I and Echo II, and V-band only observations were performed on Explorer XIX during June-July, 1967, at Akron, Ohio

(4) U-B-V-R-I photometric observations were performed on PAGEOS I, Echo I and Echo II during September-December, 1967, at Akron, Ohio. Optical and physical parameters for each satellite will be presented in summary form in the succeeding sections.

A summary description of some of the important optical and physical properties and orbit geometry of the four observed satellites is presented in Table VI.

Echo I: Photometric observations of the Echo I satellite were performed during each of the four observation periods under the present contract.

Individual passes of Echo I for the four observation periods are as follows:

I Palomar Mt., California; July-August, 1966

(a) 22 U, B, V observations: 7/17, 7/20, 7/21, 7/22, 7/24, 8/5, 8/6 (1), 8/6 (2), 8/7 (1), 8/7 (2), 8/9 (1), 8/9 (1), 8/9 (2), 8/10, 8/11, 8/12, 8/13, 8/14, 8/15, 8/16, 8/18, 8/21 (1), 8/22

(b) 1 V-band observation: 8/21 (2)

II Yuma, Arizona; February-March, 1967

(a) 10 U, B, V, R, I observations: 2/16, 2/18, 2/19, 2/20, 2/21, 3/6, 3/7, 3/8, 3/9, 3/14

(b) 1 U, B, V observation: 2/22

(c) 1 V-band (S-20) observation: 3/10

III Akron, Ohio; June-July, 1967

(a) 1 U, B, V, R, I observation: 6/13

(b) 8 U, B, V observations: 6/16, 6/20, 6/24 (1), 6/24 (2), 6/26, 6/27 (1), 6/27 (2), 7/6

IV Akron, Ohio; September-December, 1967

(a) 11 U, B, V, R, I observations: 10/3, 10/4 (1), 10/4 (2), 10/5 (1), 10/5 (2), 11/6, 11/10, 11/28, 12/5, 12/16, 12/17

TABLE VI. - CONSTRUCTION AND ORBIT PARAMETERS OF OBSERVED SATELLITES

Vehicle	Echo I	Echo II	PAGEOS I	Explorer XIX
Diameter	100 ft	135 ft	100 ft	12 ft
Satellite material description (inside-to-outside)	1. Mylar - 0.5 mil thick 2. Evaporated aluminum - 2000 Å thick 82 gores Polar caps	1. Aluminum foil - 0.18 mil thick 2. Mylar - 0.35 mil thick 3. Aluminum foil - 0.18 mil thick 4. Alodine 401-45 coating 106 gores	1. Mylar - 0.5 mil thick 2. Evaporated aluminum - 2000 Å thick 82 gores Polar caps	1. Mylar - 0.5 mil thick 2. Aluminum foil - 0.5 mil thick 3. Mylar - 0.5 mil thick 4. Aluminum foil - 0.5 mil thick 5. Zinc oxide pigmented silicone elastomer paint. 2-inch white spots over 25 percent of the surface 40 gores
Launch date	August 12, 1960	January 25, 1964	June 23, 1966	December 19, 1963
Orbital inclination	47 deg	81 deg	86 deg	79 deg
Normalized height	1000 st mi	1000 st mi	2640 st mi	1000 st mi
Reflectance* (Laboratory)				
U	0.884	0.670	0.884	
B	0.896	0.638	0.896	Aluminum foil = 0.85
V	0.896	0.718	0.896	Zinc oxide = 0.67
R	0.879	0.640	0.879	Combined = 0.80
I	0.885	0.667	0.885	
Weight				
Initially	157 lbs	617 lbs	160 lbs	18.3 lbs
Presently†	124 lbs	565 lbs	130 lbs	17.8 lbs

*Private communication: NASA-Langley to GAC.

†After inflation gas has escaped.

(b) 2 U, B, V observations: 9/26, 9/27

(c) 2 V, R, I observations: 10/1, 10/2

Table VII presents in summary form the observation periods along with number of satellite passes and data points used in the combined pass computer analysis and associated optical and physical parameters for the satellite. Also included are the original observations of Echo I performed by GAC in 1964 (Reference 1). From the visual-band data (which is deemed the most reliable) it is evident that the vapor-deposited aluminum surface of the Echo I satellite experienced no clearly measurable or significant degradation of its specularity between its orbital ages of 3.7 and 6.9 years. However, the most recent observations, taken at an orbital age of 7.2 years, indicate a marked (six-percent) drop in visual-band specularity within a few months, perhaps due to increased solar activity and/or reduction in the satellite's mean orbital altitude to below 750 st mi. This recent indication of rapid specular degradation is believed real in view of the high figure of merit derived for the last specularity determination, and the virtually independent and compelling evidence for a recent trend toward decreased surface reflectances, especially at the shorter wavelengths. This downward trend in surface reflectances (dulling and yellowing) appears to have started after the orbital age of 6.0 years, when Echo I's mean orbital height had fallen to about 825 st mi.

While Echo I's mean radius of curvature has remained quite near the design value (50 ft) for all observing periods, increased wrinkling of the surface since orbital age 6.0 years is indicated by the higher values encountered since then for the standard deviation (sigma) of the local radii of curvature.

As an example of data taken in the new spectral regions, Figure 32 shows plots of the combined computer pass reduction and analysis of the brightness level ($4\ E/E_0$) versus 8/3 Russell phase function $[8/3\ f(\psi)]$ for the Echo I V(S-1) and R-bands taken during the Autumn, 1967, observation period at Akron, Ohio. (These are the derived outputs of computer programs E-1216 and E-1214.) Plotted also is the best fit straight line through the data points. As described previously, the slope and intercept calculated from the data points determine the specularity of the satellite. The specularities for these series of data points (see Table VII) are 89.8 percent for the V (S-1) band and 83.4 percent for the R-band.

PAGEOS I: Multicolor photometric observations were performed on PAGEOS I during three observation periods under the present contract. Results are presented in summary form in Table VIII. In addition, results from the observation period at Palomar Mountain, California, during the summer of 1966 (Contract No. NAS 1-6189, Reference 3) are presented for comparison purposes.

Photometric observations of PAGEOS I passes were obtained during three periods as follows:

I Yuma, Arizona; February-March, 1967

(a) 10 U, B, V, R, I observations: 2/18, 2/19, 2/21, 2/26, 3/1, 3/5, 3/6, 3/7, 3/8, 3/9

(b) 1 U, B, V observation: 3/12

II Akron, Ohio; June, 1967

(a) 1 U, B, V, R, I observation: 6/13

(b) 4 U, B, V observations: 6/16, 6/24, 6/26, 6/27

TABLE VII. - OPTICAL AND PHYSICAL PARAMETERS OF ECHO I

Observation period	Spectral region	No. of points	Mean normalized magnitude	Sigma magnitude	Specularity (percent)	Radius of curvature (ft)	Sigma radius (ft)	Total reflectance	Figure of merit
Palomar Mt., California (23 passes) Jul-Aug, 1966	U	759	0.84	0.22	97.6	48.2	4.7	0.81	57.1
	B	377	0.66	0.20	99.3	50.6	4.6	0.91	43.5
	V (S-4)	414	0.01	0.21	96.3	50.7	4.6	0.91	43.7
Yuma, Arizona (9 passes, UBV) (8 passes, VRI) Feb-Mar, 1967	U	146	0.87	0.33	86.9	47.5	7.6	0.78	13.0
	B	146	0.71	0.31	82.0	49.8	7.4	0.87	14.1
	V (S-20)	146	0.01	0.24	95.5	50.1	5.6	0.89	18.7
	V (S-1)	133	0.02	0.25	92.5	50.0	5.8	0.89	17.9
	R	133	-0.48	0.25	90.5	50.1	6.0	0.87	17.1
	I	133	-0.82	0.29	81.3	52.6	7.4	0.95	14.7
Akron, Ohio (6 passes, UBV) Jun-Jul, 1967	U	127	1.01	0.36	121.8*	45.1	8.3	0.70	9.5
	B	127	0.74	0.29	100.0	49.1	6.9	0.85	12.1
	V (S-20)	127	0.03	0.27	95.1	50.7	6.4	0.91	13.5
Akron, Ohio (4 passes, V-20) (8 passes, UBV) (9 passes, VRI) Sep-Dec, 1967	U	74	1.02	0.30	89.6	42.5	6.5	0.62	12.4
	B	74	0.72	0.32	85.4	46.9	7.0	0.77	12.8
	V (S-20)	246	-0.00	0.36	88.7	50.2	8.3	0.87	25.0
	V (S-1)	102	-0.05	0.25	89.8	50.2	6.1	0.89	22.8
	R	102	-0.49	0.25	83.4	48.5	5.5	0.82	24.3
	I	102	-0.82	0.36	93.7	51.0	8.0	0.89	17.5
Akron, Ohio† (12 passes) Apr-Jun, 1964	V (v)	237	-0.01	0.27	96.2	51.1	6.5	0.92	31.8

*Non-random distribution of satellite intensities biased specularity determination in excess of 100 percent limit.

†Data taken under Contract No. NAS 1-3114, Amendment 5; presented here for comparison purposes.

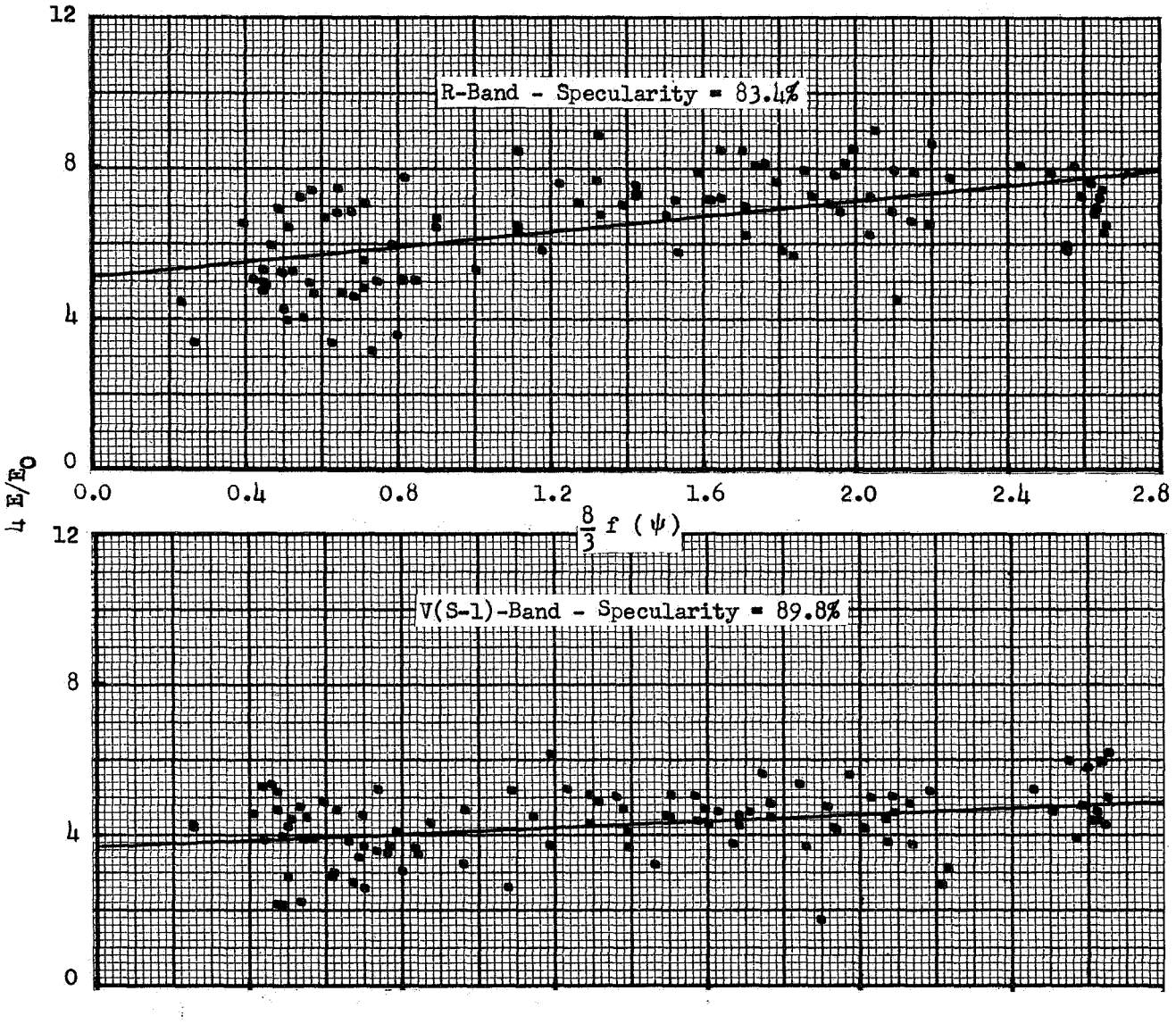

Figure 32. - Specularity of Echo I from Autumn 1967 observations

TABLE VIII. - OPTICAL AND PHYSICAL PARAMETERS OF PAGEOS I

Observation period	Spectral region	No. of points	Mean normalized magnitude	Sigma magnitude	Specularity (percent)	Radius of curvature (ft)	Sigma radius (ft)	Total reflectance	Figure of merit
Yuma, Arizona	U	465	2.94	0.28	92.8	46.5	6.4	0.75	32.8
Feb-Mar, 1967	B	465	2.76	0.26	95.5	49.1	6.1	0.85	36.1
(11 passes, UBV)	V (S-20)	465	2.09	0.27	95.0	49.6	6.4	0.87	34.7
(10 passes, VRI)	V (S-1)	300	2.13	0.30	89.4	48.7	6.3	0.84	22.6
	R	300	1.58	0.34	86.5	49.5	6.9	0.84	20.7
	I	300	1.25	0.33	84.0	50.7	8.3	0.88	17.7
Akron, Ohio	U	124	3.10	0.31	95.1	44.7	5.6	0.69	28.0
Jun, 1967	B	124	2.83	0.25	95.4	49.0	5.3	0.85	32.7
(3 passes)	V (S-20)	124	2.14	0.22	99.4	50.3	5.0	0.90	35.0
Akron, Ohio	U	325	2.95	0.23	108.6*	46.9	4.7	0.77	15.8
Sep-Oct, 1967	B	325	2.77	0.23	101.7*	49.7	5.1	0.88	15.6
(8 passes, UBV)	V (S-20)	325	2.14	0.21	97.7	49.7	4.7	0.88	16.7
(7 passes, VRI)	V (S-1)	276	2.10	0.22	103.2*	50.2	4.8	0.89	15.6
	R	276	1.61	0.22	91.0	50.5	5.2	0.89	14.3
	I	276	1.31	0.32	94.9	51.5	7.6	0.92	10.0
Palomar Mt., †	U	1323	2.92	0.23	99.3	48.6	5.1	0.83	71.4
California	B	662	2.77	0.22	99.9	50.4	5.1	0.90	51.9
Aug, 1966	V (S-4)	662	2.11	0.21	98.0	50.6	5.0	0.91	53.2
(22 passes)									

*Non-random distribution of satellite intensities biased specularity determination in excess of 100 percent limits.

†Data taken under Contract No. NAS 1-6189; presented here for comparison purposes.

The passes of 6/13 and 6/16 are not included in the combined pass computer analysis because of poor atmospheric extinction coefficients.

III Akron, Ohio; September-October, 1967

(a) 8 U, B, V, R, I observations: 9/26, 9/27 (1), 9/27 (2), 10/2, 10/3 (1), 10/3 (2), 10/4 (1), 10/4 (2)

(b) 1 V, R, I observation: 10/5

The V, R, I observations of 9/27 (2) and 10/5 were not included in the combined pass computer analysis because of poor atmospheric extinction coefficients.

It is indicated from the data presented in Table VIII that the surface of PAGEOS I has undergone little-or-no permanent change in specularity, size, or figure since the period of thermal stability began in early August, 1966. The variations in these parameters among the several observation periods is believed due in part to non-random samples of the photometric intensities resulting from the satellite's relatively slow spin rate. Some net degradation of the reflectances at the shorter wavelengths (B, and particularly U), since 1966 is indicated, and is believed real and attributable to increased solar activity.

The results as given in Table VIII are for a combined pass computer analysis, i.e., all data points are utilized for a given time period (each spectral region) to obtain definitive values of magnitude, radius of curvature, specularity, reflectance, etc., in a single computer analysis. Single pass calculations are also performed to determine the various parameters in the same manner as the combined computer pass analysis. The main value of such calculations are in the determination of rapid change in optical and/or physical properties of the satellite such as the occurrence of large excursions of radius of curvature for PAGEOS I during first shadow entry in the summer of 1966, (References 3 and 14). Figure 33 depicts the specularity of PAGEOS I for the observation of March 6, 1967. As may be seen, the specularity for the pass was 97.2 percent, which is very close to that obtained for the combined analysis value of 95.0 percent.

Comparison of Echo I and PAGEOS I satellites: Since Echo I and PAGEOS I are similar satellites, it is useful to compare the results from the photometric and polarimetric observations. Based on the more accurate visual band photometric information, the mean radius of curvature of both satellites continues to remain at or very near the design value of 50 ft. While PAGEOS I's surface figure had about the same 10 percent dispersion in local radii of curvature in late 1967 as in August 1966, the corresponding dispersion for Echo I increased markedly from 10 to 16 percent of the mean radius in this same period as its mean orbital height decreased to 750 st mi.

The visual-band specularity determinations for these satellites are plotted in Figure 34 against their respective orbital ages to yield their individual specularity histories, and more generally, a single such history for a vapor-deposited aluminum surface in earth-orbit. Figure 34 suggests that specular degradation of a few percent may occur within the first half-year in orbit, but thereafter at a rate not exceeding one-half percent per year while the satellite remains above a mean height of 825 st mi (Echo I, mid 1967). At lower mean orbital heights this specular degradation rate appears to rise markedly, perhaps to more than 20 percent per year.

Figure 35 similarly presents the total reflectance histories for Echo I and PAGEOS I as determined in the five-color bands. While the variations in the PAGEOS I data are believed due in part to non-random data samples resulting from this satellite's relatively low spin rate, some net degradation of the U and B reflectances is indicated. It should be noted that these

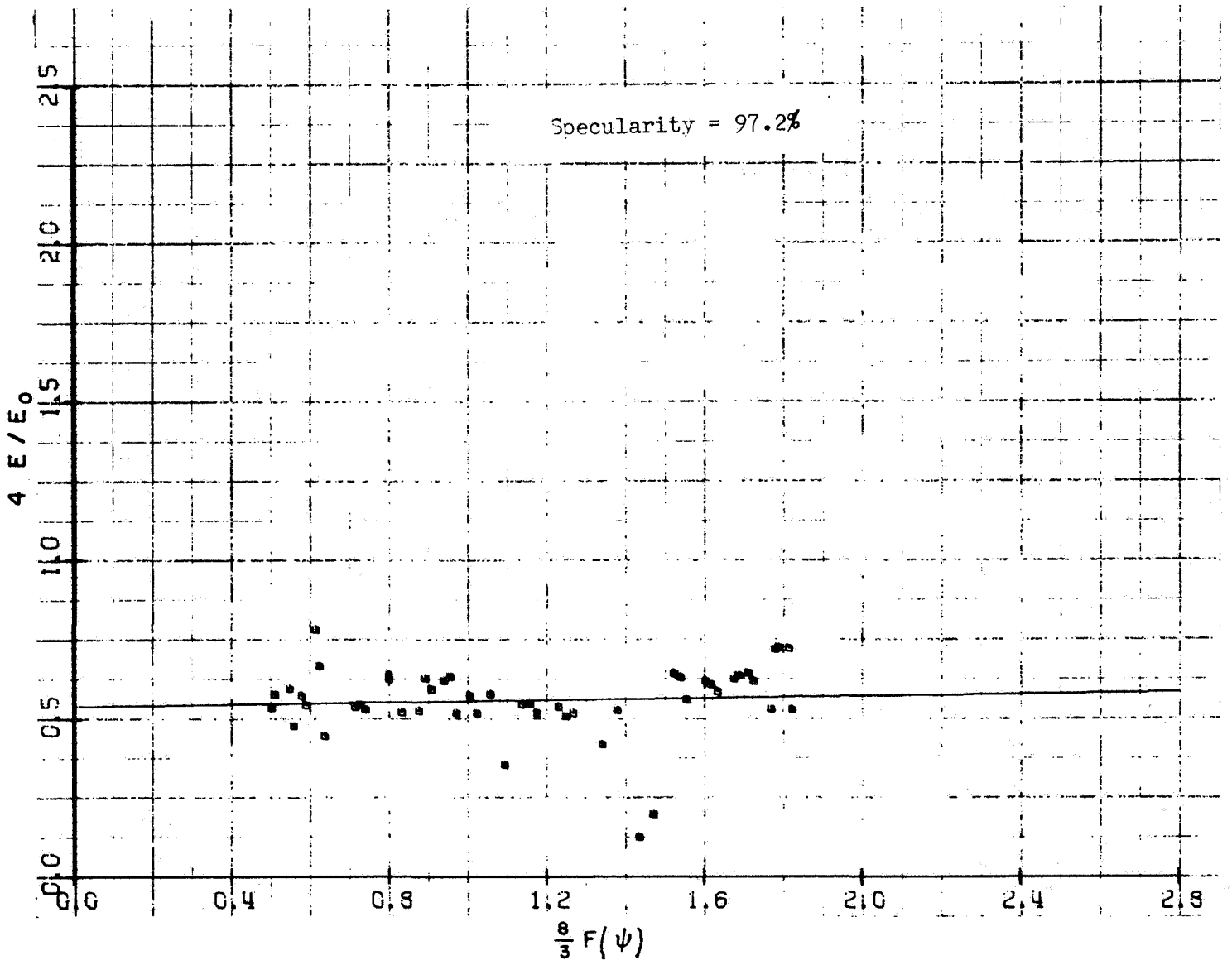

Figure 33. - Specularity of PAGEOS I from 6 March 1967 observations (V_{20}-band)

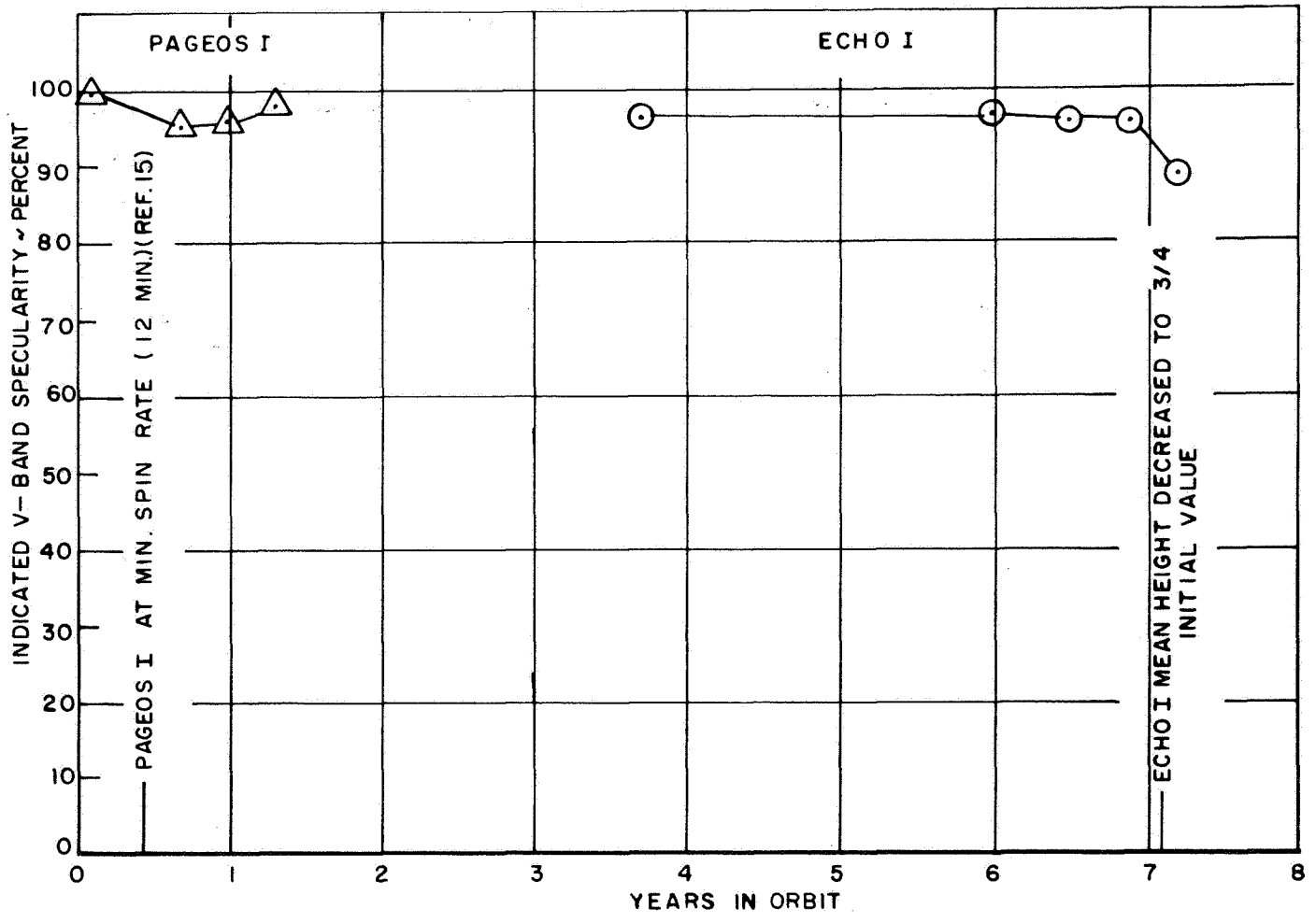

Figure 34.- Effect of time in orbit on specularity

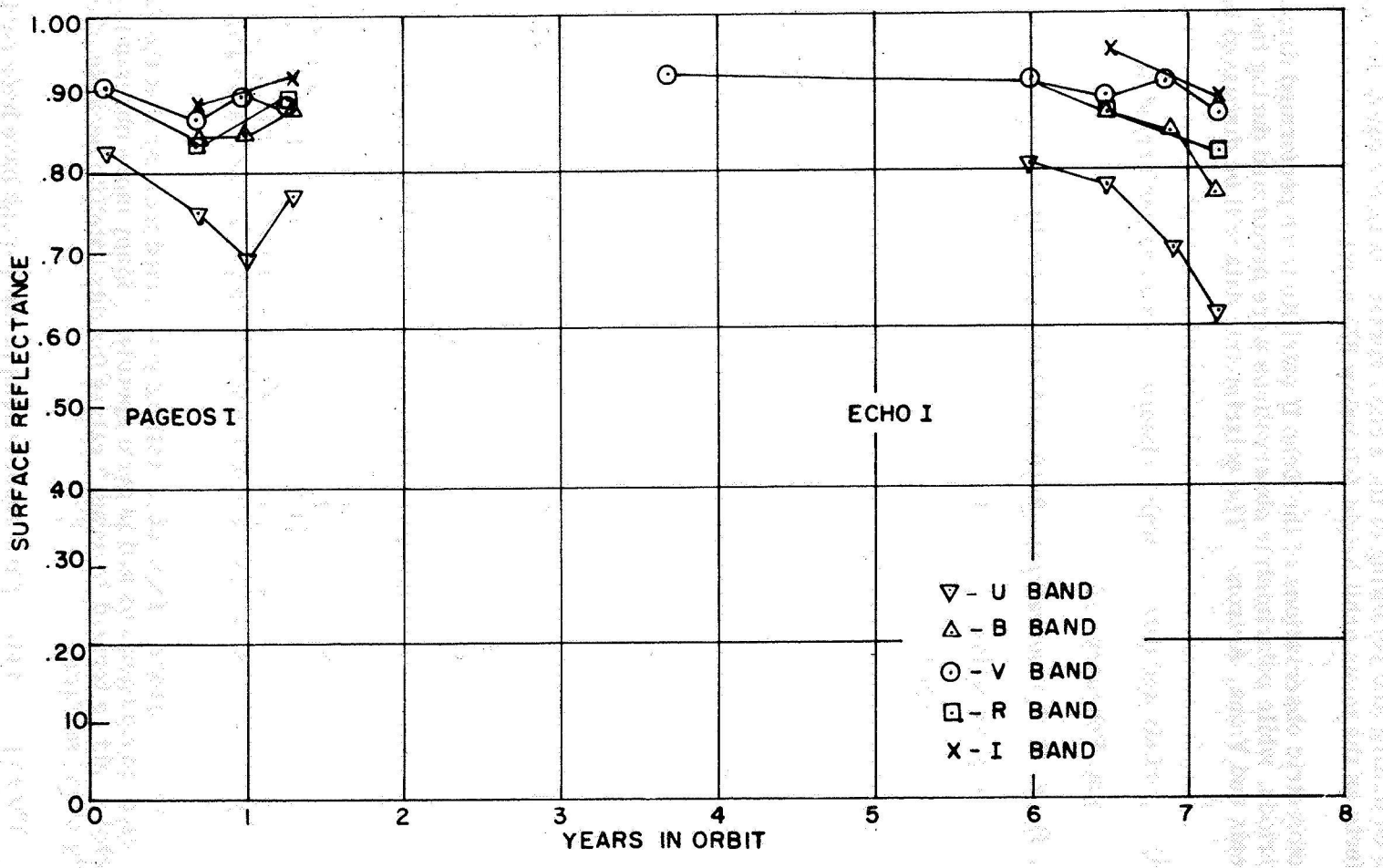

Figure 35. - Effect of time in orbit on surface reflectance

net degradations occurred in the same real time as those more clearly evident in the Echo I data, and may therefore have a common cause such as the increased solar activity in 1967. The more pronounced dulling and yellowing of the Echo I surface is likely due to the addition of atmospheric effects as the mean orbit height fell below 825 st mi.

Echo II: Photometric observations of the Echo II satellite were performed during three of the observing periods, while polarimetric observations were performed during the observation period at Phoenix and Yuma, Arizona. The polarimetric data will be discussed in a subsequent section.

The observation periods and dates in which observations were performed are as follows:

I Yuma, Arizona; February, 1967

(a) 3 U, B, V, R, I observations: 2/16, 2/18 (1), 2/18 (2)

(b) 2 U, B, V observations: 2/12 (1), 2/12 (2)

II Akron, Ohio; June, 1967

3 U, B, V observations: 6/26, 6/27, 6/28

The pass of 6/28 could not be reduced due to poor weather conditions before and after the pass.

III Akron, Ohio; November, 1967

2 U, B, V, R, I observations: 11/6, 11/28

The physical and optical properties are presented in summary in Table IX.

Laboratory measurements (Reference 16) performed on Echo II material (Alodine 401-45) in air indicated that the material was highly diffuse and that the reflectance was in the vicinity of 0.60 to 0.70 across the spectral region (see Table VI). As may be seen from the results presented in summary form in Table IX, the specularity values are well above 50 percent. Although there is a great amount of variance in the values obtained, it is evident that change in the coating has occurred due to the space environment and that the coating is now non-uniform. An interesting comparison may be made of the results obtained for Echo II and that of Echo I and/or PAGEOS I. It is to be noted that the mean normalized magnitude for Echo II in the V-band (or other bands as well) varies significantly whereas one obtains roughly the same average value for Echo I or PAGEOS I consistently. There are several reasons for this phenomenon; one might mention, (a) possibly a non-uniform surface; (b) small number of data points obtained thus far; (c) the satellite has a large change in brightness between small and large phase angles, etc.

In summary, it is quite apparent from observations performed thus far that the Echo II satellite surface is fairly inhomogeneous and is quite specular. Many more observations are required to obtain what might be termed "average" values for this satellite because of the apparent inhomogeneity of the surface.

Explorer XIX: Three photometric pass observations in the V-band have been performed on the Explorer XIX satellite. The dates of the observations and resulting optical and physical parameters are presented in Table X. In addition a combined pass computer analysis of all data points was performed and is also presented in the table. An important item which should

TABLE IX. - OPTICAL AND PHYSICAL PARAMETERS OF ECHO II

Observation period	Spectral region	No. of points	Mean normalized magnitude	Sigma magnitude	Specularity (percent)	Radius of curvature (ft)	Sigma radius (ft)	Total reflectance	Figure of merit
Yuma, Arizona	U	33	0.33	0.34	86.8	66.6	11.7	0.68	6.2
(3 passes, UBV)	B	37	0.38	0.38	64.8	67.6	12.0	0.62	7.2
(2 passes,	V (S-20)	37	-0.33	0.27	73.6	67.5	8.6	0.66	10.2
UBVRI)	V (S-1)	15	-0.64	0.22	85.7	79.0	9.0	0.91	4.2
Feb, 1967	R	15	-0.80	0.29	92.8	67.7	8.0	0.63	4.1
	I	15	-1.11	0.23	86.8	68.4	7.1	0.68	4.6
Akron, Ohio	U	20	0.80	0.26	64.8	51.4	8.1	0.40	6.1
(2 passes, UBV)	B	20	0.67	0.27	67.8	56.4	8.6	0.43	6.3
Jun, 1967	V (S-20)	20	-0.24	0.19	69.2	62.6	4.3	0.57	13.5
Akron, Ohio	U	20	1.12	0.44	46.0	54.7	4.4	0.47	11.2
(2 passes,	B	20	0.72	0.26	64.0	62.8	3.5	0.55	16.2
UBVRI)	V (S-20)	20	-0.02	0.32	56.8	66.1	4.4	0.64	13.5
Nov, 1967	V (S-1)	20	-0.07	0.33	55.6	68.0	4.7	0.68	13.2
	R	20	-0.55	0.30	59.4	67.2	5.1	0.63	11.9
	I	20	-1.10	0.32	56.3	75.9	3.9	0.84	17.7

TABLE X. - OPTICAL AND PHYSICAL PARAMETERS OF EXPLORER XIX*

Date of observation	No. of data points	Mean normalized magnitude	Sigma magnitude	Specularity (percent)	Radius of curvature (ft)	Sigma radius (ft)	Total reflectance	Figure of merit
June 16, 1967	96	4.71	0.11	86.3	6.0	0.2	0.81	71.4
June 24, 1967	110	4.71	0.22	75.6	6.1	0.7	0.83	18.0
June 27, 1967	52	4.91	0.19	76.6	5.6	0.4	0.69	22.8
Combined pass computer analysis	258	4.75	0.20	81.4	6.0	0.5	0.79	39.1

*V_{20}-Band.

be mentioned concerning this data is that the data points represent average values of intensity. Few intensity trace crests or troughs are included in the present data. Preliminary analysis of data in which crest and trough points were reduced independently show that the crest points have a high value of specularity and appear to be associated with the aluminum foil, while the trough points have a Lambertian distribution with phase angle and appear to be associated with the white epoxy paint.

From the values of specularity, radius of curvature, and reflectance obtained for data points taken on the Explorer XIX satellite up to the present, it is indicated that the satellite's surface has not measurably degraded from laboratory values for similar material. Additional observations with emphasis placed on the "troughs" or diffuse points would provide a more sensitive test for surface degradation on this satellite.

Polarimetric results. - Multicolor (UBVRI) polarimetric observations were performed by using either a rotating achromatic half-wave plate or Wollaston prism on PAGEOS I, Echo I and Echo II during January, February, and March of 1967 near Phoenix and Yuma, Arizona. The total number of polarimetric observation data points* for the satellites are listed in Table XI. Plots of Percent Polarization versus Phase Angle are presented, according to color, for the three satellites in Figures 36 through 40 along with a theoretical curve (Reference 17) of polarization for vapor deposited aluminum. The curve is strictly intended as a comparison only, since the optical parameters for the vapor deposited aluminum may not agree with those of PAGEOS I and Echo I surfaces, which are made of aluminized Mylar.

Echo I: Polarimetric measurements of Echo I were made in the U, B, and V bands, using the rotating half-wave plate. The percent polarization was determined according to the data reduction equation - and plotted versus the phase angle in Figures 36, 37, and 38. As mentioned earlier, the theoretical curve is to be used as a comparison of vapor-deposited aluminum versus the observed aluminized Mylar in space.

The data points in Figures 37 and 38 extend as far as 154 degrees phase angle for B and V-bands. These points in all three bands follow the general shape of the theoretical curve; however, they are systematically higher as one goes from V to B to U-band. This could possibly be explained as degradation in the various spectral regions; however, a more realistic explanation is that there is a difference in the design optical properties between the theoretical curve and the Echo I aluminized Mylar surface.

PAGEOS I: Polarimetric measurements of PAGEOS I were made in the U, B, V, R, and I bands using the rotating instrument head and half-wave plate. The percent polarization versus the phase angle for each color is plotted in Figure 36 through 40. These values appear systematically higher than the theoretical curve for vapor-deposited aluminum and are slightly higher than the values for Echo I in the U, B, and V bands. As for Echo I, any variation between the actual percent polarization values and those calculated for PAGEOS I are probably due to the design optical properties rather than actually showing degradation.

Echo II: Percent polarization values for Echo II are presented in Figures 36 to 38 in the U, B, and V band spectral regions. In addition, a plot of Echo II V-band percent polarization points as a function of phase angle is presented in Figure 41 along with a theoretical curve for vapor deposited aluminum and a laboratory determined curve (in air) for an Alodine coated material similar to that of Echo II (Reference 18). As may be seen from Figure 41 there is significant scatter of the data points at the lower phase angles which possibly indicates a non-uniform and/or specular surface. At higher phase angles (~100°), the data points diverge sharply from both the laboratory measured values and the theoretical curve which is indicative of a surface defined by neither of the curves. On the other hand, laboratory polarimetric

*Each "polarimetric data point" requires readings from at least 4 or 5 positions of the half-wave plate or rotating head (see Figures 24 and 25).

TABLE XI. - POLARIMETRIC OBSERVATIONS

Satellite	Color band						Date (1967)	Pass
	U	B	V_{20}	V_1	R	I		
Half-Wave Plate								
Echo I	4	1	1				2-17	-
	-	1	3				3-5	-
	1	2	-					-
Echo II	-	-	8				1-31	1st
	-	-	6				1-31	2nd
	-	-	8				2-2	1st
	-	-	10				2-2	2nd
	-	-	7				2-3	1st
	-	9	-				2-3	2nd
	-	15	-				2-5	1st
	-	11	-				2-5	2nd
	-	-	11				2-8	-
PAGEOS I	3	2	2				2-17	-
	7	6	8				2-22	-
	4	2	3				2-27	-
	8	9	8				3-10	-
	5	7	9				3-11	-
Rotating Instrument Head								
Echo II	2	-	-	-	-	-	2-7	1st
	1	-	-	-	-	-	2-7	2nd
PAGEOS I	2	2	2	2	2	2	2-28	-
	2	3	3	2	3	3	3-1	-

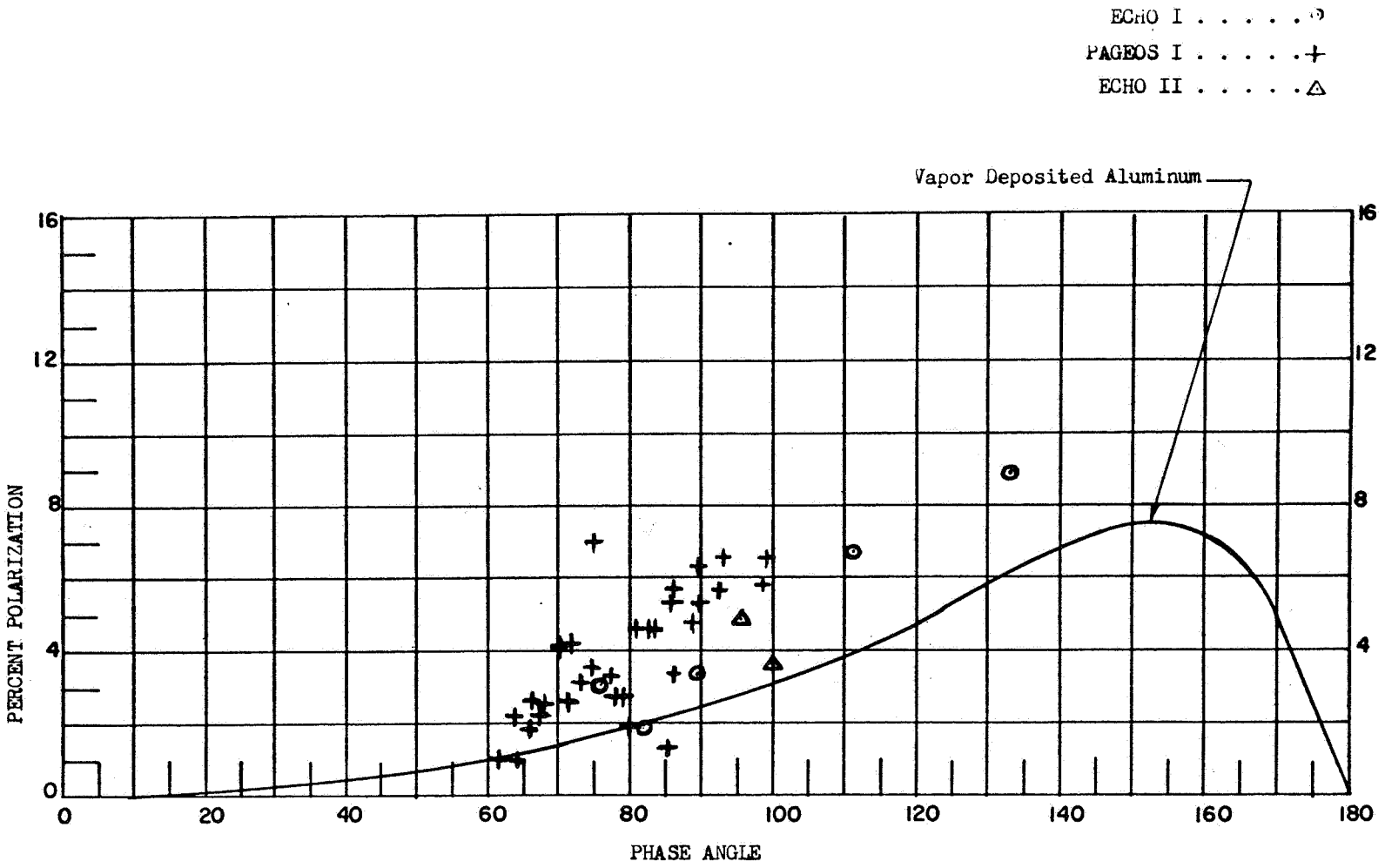

Figure 36. - Satellite Polarization Measurements - U Band

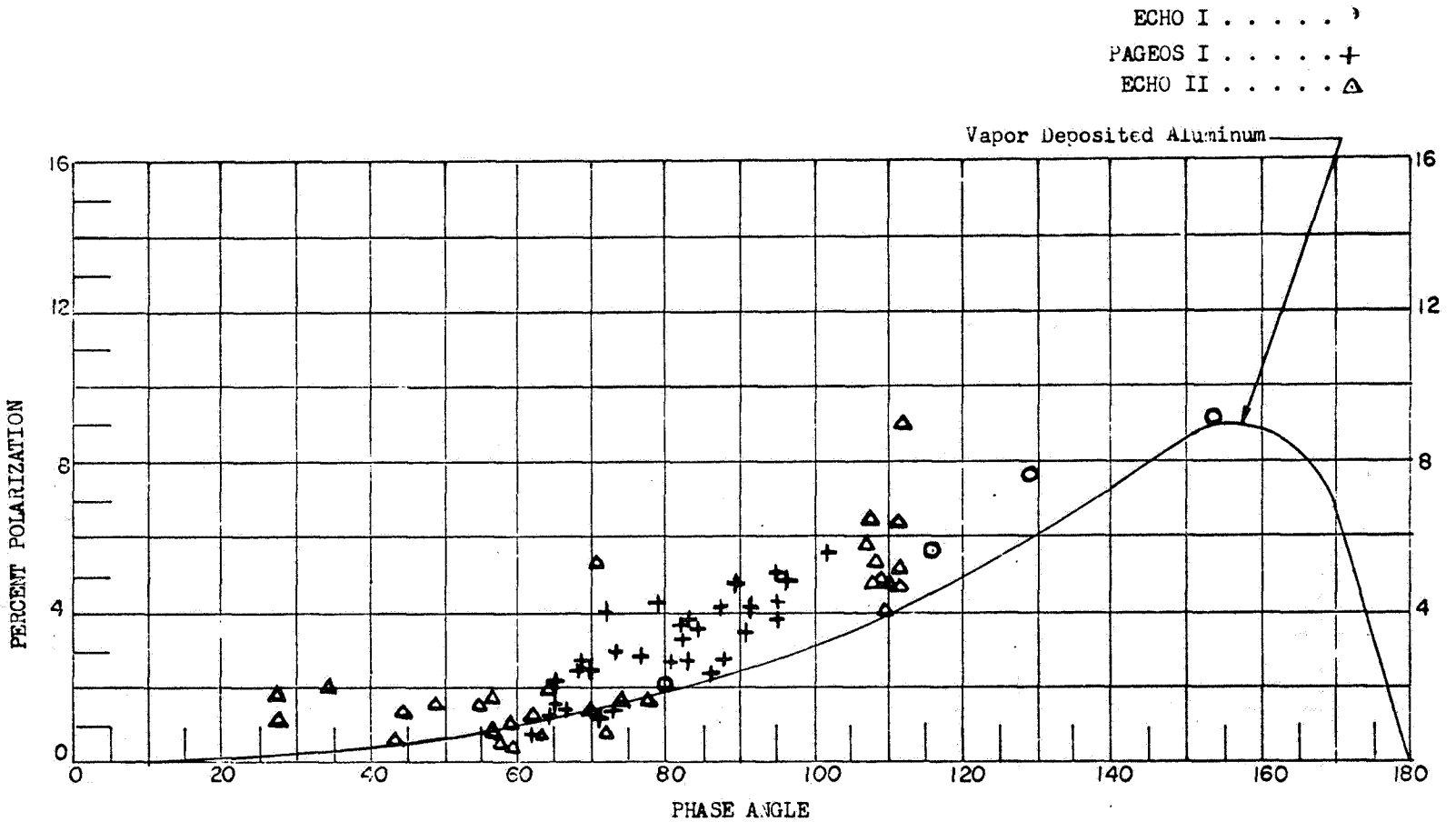

Figure 37. - Satellite Polarization Measurements - B Band

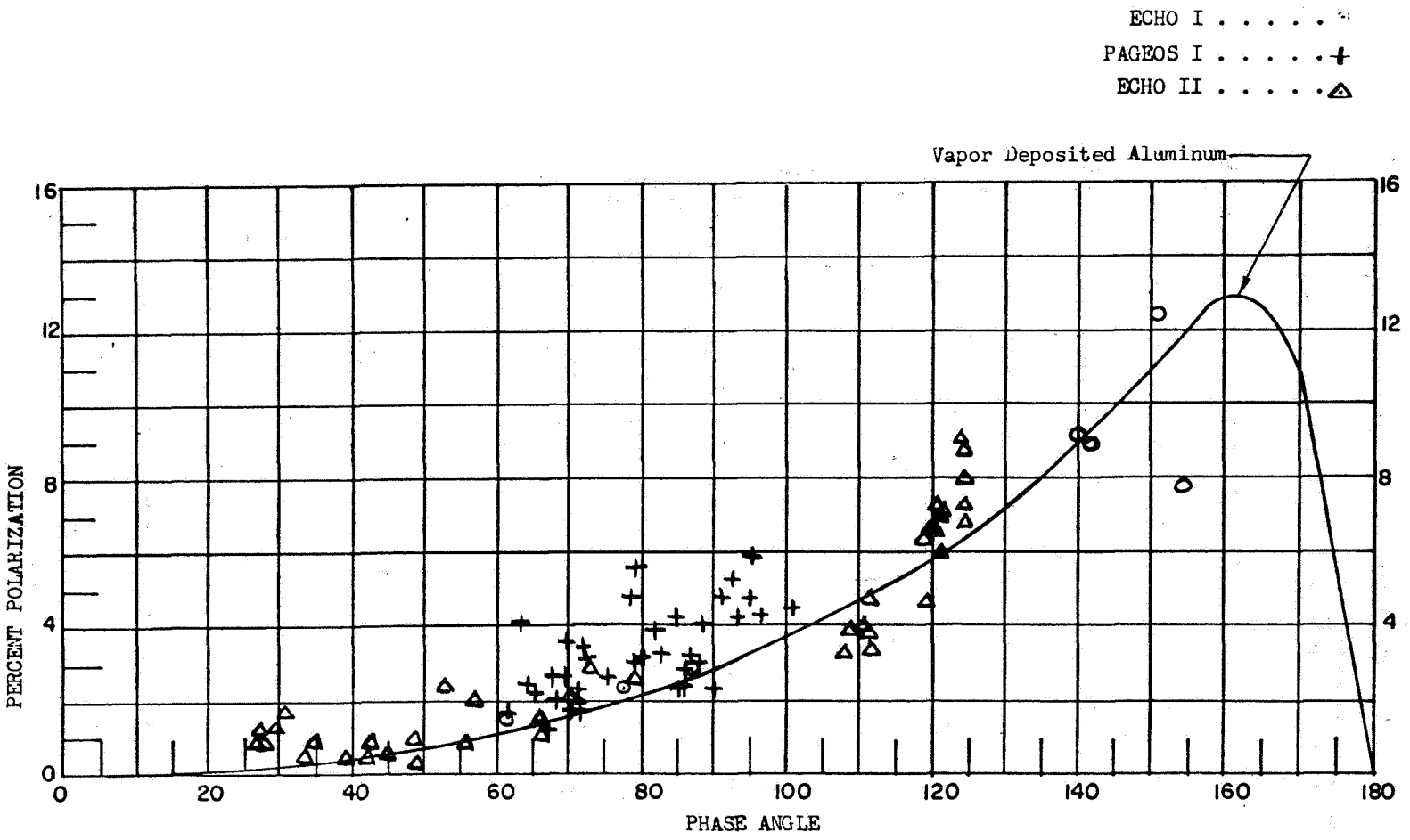

Figure 38. - Satellite Polarization Measurements - V Band

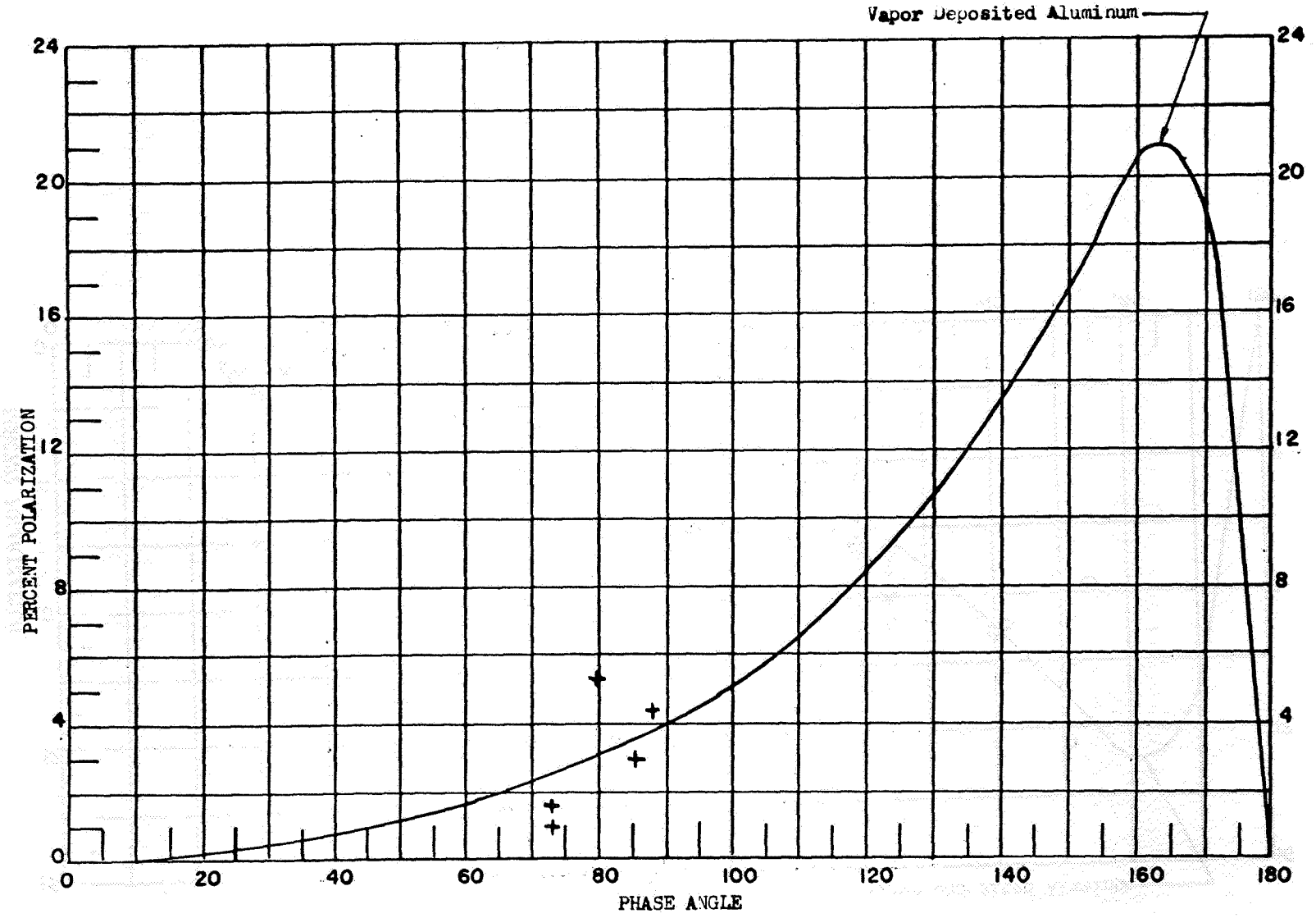

Figure 39. - Satellite Polarization Measurements - R Band

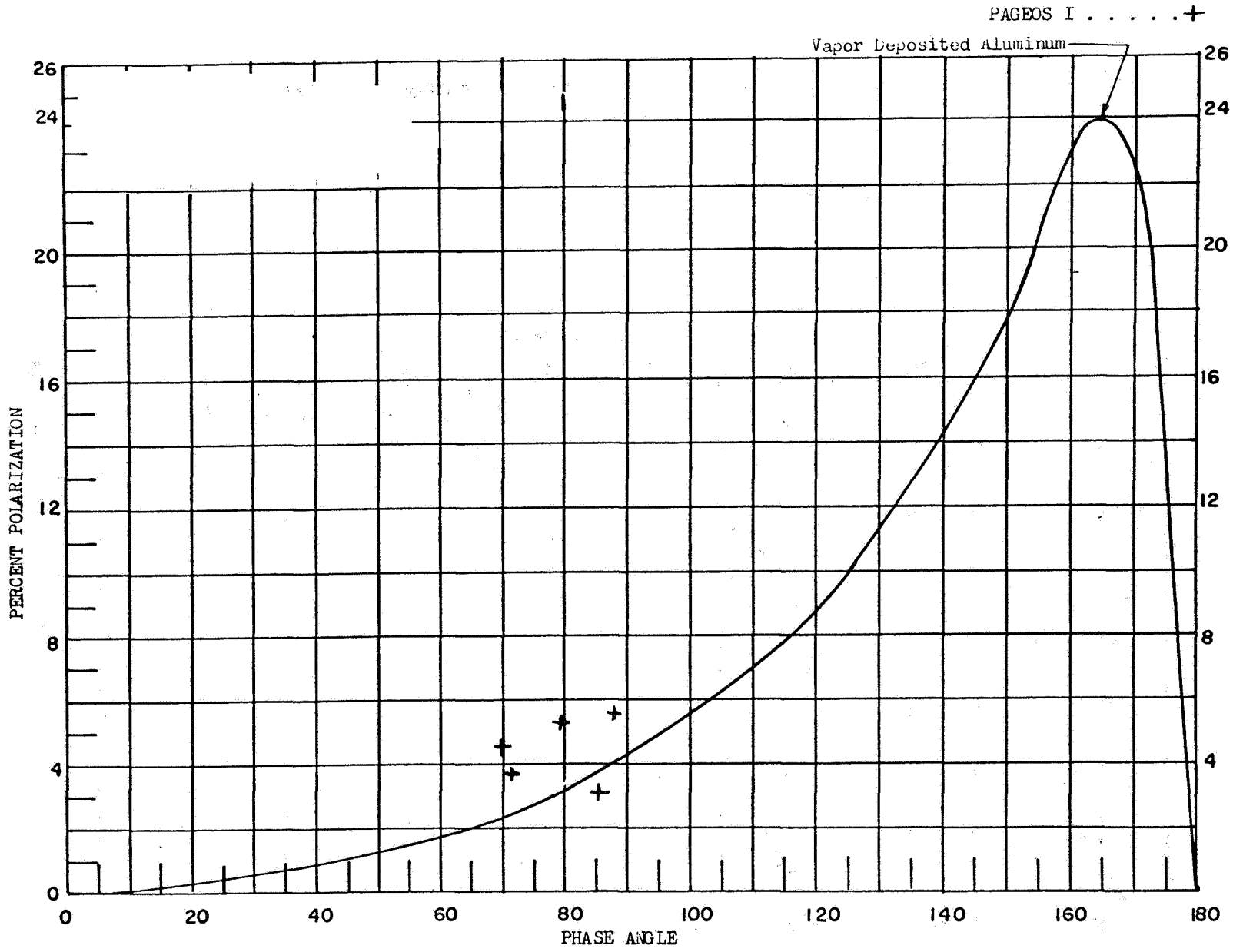

Figure 40. - Satellite Polarization Measurements - I Band

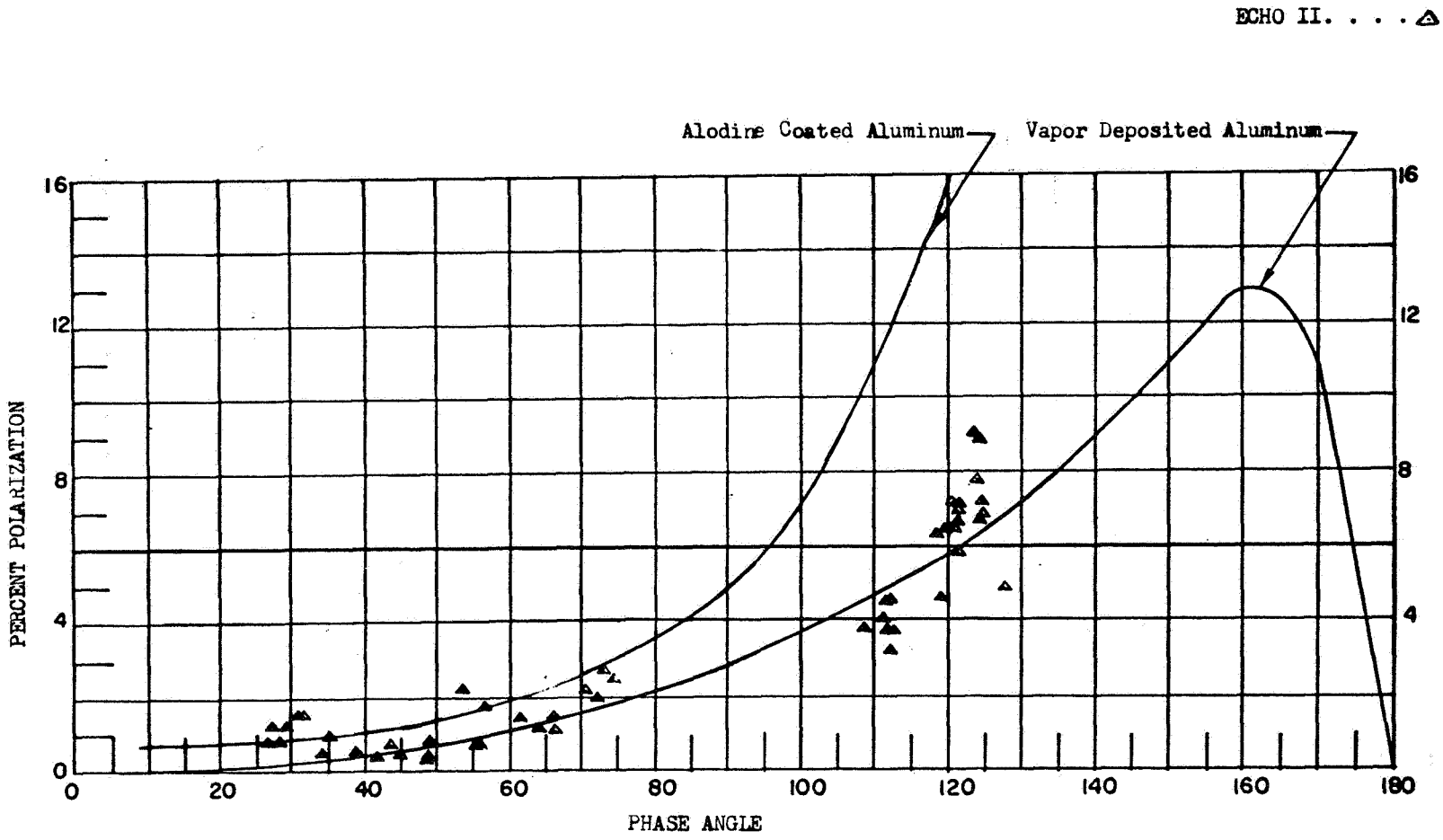

Figure 41.- Echo II Polarization Measurements - V Band

measurements in vacuum have not as yet been performed and thus comparisons of laboratory measurements of Alodine material and polarimetric observations of Echo II are not necessarily valid.

Accuracy of Results

Photometric observations of standard stars. - To aid in the determination of the accuracy of the two photometric systems in the various spectral regions, a number of independent observations were performed on the standard stars which are used in determining the primary extinction coefficients. Calculations of stellar magnitude and color indices are then performed and the values compared with those presented in Reference 6. Table XII presents data for 306 observations in each spectral region taken at Palomar Mountain, California, during July-August, 1966, in the UBV spectral regions. The average air mass of the observations was 1.5.

TABLE XII. - ACCURACY OF STANDARD STAR OBSERVATIONS AT PALOMAR

Parameter	Spectral region		
	V	B-V	U-B
Average deviation for a single observation (mag.)	0.035	0.032	0.040
Standard deviation for a single observation (mag.)	0.041	0.039	0.048
Average deviation for a single observation at 1.0 air mass (mag.)	0.023	0.021	0.027
Probable error for a single observation at 1.0 air mass (mag.)	0.018	0.018	0.022

A similar series of observations and calculations were performed for the new U-B-V-R-I photometric system during the observation period at Yuma, Arizona. For these determinations, 200 observations on 37 F-G-K spectral class standard stars were performed in each color. These data are presented in Table XIII. The average air masses for the spectral regions were as follows: UBV, 1.51; and VRI, 1.57. Since the above measurements provided data relative to the accuracies of both the original U, B, V and the new U, B, V, R, I photometric systems, no new data of this type was required to be taken in Akron for this purpose.

It is quite evident that the low values of average deviation, standard deviation, and probable error indicate a system which is operating properly with a low noise level, as well as good local weather conditions. The values shown here are true indicators of the accuracy level of the extra-atmospheric magnitudes of the various satellites.

The average deviation (A.D.) for observations at the zenith (1.0 air mass) is found by,

$$A.D._{zenith} = \frac{A.D.\ (obs.)}{\sec Z} \tag{19}$$

TABLE XIII. - ACCURACY OF STANDARD STAR OBSERVATIONS AT YUMA

Parameter	Spectral region					
	V (S-20)	B-V	U-B	V (S-1)	V-R	R-I
Average deviation for a single observation (mag.)	0.024	0.027	0.038	0.029	0.030	0.035
Standard deviation for a single observation (mag.)	0.036	0.038	0.048	0.040	0.042	0.050
Average deviation for a single observation at 1.0 air mass (mag.)	0.016	0.018	0.025	0.018	0.019	0.022
Probable error for a single observation at 1.0 air mass (mag.)	0.016	0.017	0.021	0.017	0.018	0.022

where sec Z denotes the mean of the values of the secant of the zenith distance for each star. The average probable error at the zenith for a single observation is calculated by

$$P.E._{zenith} = \frac{0.6745\sigma}{\sec Z} \qquad (20)$$

Satellite data accuracy. - The target accuracies for the multicolor photometric observations of the various satellites were as follows:

(1) Satellite magnitudes $\leq \pm 0.02$

(2) Specularity $\leq \pm 2\%$

(3) Satellite mean radius $\leq \pm 0.7$ ft

(4) Reflectance $\leq \pm 2\%$

A series of calculations of probable error values were performed for each observation period, each satellite, and each color for the above parameters.

The values of the probable errors for the four satellites, determined in accordance with the theory discussed in Reference 3, are presented in Tables XIV through XVII. The probable errors as presented here represent values determined from the mean value of all data points grouped together from each observation period.

It is believed that the relatively high probable errors for the Echo II satellite are due to; (1) the effect of the small number of data points and passes, and (2) a slow rotation rate which results in a less homogeneous set of data to legitimately represent the entire surface.

For the other satellites the probable error values, with few exceptions, are within the accuracy objectives.

TABLE XIV. - PROBABLE ERROR OF ECHO I RESULTS

Observation period	Spectral region	Radius of curvature (ft)	Specularity (percent)	Reflectance (percent)	Stellar magnitudes
Palomar Mt., California Summer, 1966	V (S-4)	±0.15	±0.07	±0.7	±0.007
	U	±0.11	±0.04	±0.5	±0.005
	B	±0.16	±0.08	±0.7	±0.007
Yuma, Arizona Winter, 1967	V (S-20)	±0.31	±0.30	±1.4	±0.014
	U	±0.43	±0.39	±1.9	±0.018
	B	±0.41	±0.31	±1.8	±0.017
	V (S-1)	±0.34	±0.31	±1.5	±0.015
	R	±0.35	±0.32	±1.5	±0.015
	I	±0.43	±0.30	±1.8	±0.017
Akron, Ohio Summer, 1967	V (S-20)	±0.38	±0.45	±1.6	±0.016
	U	±0.50	±0.71	±2.4	±0.022
	B	±0.41	±0.58	±1.8	±0.017
Akron, Ohio Autumn, 1967	V (S-20)	±0.36	±0.15	±1.5	±0.016
	U	±0.51	±0.58	±2.6	±0.024
	B	±0.55	±0.52	±2.5	±0.025
	V (S-1)	±0.41	±0.26	±1.8	±0.017
	R	±0.37	±0.23	±1.7	±0.017
	I	±0.54	±0.34	±2.3	±0.024

TABLE XV. - PROBABLE ERROR OF PAGEOS I RESULTS

Observation period	Spectral region	Radius of curvature (ft)	Specularity (percent)	Reflectance (percent)	Stellar magnitudes
Yuma, Arizona Winter, 1967	V (S-20)	±0.20	±0.09	±0.9	±0.008
	U	±0.20	±0.09	±0.9	±0.009
	B	±0.19	±0.09	±0.8	±0.008
	V (S-1)	±0.25	±0.17	±1.1	±0.012
	R	±0.27	±0.17	±1.2	±0.013
	I	±0.32	±0.20	±1.4	±0.013
Akron, Ohio Summer, 1967	V (S-20)	±0.31	±0.17	±1.3	±0.013
	U	±0.34	±0.20	±1.7	±0.019
	B	±0.32	±0.17	±1.4	±0.015
Akron, Ohio Autumn, 1967	V (S-20)	±0.18	±0.23	±0.8	±0.008
	U	±0.18	±0.28	±0.8	±0.009
	B	±0.19	±0.25	±0.8	±0,008
	V (S-1)	±0.19	±0.28	±0.8	±0.009
	R	±0.21	±0.26	±0.9	±0.009
	I	±0.31	±0.39	±1.3	±0.013

TABLE XVI. - PROBABLE ERROR OF ECHO II RESULTS

Observation period	Spectral region	Radius of curvature (ft)	Specularity (percent)	Reflectance (percent)	Stellar magnitudes
Yuma, Arizona Winter, 1967	V (S-20)	±0.95	±0.85	±3.1	±0.030
	U	±1.38	±1.86	±4.4	±0.040
	B	±1.33	±1.02	±4.3	±0.043
	V (S-1)	±1.56	±4.13	±4.3	±0.039
	R	±1.40	±4.00	±4.6	±0.050
	I	±1.23	±3.43	±3.9	±0.040
Akron, Ohio Summer, 1967	V (S-20)	±0.65	±0.84	±2.4	±0.028
	U	±1.21	±1.52	±5.0	±0.040
	B	±1.29	±1.47	±4.9	±0.040
Akron, Ohio Autumn, 1967	V (S-20)	±0.67	±0.71	±2.8	±0.049
	U	±0.66	±0.65	±3.6	±0.066
	B	±0.53	±0.65	±2.3	±0.040
	V (S-1)	±0.70	±0.70	±2.9	±0.050
	R	±0.77	±0.83	±2.9	±0.046
	I	±0.58	±0.53	±2.5	±0.048

TABLE XVII. - PROBABLE ERROR OF EXPLORER XIX RESULTS

Observation period	Spectral region	Radius of curvature (ft)	Specularity (percent)	Reflectance (percent)	Stellar magnitudes
Akron, Ohio Summer, 1967	V (S-20)	±0.02	±0.09	±0.8	±0.008

Polarimetric results. - There are two types of errors calculated in the polarimetric programs:

(1) The standard error of estimate

(2) The percent probable error of the percent polarization

The standard error of estimate of F on β for the quadratic fit

$$F = Z_1 + Z_2\beta + Z_3\beta^2 \tag{21}$$

where F (β) is used to eliminate a systematic bias in the data

$$S_e = \sqrt{\frac{\sum (f_i - F_i)^2}{n - 2}} \tag{22}$$

where

$$F = Z_1 + Z_2\beta + Z_3\beta^2$$

f_i = the data points ratios I_1/I_2

β = the position of the half-wave plate or Wollaston prism

n = number of data point ratios

The values of the standard error of estimate were used only as a comparison for a large number of zero polarized stars, since the quadratic equation is not a theoretical fit. The average value for the standard error of estimate is approximately 2 percent.

The percent probable error of P, where P is the determined percent of polarization

$$P.E.\% = \frac{0.6745\ D}{S \times P}\ (100) \tag{23}$$

where

$$S = \sum_i (X_i - \overline{X})^2$$

$$X = \cos(2\eta - k\beta)$$

$$\overline{X} = \frac{\sum X_i}{n}$$

$$D = \sum (Y_i - s_i)^2$$

k = 2 for Wollaston prism

k = 4 for half-wave plate

Y_i = theoretical value of $(I_1 - I_2)/(I_1 + I_2)$ at position i of either the Wollaston prism or half-wave plate position

s_i = the ratio of data points $\left[(I_1 - I_2)/(I_1 + I_2)\right]_i$ at position i

The probable error is calculated for each polarimetric data point. Since the percent polarization increases as a function of phase angle, it would appear that the probable error for percent polarization values at high phase angles would be much larger than for those at low phase angles. However, when calculations of the probable error were performed, it was found that this is not necessarily the case. This phenomenon is probably due to the recording of the orthogonal intensity components I_1 and I_2 separately as opposed to electronically summing and differing the two components. The error in recording of these intensities (1-2%) is far more significant at low phase angles where the difference in the two intensities is small.

Probable errors of percent polarization for each data point have been determined and average values calculated for each spectral region for the Echo I, Echo II, and PAGEOS I satellites. The average values are presented in Table XVIII.

The average probable errors show a tendency to increase with decreasing wavelengths. This may be the result of surface degradation or a decrease in achromaticity of the half-wave plate in the U- and B-band spectral regions.

TABLE XVIII. - AVERAGE VALUES OF PROBABLE ERROR OF PERCENT POLARIZATION

Satellite	Parameter	Spectral region				
		U	B	V	R	I
Echo I	Probable error of percent polarization (average)	±1.97	±1.09	±0.87		
	No. of data points	5	4	4		
Echo II	Probable error of percent polarization (average)	±0.74	±1.22	±0.80		
	No. of data points	3	34	50		
PAGEOS I	Probable error of percent polarization (average)	±1.41	±0.66	±0.51	±0.37	±0.82
	No. of data points	31	31	39	5	5

CONCLUSIONS AND RECOMMENDATIONS

Conclusions

In accordance with the results presented and discussed above, we may conclude:

(1) The following mean diameters (twice the mean radii of curvature) are inferred from the best-calibrated (visual band) photometric data:

Satellite	Mean diameter (ft)	Probable error (ft)
Echo I	100.0	±0.6
PAGEOS I	100.0	±0.5
Echo II	135.0	±1.5
Explorer XIX	12.0	±0.04

Note that these values are the same as the design diameters in each case, and therefore none of the above inflatable satellites has measurably degraded in size.

(2) While PAGEOS I's surface figure showed about the same ten percent dispersion in local radii of curvature in late 1967 as in August 1966, the corresponding dispersion for Echo I increased markedly from ten to sixteen percent of the mean radius in this same period, presumably associated with its fall in mean orbital height to 750 st mi.

(3) The long-term rate of specularity degradation in the visual band for vapor-deposited aluminum on Mylar in earth orbit above 825 st mi does not exceed one-half percent per year. (During the first half-year in orbit this specularity may drop initially by several percent. There is also indication that below mean orbital heights of 825 st mi, considerably higher specular degradation rates are encountered.)

(4) Under conditions in near-earth space environment such as existed in 1967 (near-maximum solar activity), the ultraviolet reflectance of vapor-deposited aluminum on Mylar rapidly degrades, losing about ten percent of its initial value during the year. This is evident from both Echo I and PAGEOS I data. The blue reflectance is also degraded, but at a reduced rate. The pronounced enhancement of this dulling and "yellowing" effect in the data from the lower orbiting Echo I suggests that recent interaction with the upper atmosphere is probably a contributing factor.

(5) Apparent smoothing and other indicated anomalies of the Echo II satellite are believed unreal, and actually are probably aspect effects resulting from the quite limited sample of observations for such a virtually non-rotating satellite. Some change in the Echo II original Alodine coating is suggested by the repeatedly higher than expected specularity determinations (greater than 50 percent), but the continued presence of some Alodine is indicated by the polarimetric observations.

(6) Computer analysis of separately-reduced "troughs" and "crests" on a single Explorer XIX intensity trace resulted in near zero and near one-hundred percent specularity determinations, respectively. Evidently these results represent a successful photometric discrimination between the diffuse white paint (in two-inch diameter polka-dots) and the specular bare aluminum foil. The overall specularity determination for this fast-spinning satellite of 81.4 percent is reasonable in view of the fact that about one-fourth of Explorer XIX's surface was covered by the two-inch polka-dots.

(7) The new U-B-V-R-I photometric and polarimetric instrumentation for NASA's mobile observatory has been demonstrated to perform in a highly satisfactory and accurate manner. The major limitation encountered was in frequency response due to the method in which photometric data was being recorded.

Recommendations

Based on the photometric studies to date, the following recommendations are made:

(1) That further multicolor photometric observations be performed periodically on the PAGEOS I satellite to determine reflectance, specularity and figure degradations throughout its orbital life, estimated to last through two solar cycles. The imminent orbital decay of the Echo I satellite will transfer to the surviving PAGEOS I its own acquired significance as an optical materials test and passive probe of the space environment.

(2) That, for slowly-rotating satellites, such as Echo II, considerably more photometric

observations be taken at all phase angles in order to obtain more representative values for specularity, mean radius of curvature and reflectance.

(3) That polarimetric observations of all satellites include data at the highest obtainable phase angles.

(4) That, for future analysis purposes, refined reflectance and polarimetric laboratory data be obtained under in-situ conditions at various and high phase angles of realistic spherically-curved specimens.

(5) That an adequate number of photometric observations be performed on the Explorer XIX and XXIV satellites (or other fast-rotating targets having a combination of surface coatings or materials). Such observations should be recorded on a high frequency response recorder in order to resolve intensity troughs and crests associated with both bare aluminum foil and thermal control type coatings.

(6) That future photometric observations be performed whenever possible, from sites in the southwestern United States, selected for their seeing and transparency excellence.

(7) That two five-inch, 20 magnification, elbow refractor tracking telescopes be added to the telescope complex for increased observer accessibility and efficiency. (Two such instruments were obtained and used on a short loan basis with proven value.)

(8) That instrumentation refinements be incorporated, as follows:

(a) Provision for recording the electronic difference and sum of the orthogonal intensities during polarimetric measurements

(b) Addition of indicators for gain positions of A integrator RC and B integrator RC

(c) Addition of a switch to link A integrator RC and B integrator RC together, when desired

REFERENCES

1. Photometric Measurements of Surface Characteristics of Echo I Satellite. Final Report, GER-11648, (NASA CR 200), Goodyear Aerospace Corporation, 19 June 1964.

2. Mobile 24-Inch Satellite Photometric Observatory. Final Report, NASA CR 66304, Goodyear Aerospace Corporation, 14 October 1966.

3. Hostetler, R. L.; Emmons, R. H.; Preski, R. J.; Rogers, C. L.; and Romick, D.C.: Ground-Based Photometric Surveillance of the Passive Geodetic Satellite; Goodyear Aerospace Corporation; NASA CR-791, June 1967.

4. Johnson, H. L.; and Harris, D. L. III: Three-Color Observations of 108 Stars Intended for Use as Photometric Standards. Astrophys. J., vol. 120, 1954, pp. 196-199.

5. Iriarte, B.; Johnson, H. L.; Mitchell, R. I.; and Wisniewski, W. K.: Five-Color Photometry of Bright Stars. (Includes the Arizona-Tonantzintla Catalog of 1325 Stars.) Sky and Telescope, July 1965, pp. 21-31.

6. Johnson, H. L.; Mitchell, R. I.; Iriarte, B.; and Wisniewski, W. K.: U-B-V-R-I-J-K-L Photometry of the Bright Stars. Communications of the Lunar and Planetary Laboratory; Communication No. 63, Volume 4, Part 3, p. 99, the University of Arizona Press.

7. Hardie, Robert H.: Photoelectric Reductions. Ch. 8 of Astronomical Techniques, W. A. Hiltner, ed., University of Chicago Press, Chicago, Illinois, 1962, pp. 178-208.

8. Tousey, R.: Optical Problems of the Satellite. J. Opt. Soc. Am., vol. XLVII, 1957, p. 261.

9. Tousey, R.: The Visibility of an Earth Satellite. Astronautica Acta, vol. II, 1956, p. 101.

10. Russell, H. N.: On the Albedo of the Planets and Their Satellites, Astrophys, J., vol. XLIII, April 1916 p. 123.

11. Emmons, R. H.: An Indicated Specular Degradation Rate for Aluminized Mylar Surfaces in Near-Earth Orbit from Recent Photometric Observations of the Echo I Satellite; GER-11521, Goodyear Aerospace Corporation, Akron, Ohio, 17 June 1964.

12. Behr, Alfred: Die Interstellare Polarisation des Sternlichts in Sonnenumgebung. Vandenhoeck and Ruprecht in Gottingen, Jahrgang 1959, Nr. 7.

13. Johnson, Harold L.: Interstellar Extinction in the Galaxy; Communications of the Lunar and Planetary Laboratory; Vol. 3, No. 54, p. 79, University of Arizona Press, 1965.

14. Emmons, R. H.; Rogers, C. L.; and Preski, R. J.: Photometric Observations of Artificial Satellites for Determining Optical and Physical Characteristics. Astronomical Journal, vol. 72, No. 8, October 1967, p. 939.

15. Private communication from Richard C. Vanderburgh, Aerospace Research Laboratory, Wright-Patterson Air Force Base, Ohio, to Goodyear Aerospace Corporation, May 1967.

16. Private communication from Robert B. Lee, NASA-Langley to Goodyear Aerospace Corporation; 4 April 1967.

17. American Institute of Physics Handbook, Second Edition, McGraw Hill Book Co., Inc., New York, N.Y., 1963.

18. Private communication from Robert B. Lee, NASA-Langley to Goodyear Aerospace Corporation; 11 September 1967.